Search for squarks and gluinos in final states with hadronically decaying τ-leptons, jets, and missing transverse momentum using pp collisions at $\sqrt{s} = 13$ TeV with the ATLAS detector

M. Aaboud *et al.*[*]
(ATLAS Collaboration)

(Received 21 August 2018; published 18 January 2019)

A search for supersymmetry in events with large missing transverse momentum, jets, and at least one hadronically decaying τ-lepton is presented. Two exclusive final states with either exactly one or at least two τ-leptons are considered. The analysis is based on proton-proton collisions at $\sqrt{s} = 13$ TeV corresponding to an integrated luminosity of 36.1 fb^{-1} delivered by the Large Hadron Collider and recorded by the ATLAS detector in 2015 and 2016. No significant excess is observed over the Standard Model expectation. At 95% confidence level, model-independent upper limits on the cross section are set and exclusion limits are provided for two signal scenarios: a simplified model of gluino pair production with τ-rich cascade decays, and a model with gauge-mediated supersymmetry breaking (GMSB). In the simplified model, gluino masses up to 2000 GeV are excluded for low values of the mass of the lightest supersymmetric particle (LSP), while LSP masses up to 1000 GeV are excluded for gluino masses around 1400 GeV. In the GMSB model, values of the supersymmetry-breaking scale are excluded below 110 TeV for all values of $\tan\beta$ in the range $2 \leq \tan\beta \leq 60$, and below 120 TeV for $\tan\beta > 30$.

DOI: 10.1103/PhysRevD.99.012009

I. INTRODUCTION

Supersymmetry (SUSY) [1–6] introduces a symmetry between fermions and bosons, resulting in a SUSY partner (sparticle) for each Standard Model (SM) particle with identical quantum numbers except for a difference of half a unit of spin. Squarks ($\tilde{q}$), gluinos ($\tilde{g}$), charged sleptons ($\tilde{\ell}$), and sneutrinos ($\tilde{\nu}$) are the superpartners of the quarks, gluons, charged leptons, and neutrinos, respectively. The SUSY partners of the gauge and Higgs bosons are called gauginos and higgsinos, respectively. The charged electroweak gaugino and higgsino states mix to form charginos ($\tilde{\chi}_i^{\pm}$, $i = 1, 2$), and the neutral states mix to form neutralinos ($\tilde{\chi}_j^0$, $j = 1, 2, 3, 4$). Finally, the gravitino ($\tilde{G}$) is the SUSY partner of the graviton. As no supersymmetric particle has been observed, SUSY must be a broken symmetry. To avoid large violations of baryon- or lepton-number conservation, R-parity [7] conservation is often assumed. In this case, sparticles are produced in pairs and decay through cascades involving SM particles and other sparticles until the lightest sparticle (LSP), which is stable, is produced.

Final states with τ-leptons are of particular interest in SUSY searches, although they are experimentally challenging. Light sleptons could play a role in the coannihilation of neutralinos in the early Universe, and models with light τ-sleptons are consistent with constraints on dark matter consisting of weakly interacting massive particles [8–10]. Furthermore, should SUSY or any other physics beyond the Standard Model (BSM) be discovered in leptonic final states, independent studies of all three lepton flavors are necessary to investigate the coupling structure of the new physics, especially with regard to lepton universality.

In this article, an inclusive search for squarks and gluinos produced via the strong interaction in events with jets (collimated sprays of particles from the hadronization of quarks and gluons), at least one hadronically decaying τ-lepton, and large missing transverse momentum is presented. Two SUSY models are considered: a simplified model [11–13] of gluino pair production and a model of gauge-mediated SUSY breaking (GMSB) [14–16]. If squarks and gluinos are within the reach of the Large Hadron Collider (LHC), their production may be among the dominant SUSY processes. Final states with exactly one τ-lepton (1τ) or at least two τ-leptons (2τ) provide complementary acceptance to SUSY signals. These two channels are optimized separately and the results are statistically combined. Models with a small mass splitting between gluinos or squarks and the LSP, producing soft τ-leptons in the final state, are best covered by the 1τ channel. Models

[*]Full author list given at the end of the article.

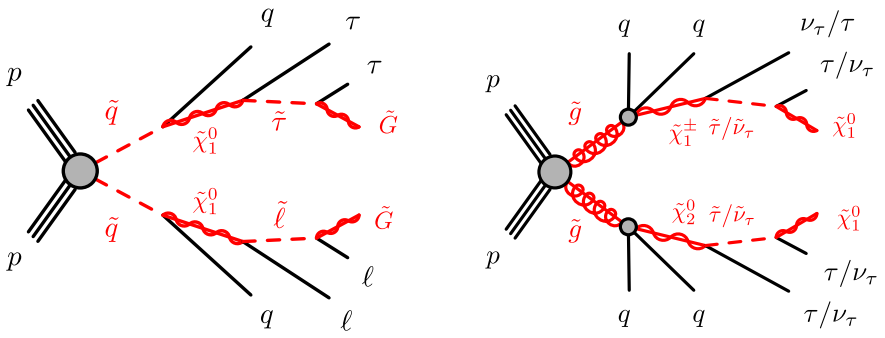

(a) GMSB model (b) Simplified model

FIG. 1. Example processes of (a) the GMSB model and (b) the simplified model of gluino pair production leading to final states with τ-leptons, jets, and missing transverse momentum.

with a heavy LSP, producing signatures with low missing transverse momentum, are more easily probed by the 2τ channel due to the lower SM background. For models with a large mass splitting, both channels provide sensitivity.

The analysis is performed using proton-proton (pp) collision data at a center-of-mass energy of $\sqrt{s}=13\,\text{TeV}$ corresponding to an integrated luminosity of 36.1 fb^{-1}, recorded with the ATLAS detector at the LHC in 2015 and 2016. For both SUSY models, the exclusion limits obtained significantly improve upon the previous ATLAS results. Besides the increase in the integrated luminosity, the results benefit from an improved analysis and statistical treatment. Previous searches in the same final state have been reported by the ATLAS [17–19] and CMS [20] collaborations.

In GMSB models, SUSY breaking is communicated from a hidden sector to the visible sector by a set of messenger fields that share the gauge interactions of the SM. SUSY is spontaneously broken in the messenger sector, leading to massive, nondegenerate messenger fields. The free parameters of GMSB models are the SUSY-breaking mass scale in the messenger sector (Λ), the messenger mass scale (M_{mes}), the number of messenger multiplets (N_5) of the $\mathbf{5}+\bar{\mathbf{5}}$ representation of SU(5), the ratio of the two Higgs-doublet vacuum expectation values at the electroweak scale ($\tan\beta$), the sign of the Higgsino mass term in the superpotential ($\text{sign}(\mu)=\pm1$), and a gravitino-mass scale factor (C_{grav}). Details of the GMSB scenarios studied herein can be found in Ref. [19].

As in previous ATLAS searches, the GMSB model is probed as a function of Λ and $\tan\beta$, while the other parameters are set to $M_{\text{mes}}=250\,\text{TeV}$, $N_5=3$, $\text{sign}(\mu)=1$, and $C_{\text{grav}}=1$. The choice of $\tan\beta$ influences the nature of the NLSP. For large values of $\tan\beta$, the NLSP is the $\tilde{\tau}_1$[1] while for lower $\tan\beta$ values, the $\tilde{\tau}_1$ and the superpartners of the right-handed electron and muon ($\tilde{e}_{\text{R}}, \tilde{\mu}_{\text{R}}$) are almost degenerate in mass. The production of squark pairs dominates at high values of Λ, with a subdominant contribution from squark-gluino production. A typical GMSB signal process is displayed in Fig. 1(a). The value of C_{grav} corresponds to prompt decays of the NLSP.

Although minimal GMSB cannot easily accommodate a Higgs boson with mass of approximately 125 GeV, various extensions exist (see, e.g., Refs. [21,22]) that remedy these shortcomings while preserving very similar signatures, in particular the natures of the LSP and the NLSP.

The simplified model of gluino pair production is inspired by generic models such as the R-parity-conserving phenomenological MSSM [23,24] with dominant gluino pair production, light $\tilde{\tau}_1$, and a $\tilde{\chi}_1^0$ LSP. Gluinos are assumed to undergo a two-step cascade decay leading to τ-rich final states, as shown in Fig. 1(b). The two free parameters of the model are the masses of the gluino ($m_{\tilde{g}}$) and the LSP ($m_{\tilde{\chi}_1^0}$). Assumptions are made about the masses of other sparticles, namely the $\tilde{\tau}_1$ and $\tilde{\nu}_\tau$ are mass degenerate, and the $\tilde{\chi}_2^0$ and $\tilde{\chi}_1^\pm$ are also mass degenerate, with

$$m_{\tilde{\chi}_1^\pm}=m_{\tilde{\chi}_2^0}=\frac{1}{2}(m_{\tilde{g}}+m_{\tilde{\chi}_1^0}),\qquad m_{\tilde{\tau}_1}=m_{\tilde{\nu}_\tau}=\frac{1}{2}(m_{\tilde{\chi}_1^\pm}+m_{\tilde{\chi}_1^0}).$$

Gluinos are assumed to decay into $\tilde{\chi}_1^\pm q\bar{q}'$ and $\tilde{\chi}_2^0 q\bar{q}$ with equal branching ratios, where q, q' denote generic first- and second-generation quarks. The neutralino $\tilde{\chi}_2^0$ is assumed to decay into $\tilde{\tau}\tau$ or $\tilde{\nu}_\tau\nu_\tau$ with equal probability, while the chargino $\tilde{\chi}_1^\pm$ is assumed to decay into $\tilde{\nu}_\tau\tau$ or $\tilde{\tau}\nu_\tau$ with equal probability. In the last step of the decay chain, $\tilde{\tau}$ and $\tilde{\nu}_\tau$ are assumed to decay into $\tau\tilde{\chi}_1^0$ and $\nu_\tau\tilde{\chi}_1^0$, respectively. All other SUSY particles are kinematically decoupled. The topology of signal events depends on the mass-splitting between the gluino and the LSP. The sparticle decay widths are assumed to be small compared to sparticle masses, such that they play no role in the kinematics.

[1]The $\tilde{\tau}_1$ is the lighter of the two τ-slepton mass eigenstates, which results from the mixing of the superpartners of the left- and right-handed τ-leptons ($\tilde{\tau}_L$, $\tilde{\tau}_R$).

II. ATLAS DETECTOR

The ATLAS experiment is described in detail in Ref. [25]. It is a multipurpose detector with a forward-backward symmetric cylindrical geometry and a solid angle[2] coverage of nearly 4π.

The inner tracking detector (ID), covering the region $|\eta| < 2.5$, consists of a silicon pixel detector, a silicon microstrip detector, and a transition radiation tracker. The innermost layer of the pixel detector, the insertable B-layer [26], was installed between Run 1 and Run 2 of the LHC. The inner detector is surrounded by a thin superconducting solenoid providing a 2 T magnetic field, and by a finely segmented lead/liquid-argon (LAr) electromagnetic calorimeter covering the region $|\eta| < 3.2$. A steel/scintillator-tile hadronic calorimeter provides coverage in the central region $|\eta| < 1.7$. The end cap and forward regions, covering the pseudorapidity range $1.5 < |\eta| < 4.9$, are instrumented with electromagnetic and hadronic LAr calorimeters, with steel, copper, or tungsten as the absorber material. A muon spectrometer system incorporating large superconducting toroidal air-core magnets surrounds the calorimeters. Three layers of precision wire chambers provide muon tracking coverage in the range $|\eta| < 2.7$, while dedicated fast chambers are used for triggering in the region $|\eta| < 2.4$.

The trigger system is composed of two stages [27]. The level-1 trigger, implemented with custom hardware, uses information from calorimeters and muon chambers to reduce the event rate from 40 MHz to a maximum of 100 kHz. The high-level trigger reduces the data acquisition rate to about 1 kHz. It is software based and runs reconstruction algorithms similar to those used in the offline reconstruction.

III. DATA AND SIMULATED EVENT SAMPLES

The data used in this analysis consist of pp collisions at a center-of-mass energy of $\sqrt{s} = 13$ TeV delivered by the LHC with a 25 ns bunch spacing and recorded by the ATLAS detector in 2015 and 2016. The average number of pp interactions per bunch crossing, $\langle\mu\rangle$, was 13.4 in 2015 and 25.1 in 2016. Data quality requirements are applied to ensure that all subdetectors were operating normally, and that LHC beams were in stable collision mode. The integrated luminosity of the resulting data set is 36.1 fb^{-1}.

[2]ATLAS uses a right-handed coordinate system with its origin at the nominal interaction point in the center of the detector and the z axis along the beam pipe. The x axis points from the interaction point to the center of the LHC ring and the y axis points upward. Cylindrical coordinates (r, ϕ) are used in the transverse plane, ϕ being the azimuthal angle around the beam pipe. The pseudorapidity is defined in terms of the polar angle θ as $\eta = -\ln\tan(\theta/2)$. Rapidity is defined as $y = 0.5\ln[(E + p_z)/(E - p_z)]$ where E denotes the energy and p_z represents the momentum component along the z axis.

Monte Carlo (MC) simulations are used to model both the SUSY signals and SM backgrounds, except for multijet production, which is evaluated from data. Soft pp interactions (pileup) were included in the simulation using the PYTHIA 8.186 [28] generator with the A2 [29] set of tuned parameters (minimum-bias tune) and MSTW2008LO [30] parton distribution function (PDF) set. Generated events were reweighted such that the $\langle\mu\rangle$ distribution of the simulation matches the one in data. For SM background samples, the interactions between particles and the detector material were simulated [31] using GEANT4 [32] and a detailed description of the ATLAS detector. For signal samples, a parametrized fast simulation was used to describe the energy deposits in the calorimeters [33].

The W + jets and Z + jets (V + jets) processes were simulated with the SHERPA [34] generator using version 2.2.1. Matrix elements (ME) were calculated for up to two partons at next-to-leading order (NLO) and up to four additional partons at leading order (LO) in perturbative QCD using the OPENLOOPS [35] and COMIX [36] ME generators, respectively. The phase space merging between the SHERPA parton shower (PS) [37] and MEs followed the ME + PS@NLO prescription [38]. The NNPDF3.0nnlo [39] PDF set was used in conjunction with dedicated parton-shower tuning. The inclusive cross sections were normalized to a next-to-next-to-leading-order (NNLO) calculation [40] in perturbative QCD based on the FEWZ program [41]. An additional $W(\tau\nu)$ sample is used for evaluating systematic uncertainties; this was generated with MG5_aMC@NLO v2.2.3 [42] interfaced to PYTHIA 8.186 with the A14 tune [43] for the modeling of the PS, hadronization, and underlying event. The ME calculation was performed at tree level and includes the emission of up to four additional partons. The PDF set used for the generation was NNPDF23LO [44].

For the simulation of $t\bar{t}$ events, the POWHEG-BOX v2 [45] generator was used with the CT10 [46] PDF set for the ME calculation. Electroweak single-top-quark production in the s-channel, t-channel, and Wt final state was generated using POWHEG-BOX v1. The PS, hadronization, and underlying event were simulated using PYTHIA 6.428 [47] with the CTEQ6L1 [48] PDF set and the corresponding Perugia 2012 tune [49]. Cross sections were calculated at NNLO in perturbative QCD with resummation of next-to-next-to-leading-logarithm (NNLL) soft gluon terms using the TOP++ 2.0 program [50].

Diboson production was simulated using SHERPA 2.2.1 and 2.2.2 with the NNPDF3.0nnlo PDF set. Processes with fully leptonic final states were calculated with up to one parton for the 4ℓ, $2\ell + 2\nu$ samples or no parton for the $3\ell + 1\nu$ samples at NLO and up to three additional partons at LO. Diboson processes with one of the bosons decaying hadronically and the other leptonically were simulated with up to one parton for the ZZ or no parton for the WW and WZ samples at NLO, and up to three additional partons at

LO. The cross section provided by the generator is used for these samples.

The simplified-model signal samples were generated using MG5_aMC@NLO v2.2.3 interfaced to Pythia 8.186 with the A14 tune. The ME calculation was performed at tree level and includes the emission of up to two additional partons. The PDF set used for the generation was NNPDF23LO. The ME-PS matching was performed using the CKKW-L prescription, with a matching scale set to one quarter of the gluino mass. The GMSB signal samples were generated with the Herwig++ 2.7.1 [51] generator, with CTEQ6L1 PDFs and the UE-EE-5-CTEQ6L1 tune [52], using input files generated in the SLHA format with the SPheno v3.1.12 [53] program. The PS evolution was performed using an algorithm described in Refs. [51,54–56]. Signal cross sections were calculated to next-to-leading order in the strong coupling constant, adding the resummation of soft gluon emission at next-to-leading-logarithm accuracy (NLO + NLL) [57–61]. The nominal cross section and its uncertainty were taken from an envelope of cross-section predictions using different PDF sets and factorization and renormalization scales, as described in Ref. [62].

IV. EVENT RECONSTRUCTION

This search is based on final states with jets, hadronically decaying τ-leptons, and missing transverse momentum. In addition, muons and b-tagged jets are used for background modeling studies, while electrons are only used for the missing transverse momentum calculation.

Interaction vertices are reconstructed using inner-detector tracks with transverse momentum $p_{\mathrm{T}} > 400\,\mathrm{MeV}$ [63]. Primary vertex candidates are required to have at least two associated tracks, and the candidate with the largest $\sum p_{\mathrm{T}}^2$ is defined as the primary vertex. Events without a reconstructed primary vertex are rejected.

Jets are reconstructed using the anti-k_t clustering algorithm [64,65] with a distance parameter $R = 0.4$. Clusters of calorimeter cells [66], calibrated at the electromagnetic energy scale, are used as input. The jet energy is calibrated using a set of global sequential calibrations [67,68]. Jets are required to have $p_{\mathrm{T}} > 20$ GeV and $|\eta| < 2.8$. A jet-vertex-tagging algorithm [69] is used to discriminate hard-interaction jets from pileup jets for jets with $|\eta| < 2.4$ and $p_{\mathrm{T}} < 60$ GeV. Events with jets originating from cosmic rays, beam background, or detector noise are rejected [70]. Jets containing b-hadrons (b-jets) are identified using a multivariate algorithm exploiting the long lifetime, high decay multiplicity, hard fragmentation, and large mass of b-hadrons [71]. The b-tagging algorithm identifies b-jets with an efficiency of approximately 70% in simulated $t\bar{t}$ events. The rejection factors for c-jets, hadronically decaying τ-leptons, and light-quark or gluon jets are approximately 8, 26 and 440, respectively [72].

Muon candidates are reconstructed in the region $|\eta| < 2.5$ from muon spectrometer tracks matching ID tracks. Muons are required to have $p_{\mathrm{T}} > 10$ GeV and pass *medium* identification requirements [73], based on the number of hits in the ID and muon spectrometer, and the compatibility of the charge-to-momentum ratios measured in the two detector systems. Events containing poorly reconstructed muons or cosmic-ray muon candidates are rejected. Details of the electron reconstruction are given in Refs. [74,75].

Hadronically decaying τ-leptons are reconstructed [76] from anti-k_t jets within $|\eta| < 2.5$ calibrated with a local cluster weighting technique [77]. The τ-lepton candidates are built from clusters of calorimeter cells within a cone of size $\Delta R_\eta \equiv \sqrt{(\Delta\eta)^2 + (\Delta\phi)^2} = 0.2$ centered on the jet axis. A boosted regression tree is used to calibrate the energy of reconstructed τ-leptons. It exploits shower-shape information from the calorimeter, the track multiplicity, the amount of pileup, and information from particle-flow reconstruction [78] that aims to identify charged and neutral hadrons from the τ-lepton decay. The τ-leptons are required to have $p_{\mathrm{T}} > 20$ GeV, and candidates reconstructed within the transition region between the barrel and end cap calorimeters, $1.37 < |\eta| < 1.52$, are discarded. The τ-leptons are required to have either one or three associated tracks, with a charge sum of ± 1. A boosted-decision-tree discriminant is used to separate jets from τ-leptons. It relies on track variables from the inner detector as well as shower-shape variables from the calorimeters. The analysis makes use of *loose* and *medium* τ-leptons, corresponding to identification efficiencies of 60% and 55%, respectively, for one-track τ-leptons and 50% and 40%, respectively, for three-track τ-leptons. Electrons reconstructed as one-track τ-leptons are rejected by imposing a p_{T}- and $|\eta|$-dependent requirement on the likelihood identification variable of the electron, which provides a constant efficiency of 95% for real τ-leptons, with a rejection factor for electrons ranging from 30 to 150 depending on the $|\eta|$ region. Like for jets, events with τ-lepton candidates close to inactive calorimeter regions are rejected.

The missing transverse momentum vector $\boldsymbol{p}_{\mathrm{T}}^{\mathrm{miss}}$, whose magnitude is denoted by $E_{\mathrm{T}}^{\mathrm{miss}}$, is defined as the negative vector sum of the transverse momenta of all identified and calibrated physics objects (electrons, muons, jets, and τ-leptons) and an additional soft term. The soft term is constructed from all the tracks with $p_{\mathrm{T}} > 400$ MeV which originate from the primary vertex but are not associated with any physics object. This track-based definition makes the soft term largely insensitive to pileup [79].

After the reconstruction, an *overlap-removal* procedure is applied to remove ambiguities in case the same object is reconstructed by different algorithms. The successive steps of this procedure are summarized in Table I, where the overlap of reconstructed objects is defined in terms of the distance between objects $\Delta R_y \equiv \sqrt{(\Delta y)^2 + (\Delta\phi)^2}$.

TABLE I. Overview of the successive steps in the overlap-removal procedure.

	Object discarded	Object kept	Matching condition
1.	Loose τ	Electron	$\Delta R_y < 0.2$
2.	Loose τ	Muon	$\Delta R_y < 0.2$
3.	Electron	Muon	Shared inner-detector track
4.	Jet	Electron	$\Delta R_y < 0.2$ and jet not b-tagged
5.	Electron	Jet	$\Delta R_y < 0.4$
6.	Jet	Muon	$\Delta R_y < 0.2$, jet with ≤ 2 tracks and not b-tagged
7.	Muon	Jet	$\Delta R_y < 0.4$
8.	Jet	Loose τ	$\Delta R_y < 0.2$

First, *loose* τ candidates are discarded if they overlap with an electron or muon (steps 1 and 2). If an electron and a muon are reconstructed using the same inner-detector track, the electron is discarded (step 3). For overlapping light leptons (electrons and muons) and jets, the jet is kept in cases where the lepton is likely to result from a heavy-flavor hadron decay within the jet, otherwise the lepton is kept (steps 4–7). Finally, if a jet is also reconstructed as a *loose* τ-lepton, the jet is discarded (step 8).

V. EVENT SELECTION

A preselection common to the 1τ and 2τ channels is applied. Events are required to pass the missing transverse momentum trigger with the lowest threshold and no bandwidth limitation. To select a phase space where the trigger is fully efficient, the offline selection requires $E_{\mathrm{T}}^{\mathrm{miss}} > 180\,\mathrm{GeV}$ and a leading jet with $p_{\mathrm{T}} > 120\,\mathrm{GeV}$. Furthermore, an additional jet with $p_{\mathrm{T}} > 25$ GeV is required. The two leading jets are required to be separated from $\boldsymbol{p}_{\mathrm{T}}^{\mathrm{miss}}$ by at least 0.4 in ϕ, to reject multijet background where large $E_{\mathrm{T}}^{\mathrm{miss}}$ can arise from jet energy mismeasurements. The 1τ channel requires exactly one *medium* τ-lepton while the 2τ channel requires at least two *medium* τ-lepton. The preselection is summarized in Table II.

To isolate signatures of potential SUSY processes from known SM background, additional kinematic variables are utilized:

(i) The transverse mass of the system formed by $\boldsymbol{p}_{\mathrm{T}}^{\mathrm{miss}}$ and the momentum $\boldsymbol{p}$ of a reconstructed object,

$$m_{\mathrm{T}} \equiv m_{\mathrm{T}}(\boldsymbol{p}, \boldsymbol{p}_{\mathrm{T}}^{\mathrm{miss}}) = \sqrt{2 p_{\mathrm{T}} E_{\mathrm{T}}^{\mathrm{miss}} (1 - \cos\Delta\phi(\boldsymbol{p}, \boldsymbol{p}_{\mathrm{T}}^{\mathrm{miss}}))},$$

where $\Delta\phi(\boldsymbol{p}, \boldsymbol{p}_{\mathrm{T}}^{\mathrm{miss}})$ denotes the azimuthal angle between the momentum of the reconstructed object and the missing transverse momentum. For events where a lepton ℓ and the missing transverse momentum both originate from a $W(\ell\nu)$ decay, the m_{T}^{ℓ} distribution exhibits a Jacobian peak at the W boson mass. The transverse mass of various objects is used in this analysis, most notably the transverse mass of the reconstructed τ-lepton.

(ii) The $m_{\mathrm{T2}}^{\tau\tau}$ variable [80,81], also called *stransverse mass*, computed as

$$m_{\mathrm{T2}}^{\tau\tau} = \min_{\boldsymbol{p}_{\mathrm{T}}^{a} + \boldsymbol{p}_{\mathrm{T}}^{b} = \boldsymbol{p}_{\mathrm{T}}^{\mathrm{miss}}} (\max\,[m_{\mathrm{T}}(\boldsymbol{p}^{\tau_1}, \boldsymbol{p}_{\mathrm{T}}^{a}), m_{\mathrm{T}}(\boldsymbol{p}^{\tau_2}, \boldsymbol{p}_{\mathrm{T}}^{b})]),$$

where (a, b) refers to two invisible particles that are assumed to be produced with transverse momentum vectors $\boldsymbol{p}_{\mathrm{T}}^{a,b}$. In this calculation, (a, b) are assumed to be massless. The $m_{\mathrm{T2}}^{\tau\tau}$ distribution has a kinematic endpoint for processes where massive particles are pair-produced, each particle decaying into a τ-lepton and an undetected particle. When more than two τ-leptons are produced in a decay chain, there is no way to *a priori* select the pair leading to the desired characteristic. Therefore, $m_{\mathrm{T2}}^{\tau\tau}$ is calculated using all possible τ-lepton pairs and the largest value is chosen.

(iii) The scalar sum of the transverse momenta of all τ-leptons and jets, $H_{\mathrm{T}} = \sum_i p_{\mathrm{T}}^{\tau_i} + \sum_j p_{\mathrm{T}}^{\mathrm{jet}_j}$.

TABLE II. Summary of the preselection criteria applied in the 1τ and 2τ channels. N_{jet} and N_{τ} are the number of jets and τ-leptons respectively; other variables are defined in the text.

Subject of selection	1τ channel	2τ channel
Trigger	$E_{\mathrm{T}}^{\mathrm{miss}} > 180$ GeV, $p_{\mathrm{T}}^{\mathrm{jet}_1} > 120$ GeV	
Jets	$N_{\mathrm{jet}} \geq 2$, $p_{\mathrm{T}}^{\mathrm{jet}_2} > 25$ GeV	
Multijet events	$\Delta\phi(\boldsymbol{p}_{\mathrm{T}}^{\mathrm{jet}_{1,2}}, \boldsymbol{p}_{\mathrm{T}}^{\mathrm{miss}}) > 0.4$	
τ-leptons	$N_{\tau} = 1$	$N_{\tau} \geq 2$

Figure 2 shows examples of kinematic distributions after the preselection and after applying background normalization factors as described in Sec. VI. The dominant backgrounds in the 1τ channel are $t\bar{t}$ production and $W(\tau\nu)$ + jets events, with subdominant contributions from $Z(\nu\nu)$ + jets and $Z(\tau\tau)$ + jets. In the 2τ channel, the spectrum is dominated by $t\bar{t}$, $W(\tau\nu)$ + jets and $Z(\tau\tau)$ + jets events. The multijet background does not contribute significantly while contributions from the diboson background are only relevant at high values of $m_{\mathrm{T}}^{\tau_1} + m_{\mathrm{T}}^{\tau_2}$.

Multiple phase space regions are then defined. A set of signal regions (SRs) with stringent kinematic requirements and low background contribution is designed to target the different signatures and kinematic configurations of the two SUSY models. A set of control regions (CRs) with negligible signal yield is used to constrain the normalization of the dominant backgrounds in phase space regions close to the SRs. The determination of background normalization factors and the search for a possible signal are performed simultaneously by fitting a signal-plus-background model to

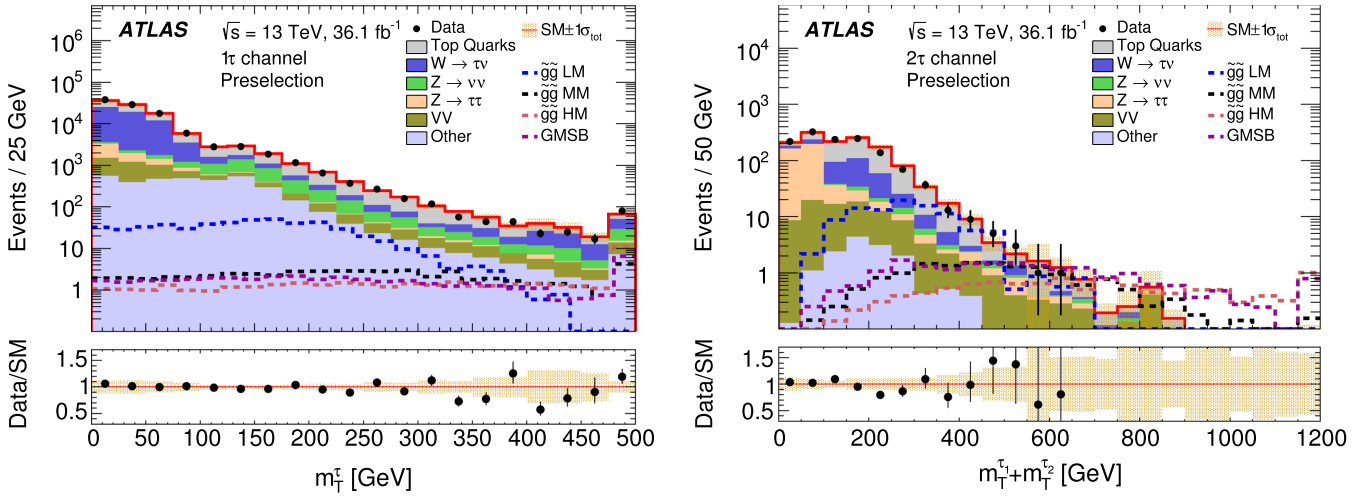

(a) (b)

FIG. 2. Distributions of (a) the τ-lepton transverse mass m_{T}^{τ} in the 1τ channel and (b) the sum of τ-lepton transverse masses $m_{\mathrm{T}}^{\tau_1} + m_{\mathrm{T}}^{\tau_2}$ in the 2τ channel after the preselection, after applying data-driven normalization factors to the main backgrounds. The last bin includes overflow events. The total uncertainty in the background prediction is shown as a shaded band. The contribution labeled as "Other" includes multijet events and the $V+$jets processes not explicitly listed in the legend. Signal predictions are overlaid for several benchmark model points. For the simplified model, LM, MM, and HM refer to low, medium, and high mass-splitting scenarios, with $(m_{\tilde{g}}, m_{\tilde{\chi}_1^0})$ set to (1065,825) GeV, (1625,905) GeV, and (1705,345) GeV, respectively. The GMSB benchmark model corresponds to $\Lambda = 120$ TeV and $\tan\beta = 40$.

the data in the CRs and SRs. Validation regions (VRs) are defined in phase space regions between CRs and SRs. The VRs are not included in the fit; they are used to compare the fitted background predictions with the observed data in the vicinity of SRs to validate the background extrapolation before unblinding the SRs. The CRs, VRs and SRs are mutually exclusive and therefore statistically independent.

TABLE III. Summary of the signal region definitions in the 1τ channel. These requirements are applied in addition to the preselection. The variables are defined in the text.

	1τ SRs	
Subject of selection	Compressed	Medium mass
τ-leptons	$20 < p_{\mathrm{T}}^{\tau} < 45$ GeV	$p_{\mathrm{T}}^{\tau} > 45$ GeV
Event kinematics	$E_{\mathrm{T}}^{\mathrm{miss}} > 400$ GeV	
	$m_{\mathrm{T}}^{\tau} > 80$ GeV	$m_{\mathrm{T}}^{\tau} > 250$ GeV
	...	$H_{\mathrm{T}} > 1000$ GeV

In the 1τ channel, two SRs are defined for the simplified model, as summarized in Table III. The 1τ compressed SR targets small mass differences between the gluino and the LSP, up to ≈300 GeV. It exploits topologies where the pair of gluinos recoils against a high-p_{T} jet from initial-state radiation (ISR). While τ-leptons and additional jets from gluino decays typically have low p_{T}, such ISR events have substantial $E_{\mathrm{T}}^{\mathrm{miss}}$ since both LSPs tend to be emitted opposite to the ISR jet in the transverse plane. A requirement on the transverse mass is used to suppress $W(\tau\nu)+$jets events as well as semileptonic $t\bar{t}$ events with a τ-lepton in the final state. The 1τ medium-mass SR targets larger mass-splittings, motivating a more stringent m_{T}^{τ} criterion and an H_{T} requirement.

These two SRs also provide sensitivity to GMSB signals at low $\tan\beta$, in cases where only one τ-lepton decays hadronically and is reconstructed within the detector acceptance. At high $\tan\beta$, the 1τ channel is not competitive due to the large multiplicity of τ-leptons in signal events.

TABLE IV. Summary of the signal region definitions in the 2τ channel. These requirements are applied in addition to the preselection. The variables are defined in the text on the last line of the Compressed SR, High mass SR and GMSB SR, to make it clear that the 7 bins are only relevant for the multibin SR.

	2τ SRs			
Subject of selection	Compressed	High mass	Multibin	GMSB
Event kinematics	$m_{\mathrm{T2}}^{\tau\tau} > 70$ GeV	$m_{\mathrm{T}}^{\tau_1} + m_{\mathrm{T}}^{\tau_2} > 350$ GeV	$m_{\mathrm{T}}^{\tau_1} + m_{\mathrm{T}}^{\tau_2} > 150$ GeV	$m_{\mathrm{T}}^{\tau_1} + m_{\mathrm{T}}^{\tau_2} > 150$ GeV
	$H_{\mathrm{T}} < 1100$ GeV	$H_{\mathrm{T}} > 1100$ GeV	$H_{\mathrm{T}} > 800$ GeV	$H_{\mathrm{T}} > 1900$ GeV
	$m_{\mathrm{T}}^{\mathrm{sum}} > 1600$ GeV	...	$N_{\mathrm{jet}} \geq 3$	...
	...	...	7 bins in $m_{\mathrm{T}}^{\tau_1} + m_{\mathrm{T}}^{\tau_2}$	...

In the 2τ channel, three SRs are defined for the simplified model, as summarized in Table IV. The compressed and high-mass SRs target signals with small and large mass-splittings, respectively. The 2τ multibin SR exploits the shape difference between signal and background distributions, in contrast to the other SRs which only exploit the total yields. The multibin approach is less model dependent than a single-bin SR designed to probe a narrow part of the model parameter space, and it provides increased sensitivity to both small and large mass-splittings.

The 2τ compressed SR has a requirement on $m_{\mathrm{T2}}^{\tau\tau}$ to exploit the kinematic endpoint of $Z(\tau\tau)+\text{jets}$ and dileptonic $t\bar{t}$ events. A requirement on $m_{\mathrm{T}}^{\mathrm{sum}} \equiv m_{\mathrm{T}}^{\tau_1} + m_{\mathrm{T}}^{\tau_2} + \sum_i m_{\mathrm{T}}^{\mathrm{jet}_i}$ is imposed to take advantage of the large $E_{\mathrm{T}}^{\mathrm{miss}}$ and the high multiplicities of jets and τ-leptons that are expected from gluino decays and the boosted topologies. The upper bound on H_{T} allows a combination with the high-mass SR, and does not affect the sensitivity to compressed signals. The 2τ high-mass SR includes a stringent requirement on $m_{\mathrm{T}}^{\tau_1} + m_{\mathrm{T}}^{\tau_2}$ that reduces the contribution from $Z(\tau\tau)+\text{jets}$ events. The τ-leptons from high-p_{T} Z bosons have a small separation in ϕ, which results in low values of $m_{\mathrm{T}}^{\tau_1} + m_{\mathrm{T}}^{\tau_2}$ given that the τ-neutrinos producing $E_{\mathrm{T}}^{\mathrm{miss}}$ are collimated with the visible decay products of τ-leptons. An H_{T} requirement is applied to significantly reduce background from $t\bar{t}$ and $W(\tau\nu)+\text{jets}$ events. The multibin SR uses looser selection criteria than the high-mass SR, and comprises seven bins in $m_{\mathrm{T}}^{\tau_1} + m_{\mathrm{T}}^{\tau_2}$.

A dedicated SR is defined for the GMSB model, based on the high-mass SR. To accommodate the more complex production and decay processes and the higher mass reach in the GMSB model, the minimum $m_{\mathrm{T}}^{\tau_1} + m_{\mathrm{T}}^{\tau_2}$ requirement, which depends on specific decay topologies, is lowered while the minimum H_{T} requirement is raised. The selection criteria defining the GMSB SR in the 2τ channel are summarized in Table IV.

For the simplified model, the two SRs of the 1τ channel can be statistically combined in a simultaneous fit with either the compressed and high-mass SRs of the 2τ channel or the multibin SR of the 2τ channel, as the multibin SR is not mutually exclusive to the other 2τ SRs. For each benchmark point in the parameter space, the most sensitive expected result of these two fits is used. For the GMSB interpretation, the 1τ SRs are combined with the 2τ GMSB SR and the 2τ compressed SR.

VI. BACKGROUND ESTIMATION

Events from $W(\tau\nu)+\text{jets}$, $t\bar{t}$ and, to a smaller extent, diboson production are significant backgrounds in all SRs. Additionally, $Z(\nu\nu)+\text{jets}$ plays a role in the 1τ channel, while $Z(\tau\tau)+\text{jets}$ is an important background in some of the 2τ SRs. Multijet production makes a minor contribution in the 1τ channel. Dedicated control regions are used to constrain the normalization of all these backgrounds, except for diboson processes, which are normalized to their respective theoretical cross sections.

The τ-leptons selected in the Standard Model background events are either prompt leptons from electroweak boson decays (*true τ-leptons*), or reconstructed objects such as jets that are misidentified as τ-leptons (*fake τ-leptons*). Backgrounds that contribute almost exclusively to a single channel, with only fake or only true τ-leptons, are each normalized with a single normalization factor. This is the case for $Z(\nu\nu)+\text{jets}$, multijet and $Z(\tau\tau)+\text{jets}$ events. The associated control regions are named $Z(\nu\nu)$ CR, multijet CR and $Z(\tau\tau)$ CR. For both the $W(\tau\nu)+\text{jets}$ and $t\bar{t}$ backgrounds, which contribute to both the 1τ and the 2τ SRs with different multiplicities of true and fake τ-leptons, three normalization factors are used. A normalization factor for true τ-leptons is used to correct for differences in the τ-lepton reconstruction and identification efficiencies between data and simulation. A normalization factor for fake τ-leptons accounts for multiple sources of potential mismodeling in the simulation: the quark/gluon composition of jets misidentified as τ-leptons, the parton shower and hadronization models of the generator, and the modeling of particle shower shapes in the calorimeter, which mainly depends on the GEANT4 hadronic interaction model and the modeling of the ATLAS detector. An overall normalization factor accounts for the modeling of the background kinematics and acceptance, and absorbs the theoretical uncertainties in the cross-section computation, as well as the experimental uncertainties in the measured integrated luminosity of the data. The corresponding CRs are named W/top true-τ CR, W/top fake-τ CR, and W/top kinematic CR, respectively. The separation between W and top CRs is achieved by requiring the absence or presence of a b-tagged jet.

The kinematic CRs require a muon and no τ candidate, to be independent of the τ-lepton reconstruction and identification. An upper bound on m_{T}^{μ} is applied to select $W(\mu\nu)+\text{jets}$ events and top-quark background with a muon in the final state. The true-τ CRs target $W(\tau\nu)+\text{jets}$ and semileptonic top-quark processes with a true τ-lepton. They are based on events with a τ-lepton, jets, and $E_{\mathrm{T}}^{\mathrm{miss}}$. Contributions from fake τ-leptons are suppressed by a requirement on m_{T}^{τ}. The fake-τ CRs target $W(\mu\nu)+\text{jets}$ and top-quark processes with a final-state muon, with a jet misidentified as a τ-lepton. They use the same baseline selection as kinematic CRs, but a τ candidate is required. Events with large m_{T}^{μ} values are discarded to suppress the top-quark background with a muon and a true τ-lepton. In the W fake-τ CR, the invariant mass of the reconstructed τ-lepton and the muon $m_{\tau\mu}$ is required to be large to suppress $Z(\tau\tau)$ events where one of the τ-leptons decays into a muon. The $Z(\nu\nu)$ CR requires one τ-lepton, has a lower bound on m_{T}^{τ} to suppress background with real τ-leptons, a requirement on $E_{\mathrm{T}}^{\mathrm{miss}}/m_{\mathrm{eff}}$, where $m_{\mathrm{eff}} = H_{\mathrm{T}} + E_{\mathrm{T}}^{\mathrm{miss}}$, to reject multijet events, and requirements on the $\Delta\phi$ separations between the missing transverse momentum and the highest-p_{T} jet and τ-lepton, to exploit the background topology. The $Z(\tau\tau)$ CR is designed by inverting the

$m_{\mathrm{T}}^{\tau_1} + m_{\mathrm{T}}^{\tau_2}$ and H_{T} requirements from the 2τ SRs. This selection requires two medium τ-leptons of opposite electric charge and imposes an upper bound on the invariant mass of the τ-lepton pair to suppress dileptonic top-quark contributions. Both Z CRs employ a veto on b-tagged jets to suppress contributions from top-quark processes. A simultaneous fit over all CRs is performed using HistFitter [82] to extract the normalization factors.

The multijet background contributes when jets are misidentified as τ-leptons and large missing transverse momentum is induced by jet energy mismeasurements. This, together with the very large production cross section, makes it difficult to simulate a sufficient number of multijet events with the required accuracy, so this background is estimated from data [83]. A data sample with high purity in multijet events is selected using single-jet triggers. Events with well-measured jets are retained by applying an upper bound on the $E_{\mathrm{T}}^{\mathrm{miss}}$ significance [19], except for events where the leading b-tagged jet is aligned with $\boldsymbol{p}_{\mathrm{T}}^{\mathrm{miss}}$. The latter exception avoids too large of a suppression of high-p_{T} b-hadrons decaying semileptonically and producing high-p_{T} neutrinos. Jet energies are then smeared according to the jet energy resolution obtained from simulation and corrected to better describe the data. The smearing is performed multiple times for each selected event, leading to a large pseudo-data set where $E_{\mathrm{T}}^{\mathrm{miss}}$ originates from resolution effects and which includes an adequate fraction of jets misidentified as τ-leptons. A subtraction is performed to account for the small contamination from $t\bar{t}$ events satisfying this kinematic configuration. The normalization of the pseudo-data is constrained in the simultaneous fit using a multijet CR where either of the two leading jets is aligned with $\boldsymbol{p}_{\mathrm{T}}^{\mathrm{miss}}$.

The selection criteria defining the various CRs are summarized in Tables V and VI. Figure 3 illustrates the background modeling in CRs after the fit. The fitted normalization factors do not deviate from unity by more than 15% and are compatible with unity within one standard deviation when considering all systematic uncertainties, except for the $Z(\nu\nu)+\text{jets}$ background, where the normalization factor reaches 1.44 ± 0.29.

TABLE V. Summary of the W and top control regions. These requirements are applied in addition to the trigger, jet, and multijet requirements of the preselection. The variables N_τ, N_{jet}, N_μ, and $N_{b\text{-jet}}$ are the number of τ-leptons, jets, muons, and b-tagged jet, respectively; other variables are defined in the text.

Subject of selection	W/top kinematic CR	W/top true-τ CR	W/top fake-τ CR
τ-leptons	$N_\tau = 0$	$N_\tau = 1$	
Jets	$N_{\text{jet}} \geq 3$		$\cdots$
Muons	$N_\mu = 1$	$N_\mu = 0$	$N_\mu = 1$
W/top separation		$N_{b\text{-jet}} = 0/\geq 1$	
Event kinematics		$H_{\mathrm{T}} < 800$ GeV	
		$E_{\mathrm{T}}^{\mathrm{miss}} < 300$ GeV	
	$m_{\mathrm{T}}^{\mu} < 100$ GeV	$m_{\mathrm{T}}^{\tau} < 80$ GeV	$m_{\mathrm{T}}^{\mu} < 100$ GeV
	$\cdots$	$\cdots$	$m_{\tau\mu} > 60$ GeV (W CR)

TABLE VI. Summary of the $Z(\nu\nu)$, $Z(\tau\tau)$, and multijet control regions. These requirements are applied in addition to the trigger and jet requirements of the preselection. The variables N_τ and N_μ are the number of τ-leptons, and muons, respectively; q_{τ_i} is the charge of τ-lepton i; other variables are defined in the text.

Subject of selection	$Z(\nu\nu)$ CR	$Z(\tau\tau)$ CR	Multijet CR
τ-leptons	$N_\tau = 1$	$N_\tau \geq 2, q_{\tau_1} = -q_{\tau_2}$	$N_\tau = 1$
Multijet events	$\Delta\phi(\boldsymbol{p}_{\mathrm{T}}^{\mathrm{jet}_{1,2}}, \boldsymbol{p}_{\mathrm{T}}^{\mathrm{miss}}) > 0.4$		$\Delta\phi(\boldsymbol{p}_{\mathrm{T}}^{\mathrm{jet}_{1,2}}, \boldsymbol{p}_{\mathrm{T}}^{\mathrm{miss}}) < 0.3$
Muons	$N_\mu = 0$	$\cdots$	$\cdots$
Top suppression	$N_{b\text{-jet}} = 0$		$\cdots$
Event kinematics	$H_{\mathrm{T}} < 800$ GeV		$\cdots$
	$E_{\mathrm{T}}^{\mathrm{miss}} < 300$ GeV	$\cdots$	$\cdots$
	$100 \leq m_{\mathrm{T}}^{\tau} < 200$ GeV	$m_{\mathrm{T}}^{\tau_1} + m_{\mathrm{T}}^{\tau_2} < 100$ GeV	$100 < m_{\mathrm{T}}^{\tau} < 200$ GeV
	$E_{\mathrm{T}}^{\mathrm{miss}}/m_{\mathrm{eff}} > 0.3$	$m_{\mathrm{T2}} < 70$ GeV	$E_{\mathrm{T}}^{\mathrm{miss}}/m_{\mathrm{eff}} < 0.2$
	$\Delta\phi(\boldsymbol{p}_{\mathrm{T}}^{\mathrm{jet}_1}, \boldsymbol{p}_{\mathrm{T}}^{\mathrm{miss}}) > 2.0$	$\cdots$	$\cdots$
	$\Delta\phi(\boldsymbol{p}_{\mathrm{T}}^{\tau_1}, \boldsymbol{p}_{\mathrm{T}}^{\mathrm{miss}}) > 1.0$	$\cdots$	$\cdots$

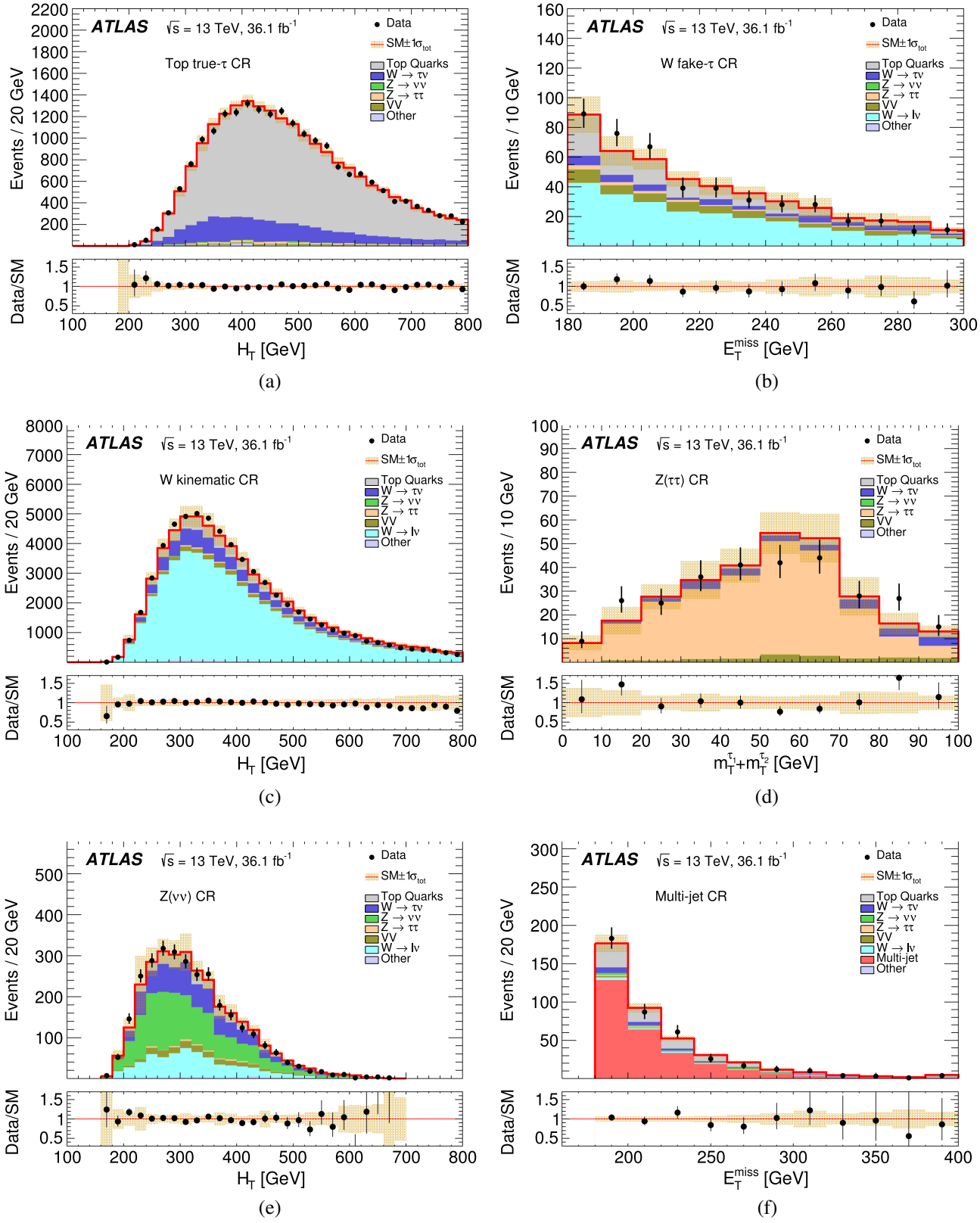

FIG. 3. (a) Scalar sum of transverse momenta of τ-leptons and jets H_{T} in the top true-τ CR, (b) missing transverse momentum $E_{\mathrm{T}}^{\mathrm{miss}}$ in the W fake-τ CR, (c) H_{T} in the W kinematic CR, (d) sum of τ-lepton transverse masses $m_{\mathrm{T}}^{\tau_1} + m_{\mathrm{T}}^{\tau_2}$ in the $Z(\tau\tau)$ CR, (e) H_{T} in the $Z(\nu\nu)$ CR, and (f) $E_{\mathrm{T}}^{\mathrm{miss}}$ in the multijet CR, illustrating the background modeling in the CRs after the fit. The contribution labeled as "Other" includes multijet events (except for the multijet CR) and the V + jets processes not explicitly listed in the legend. The last bin of each distribution includes overflow events. The total uncertainty in the background prediction is shown as a shaded band.

TABLE VII. Validation regions for the 1τ channel. These requirements are applied in addition to the preselection. The variables are defined in the text.

	1τ medium-mass VRs			1τ compressed VRs	
Subject of selection	H_{T}	$E_{\mathrm{T}}^{\mathrm{miss}}$	m_{T}^{τ}	$E_{\mathrm{T}}^{\mathrm{miss}}$	m_{T}^{τ}
τ-leptons	$p_{\mathrm{T}}^{\tau} > 45$ GeV			$20 < p_{\mathrm{T}}^{\tau} < 45$ GeV	
Event kinematics	$m_{\mathrm{T}}^{\tau} < 250$ GeV		$m_{\mathrm{T}}^{\tau} > 250$ GeV	$m_{\mathrm{T}}^{\tau} < 80$ GeV	$m_{\mathrm{T}}^{\tau} > 80$ GeV
	$E_{\mathrm{T}}^{\mathrm{miss}} < 400$ GeV	$E_{\mathrm{T}}^{\mathrm{miss}} > 400$ GeV	$E_{\mathrm{T}}^{\mathrm{miss}} < 400$ GeV	$E_{\mathrm{T}}^{\mathrm{miss}} > 400$ GeV	$E_{\mathrm{T}}^{\mathrm{miss}} < 400$ GeV
	$H_{\mathrm{T}} > 1000$ GeV	$H_{\mathrm{T}} < 1000$ GeV		...	...

TABLE VIII. Validation regions for the 2τ channel. These requirements are applied in addition to the preselection. The variables are defined in the text.

Subject of selection	$2\tau W/\mathrm{Top}$ VR	$Z(\tau\tau)$ VR
$W/$top separation	$N_{b\text{-jet}} = 0/\geq 1$	...
Event kinematics	$H_{\mathrm{T}} < 800$ GeV	$H_{\mathrm{T}} > 800$ GeV
	$m_{\mathrm{T}}^{\tau_1} + m_{\mathrm{T}}^{\tau_2} > 150$ GeV	$m_{\mathrm{T}}^{\tau_1} + m_{\mathrm{T}}^{\tau_2} < 150$ GeV
	$m_{\mathrm{T2}}^{\tau\tau} < 60$ GeV	

Validation regions are used to verify that the background is well modeled after the fit in kinematic regions close to the SRs. In the 1τ channel, three VRs are defined for the medium-mass SR and two for the compressed SR, while three VRs are used for the 2τ channel. Their selection criteria are summarized in Tables VII and VIII. The level of agreement between data and background in the VRs is illustrated in Figs. 4 and 5. Distributions are found to be well modeled in both channels. The comparison between the numbers of observed events and the predicted background yields is displayed in Fig. 6. Agreement well within one standard deviation is observed.

VII. SYSTEMATIC UNCERTAINTIES

Theoretical and experimental systematic uncertainties are evaluated for all simulated processes. The uncertainties from theory include PDF, α_{S} and scale uncertainties, and generator modeling uncertainties. Experimental uncertainties are related to the reconstruction, identification, and calibration of final-state objects. Specific uncertainties are evaluated for the multijet background, which is estimated from data.

For $V+$jets and diboson samples, systematic uncertainties related to PDFs, α_{S}, and scales are evaluated using alternative weights from the generator. The PDF uncertainty is obtained as the standard deviation of the 100 PDF variations from the NNPDF3.0nnlo set. The effect of the uncertainty in α_{S} is computed as half the difference resulting from the $\alpha_{\mathrm{S}} = 0.119$ and $\alpha_{\mathrm{S}} = 0.117$ parametrizations. The renormalization scale μ_{R} and factorization scale μ_{F} are varied up and down by a factor of 2 and all combinations are evaluated, except for the $(2\mu_{\mathrm{R}}, \frac{1}{2}\mu_{\mathrm{F}})$ and $(\frac{1}{2}\mu_{\mathrm{R}}, 2\mu_{\mathrm{F}})$ variations, which would lead to large $\log(\mu_{\mathrm{R}}/\mu_{\mathrm{F}})$ contributions to the cross section. The scale uncertainty is computed as half the difference between the two combinations yielding the largest and smallest deviations from the nominal prediction. Uncertainties due to the resummation and CKKW matching scales for $V+$jets samples are found to be negligible. Additional generator modeling uncertainties are considered for the dominant $W(\tau\nu)+$jets background. An uncertainty is derived to cover a mismodeling of the H_{T} distribution observed in the W kinematic CR (cf. Figure 3(c)). In addition, predictions from SHERPA and MG5_aMC@NLO+PYTHIA8 are compared, and the difference is taken as a systematic uncertainty. For the diboson background, which is not normalized to data in the fit, the uncertainty in the cross section is also taken into account.

For top quark pair production, uncertainties due to PDF and scale variations are derived using POWHEG+PYTHIA8 and applied to the nominal predictions from POWHEG+PYTHIA6. Generator modeling uncertainties are assessed from comparisons with alternative generator samples. An uncertainty in the hard-scattering model is evaluated by comparing predictions from MG5_aMC@NLO+HERWIG++ and POWHEG-BOX+HERWIG++. An uncertainty due to the parton shower and hadronization models is evaluated by comparing predictions from POWHEG-BOX+PYTHIA6 and POWHEG-BOX+HERWIG++. An uncertainty due to the ISR modeling is assessed by varying the POWHEG-BOX parameter which controls the transverse momentum of the first additional parton emission beyond the Born configuration. For the small contributions from single-top-quark production and $t\bar{t}+V$ events, uncertainties in the cross sections are taken into account.

Systematic uncertainties affecting jets arise from the jet energy scale [84], jet energy resolution [85], and efficiency corrections for jet-vertex-tagging [69] as well as b-tagging

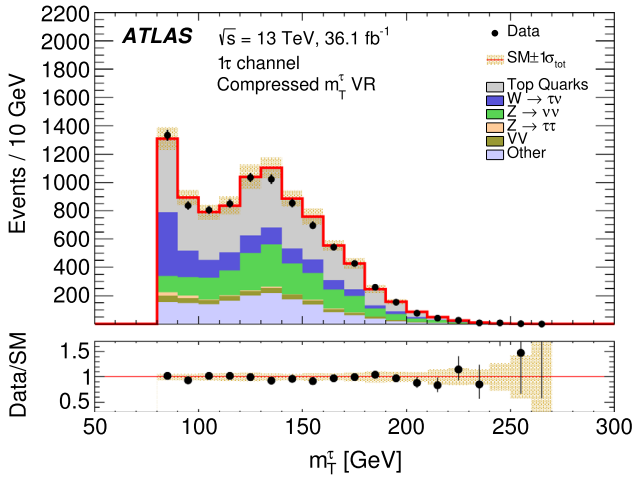

(a)

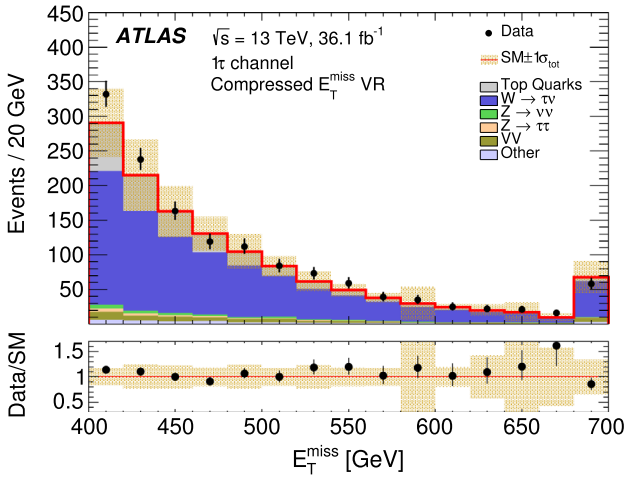

(b)

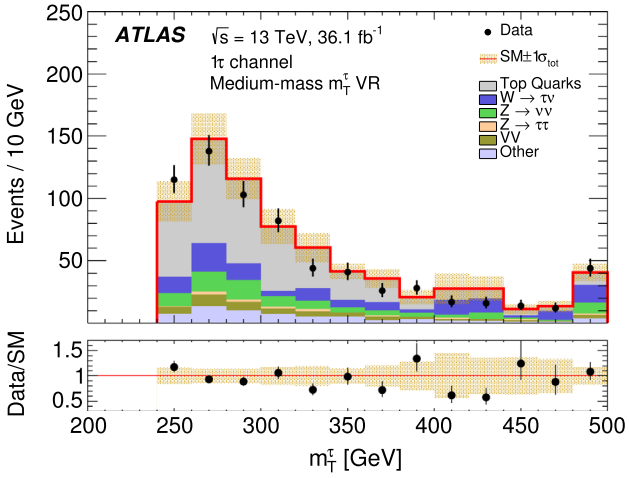

(c)

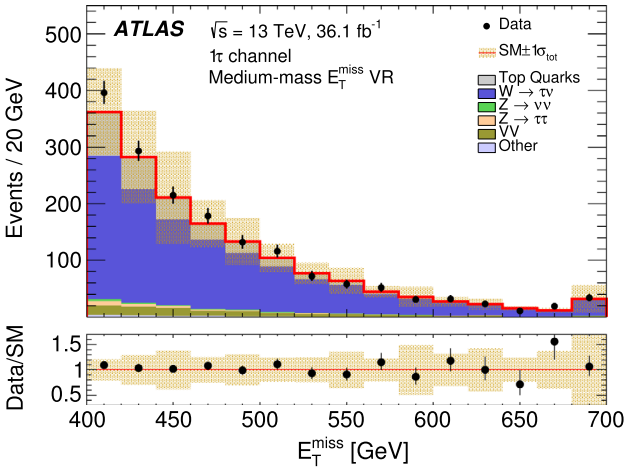

(d)

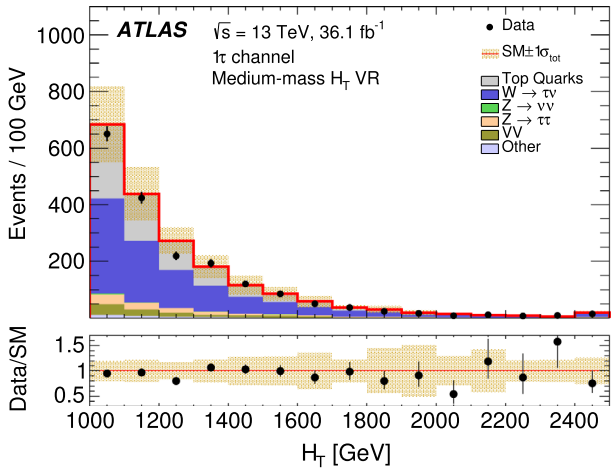

(e)

FIG. 4. Distributions of (a) τ-lepton transverse mass m_{T}^{τ} in the compressed m_{T}^{τ} VR, (b) missing transverse momentum $E_{\mathrm{T}}^{\mathrm{miss}}$ in the compressed $E_{\mathrm{T}}^{\mathrm{miss}}$ VR, (c) m_{T}^{τ} in the medium-mass m_{T}^{τ} VR, (d) $E_{\mathrm{T}}^{\mathrm{miss}}$ in the medium-mass $E_{\mathrm{T}}^{\mathrm{miss}}$ VR, and (e) scalar sum of τ-lepton and jet transverse momenta H_{T} in the medium-mass H_{T} VR, illustrating the background modeling in the VRs of the 1τ channel after the fit. The normalization factors obtained in the CRs are applied. The contribution labeled as "Other" includes multijet events and the $V+$ jets processes not explicitly listed in the legend. The last bin of each distribution includes overflow events. The total uncertainty in the background prediction is shown as a shaded band.

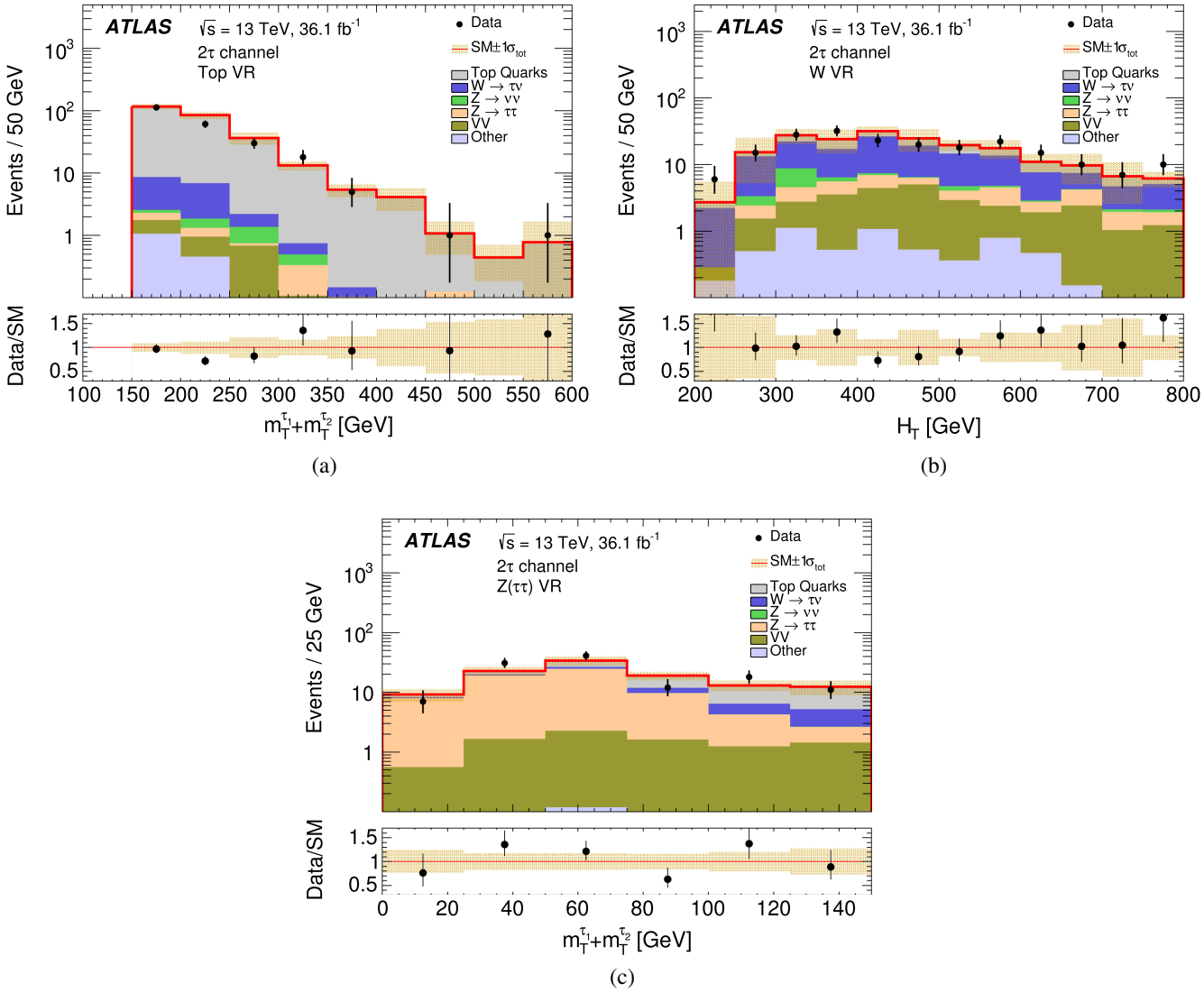

FIG. 5. (a) Sum of τ-lepton transverse masses $m_{\mathrm{T}}^{\tau_1} + m_{\mathrm{T}}^{\tau_2}$ in the top VR, (b) scalar sum of τ-lepton and jet transverse momenta H_{T} in the W VR, and (c) $m_{\mathrm{T}}^{\tau_1} + m_{\mathrm{T}}^{\tau_2}$ in the Z VR, illustrating the background modeling in the VRs of the 2τ channel after the fit. The normalization factors obtained in the CRs are applied. The contribution labeled as "Other" includes multijet events and the V + jets processes not explicitly listed in the legend. The last bin of each distribution includes overflow events. The total uncertainty in the background prediction is shown as a shaded band.

[86]. Jet energy scale uncertainties are mainly determined from measurements of the p_{T} balance in the calorimeter in Z/γ + jet and multijet events. Remaining uncertainties arise from the relative calibration of forward and central jets, jet flavor composition, pileup, and punch-through for high-p_{T} jets not fully contained in the calorimeters. A set of five uncertainties that comprises contributions from both absolute and *in situ* energy calibrations and which preserves the dominant correlations in the (p_{T}, η) phase space is used. An uncertainty in the jet energy resolution is applied to jets in the simulation as a Gaussian energy smearing.

Systematic uncertainties affecting true τ-leptons are related to the reconstruction and identification efficiencies, the electron rejection efficiency, and the energy scale calibration [87]. The uncertainties in the reconstruction efficiency are estimated by varying parameters in the simulation such as the detector material, underlying event, and hadronic shower model. Uncertainties in the identification efficiency and *in situ* energy calibration, which are derived in $Z(\tau\tau)$ events with a hadronically decaying τ-lepton and a muon, arise from the modeling of true- and fake-τ-lepton templates. The uncertainty in the energy scale also includes nonclosure of the calibration found in simulation and a single-pion response uncertainty. In the case of fake τ-leptons, the misidentification rate in the simulation is largely constrained by the fit to data in the CRs. The process-dependence of the misidentification rate is accounted for by the use of different normalization

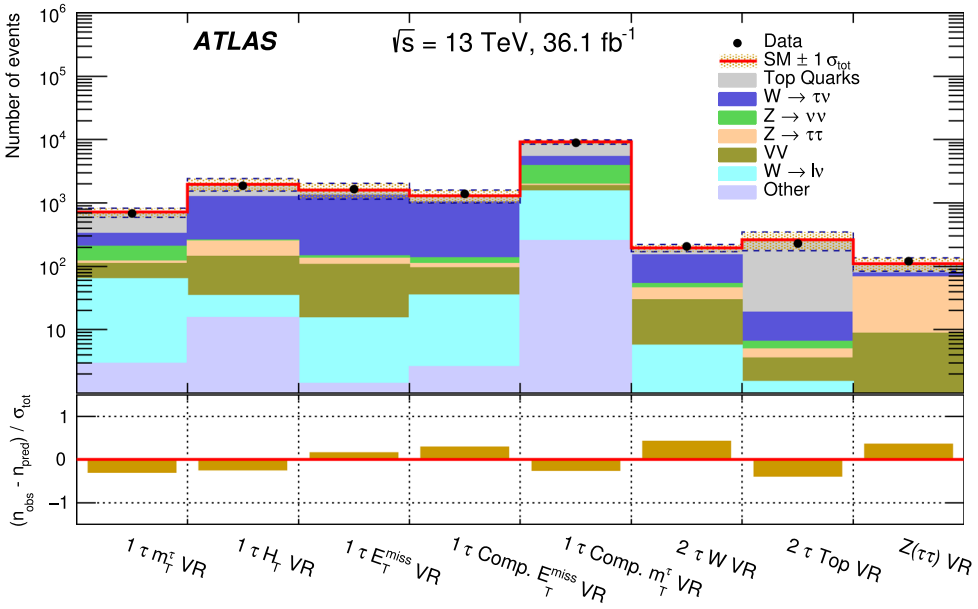

FIG. 6. Number of observed events n_{obs} and predicted background yields in the validation regions n_{pred} of the 1τ and 2τ channels. The background predictions are scaled using normalization factors derived in the control regions. The total uncertainty in the background predictions σ_{tot} is shown as a shaded band. The lower panel displays the significance of the deviation of the observed from the expected yield.

factors for the various backgrounds. Uncertainties in the extrapolation from the CRs to the VRs and SRs are covered by generator modeling uncertainties.

In the case of signal samples, which undergo fast calorimeter simulation, dedicated uncertainties take into account the difference in performance between full and fast simulation. These uncertainties include nonclosure of the energy calibration for both the jets and τ-leptons, as well as differences in reconstruction and identification efficiencies for τ-leptons.

Systematic uncertainties in the missing transverse momentum originate from uncertainties in the energy or momentum calibration of jets, τ-leptons, electrons, and muons, which are propagated to the $E_{\text{T}}^{\text{miss}}$ calculation. Additional uncertainties are related to the calculation of the track-based soft term. These uncertainties are derived by studying the p_{T} balance between the soft term and the hard term composed of all reconstructed objects, in $Z(\mu\mu)$ events. Soft-term uncertainties include scale uncertainties along the hard-term axis, and resolution uncertainties along and perpendicular to the hard-term axis [88].

A systematic uncertainty accounts for the modeling of pileup in the simulation, which affects the correlation between the average number of interactions per bunch crossing and the number of reconstructed primary vertices. The modeling mostly depends on the minimum-bias tune and the longitudinal size of the pp interaction region used in the simulation.

Systematic uncertainties in the small multijet background contribution are due to the limited numbers of events in the input data set satisfying the $E_{\text{T}}^{\text{miss}}$ significance requirement, the jet resolution parametrization used for jet energy smearing, and the $t\bar{t}$ background subtraction.

The uncertainty in the combined 2015 + 2016 integrated luminosity is 2.1%. It is derived, following a methodology similar to that detailed in Ref. [89], from a calibration of the luminosity scale using x-y beam-separation scans performed in August 2015 and May 2016.

The impact of the main systematic uncertainties on the total background predictions in the SRs of the 1τ and 2τ channels is summarized in Table IX. These uncertainties are shown after the background fit, assuming that no signal is present in the CRs. In both channels, generator modeling uncertainties for the W + jets and $t\bar{t}$ backgrounds are the largest sources of systematic uncertainty. Other dominant uncertainties are jet energy calibration and τ-lepton identification, which contributes more in the 2τ channel. Uncertainties in the b-tagging efficiency and $E_{\text{T}}^{\text{miss}}$ calibration have little impact on background predictions, and those affecting electrons and muons are negligible.

VIII. RESULTS

Kinematic distributions for the SRs of the 1τ and 2τ channels are shown in Figs. 7 and 8, respectively. In these plots, all selection criteria defining the respective SRs are applied, except for the one on the variable which is displayed. Data and fitted background predictions are compared, and signal predictions from several benchmark models are overlaid. Variables providing the most

TABLE IX. Dominant systematic uncertainties in the total background predictions, for the signal regions of the 1τ (top) and 2τ (bottom) channels after the normalization fit in the control regions. The total systematic uncertainty accounts for other minor contributions not listed in this table. Due to nontrivial correlations between the various sources in the combined fit, the total uncertainty is not identical to the sum in quadrature of the individual components.

Source of uncertainty	1τ compressed SR	1τ medium-mass SR
Top generator modeling	6%	11%
$V+$jets generator modeling	7%	5%
Jet energy scale and resolution	7%	7%
τ-lepton energy scale	<1%	2.9%
τ-lepton identification	1.5%	3.3%
PDFs	1.9%	13%
Limited simulation sample size	1.8%	6%
Background normalization uncertainty	12%	11%
Total	10%	19%

Source of uncertainty	2τ compressed SR	2τ high-mass SR	2τ GMSB SR
Top generator modeling	31%	18%	14%
$V+$jets generator modeling	7%	15%	21%
Jet energy scale and resolution	15%	9%	5%
τ-lepton energy scale	4%	6%	1.7%
τ-lepton identification	5%	10%	9%
PDFs	2.0%	4%	10%
Limited simulation sample size	10%	8%	21%
Background normalization uncertainty	13%	13%	13%
Total	35%	30%	38%

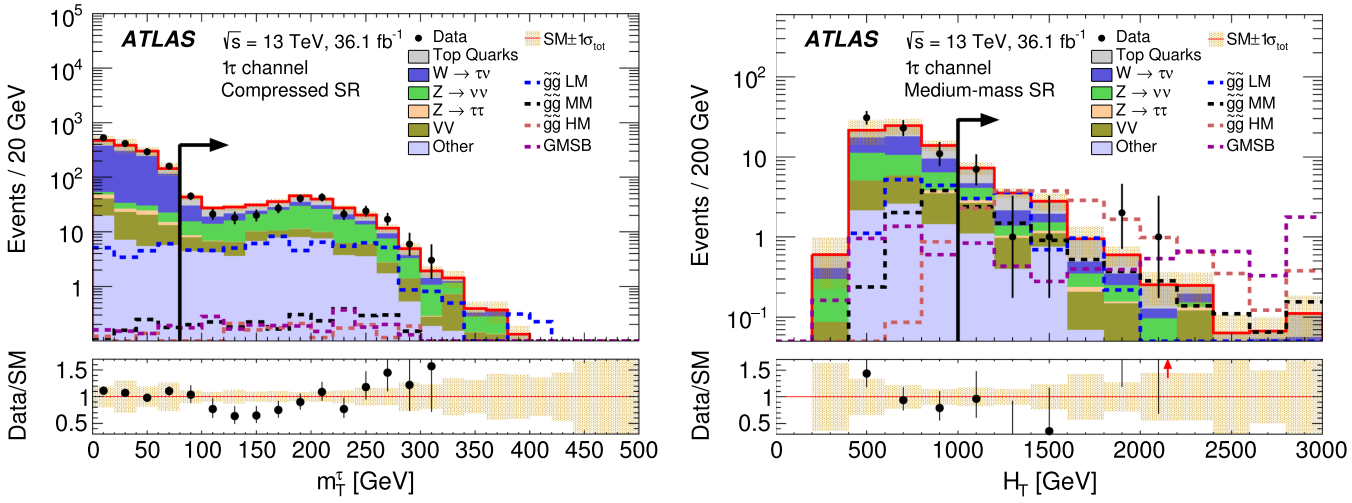

(a) (b)

FIG. 7. Distributions of kinematic variables in extended SR selections of the 1τ channel after the fit: (a) τ-lepton transverse mass m_{T}^{τ} in the compressed SR without the $m_{\mathrm{T}}^{\tau} > 80$ GeV requirement and (b) scalar sum of τ-lepton and jet transverse momenta H_{T} in the medium-mass SR without the $H_{\mathrm{T}} > 1000$ GeV requirement. The contribution labeled as "Other" includes multijet events and the $V+$jets processes not explicitly listed in the legend. The last bin of each distribution includes overflow events. The total uncertainty in the background prediction is shown as a shaded band. Arrows in the Data/SM ratio indicate bins where the entry is outside the plotted range. The signal region is indicated by the arrow in the upper pane. Signal predictions are overlaid for several benchmark models. For the simplified model, LM, MM and HM refer to low, medium, and high mass-splitting scenarios, with $(m_{\tilde{g}}, m_{\tilde{\chi}_1^0})$ set to (1065,825) GeV, (1625,905) GeV, and (1705,345) GeV, respectively. The GMSB benchmark model corresponds to $\Lambda = 120$ TeV and $\tan\beta = 40$.

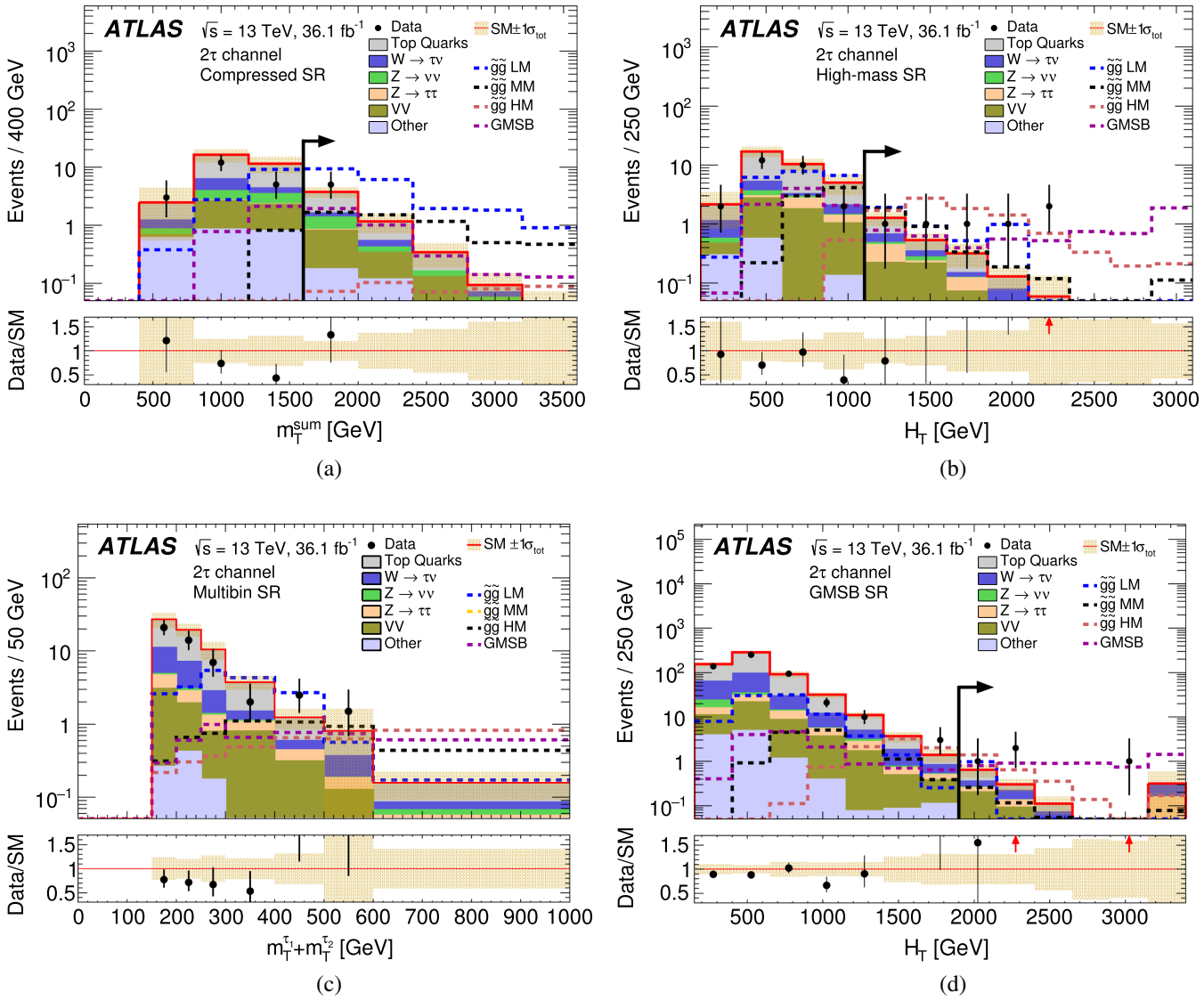

FIG. 8. Distributions of kinematic variables in extended SR selections of the 2τ channel after the fit: (a) sum of transverse masses of τ-leptons and jets $m_{\mathrm{T}}^{\mathrm{sum}}$ in the compressed SR without the $m_{\mathrm{T}}^{\mathrm{sum}} > 1600$ GeV requirement, (b) scalar sum of transverse momenta of τ-leptons and jets H_{T} in the high-mass SR without the $H_{\mathrm{T}} > 1100$ GeV requirement, (c) sum of transverse masses of τ-leptons $m_{\mathrm{T}}^{\tau_1} + m_{\mathrm{T}}^{\tau_2}$ in the multibin SR, and (d) H_{T} in the GMSB SR without the $H_{\mathrm{T}} > 1900$ GeV requirement. The contribution labeled as "Other" includes multijet events and the $V+$jets processes not explicitly listed in the legend. The last bin of each distribution includes overflow events. The total uncertainty in the background prediction is shown as a shaded band. Arrows in the Data/SM ratio indicate bins where the entry is outside the plotted range. The signal region is indicated by the arrow in the upper pane. Signal predictions are overlaid for several benchmark models. For the simplified model, LM, MM, and HM refer to low, medium, and high mass-splitting scenarios, with $(m_{\tilde{g}}, m_{\tilde{\chi}_1^0})$ set to (1065,825) GeV, (1625,905) GeV, and (1705,345) GeV, respectively. The GMSB benchmark model corresponds to $\Lambda = 120$ TeV and $\tan\beta = 40$.

discrimination between signal and background are displayed. The $m_{\mathrm{T}}^{\tau_1} + m_{\mathrm{T}}^{\tau_2}$ distribution which is used for the multibin SR of the 2τ channel is also shown.

Good agreement between data and background expectation is observed. A small discrepancy is observed for $m_{\mathrm{T}}^{\tau} < 200$ GeV in the 1τ compressed SR [cf. Fig. 7(a)]. This region has been studied in detail and no particular problem has been identified. Given that the deviation is only observed in a restricted region and it is below two standard deviations in all bins, no significant impact on the result is expected.

The numbers of observed events and expected background events in the SRs of the 1τ and 2τ channels are reported in Tables X and XI, respectively. In the high-mass and GMSB SRs of the 2τ channel that both require high H_{T}, a small excess of data with a significance of below 2 standard deviations is observed. Apart from that, no significant deviation of data from the SM prediction is

TABLE X. Number of observed events and predicted background yields in the two signal regions of the 1τ channel. The background prediction is scaled using normalization factors derived in the control regions. The numbers in brackets give the background prediction before application of the fitted normalization factors. All systematic and statistical uncertainties are included in the quoted uncertainties. The bottom part of the table shows the observed and expected model-independent upper limits at 95% C.L. on the number of signal events S^{95}_{obs} and S^{95}_{exp}, respectively, the corresponding observed upper limit on the visible cross section $\langle\sigma_{\mathrm{vis}}\rangle^{95}_{\mathrm{obs}}$, the confidence level observed for the background-only hypothesis $\mathrm{CL_b}$, the p_0 value, and corresponding significance Z. If the number of observed events is smaller than the expected background yield, the p_0 value is set to 0.5, corresponding to a significance of 0.0 standard deviations.

1τ channel	Compressed SR		Medium-mass SR	
Data		286		12
Total background	[290]	320 ± 32	[15.2]	15.9 ± 3.0
Top quarks	[66]	77 ± 21	[5.2]	5.8 ± 1.6
$W(\tau\nu) + \text{jets}$	[57]	51 ± 18	[2.4]	2.2 ± 1.7
$Z(\nu\nu) + \text{jets}$	[77]	110 ± 24	[1.5]	2.2 ± 0.5
Other $V + \text{jets}$	[52]	45 ± 10	[1.9]	1.7 ± 0.4
Diboson	[28]	28 ± 5	[3.0]	3.0 ± 0.6
Multijet	[10.0]	9.2 ± 1.2	[1.24]	1.14 ± 0.14
S^{95}_{obs} (S^{95}_{exp})		49.5 ($64.3^{+24.1}_{-14.9}$)		7.7 ($10.0^{+4.3}_{-2.7}$)
$\langle\sigma_{\mathrm{vis}}\rangle^{95}_{\mathrm{obs}}$[fb]		1.37		0.21
$\mathrm{CL_b}$		0.18		0.24
p_0(Z)		0.5 (0.0)		0.5 (0.0)

observed in any of the five single-bin SRs and the seven bins of the multibin SR. Upper limits are set at the 95% confidence level (C.L.) on the number of signal events, or equivalently, on the signal cross section.

The one-sided profile-likelihood-ratio test statistic is used to assess the probability that the observed data is compatible with the background-only and signal-plus-background hypotheses. Systematic uncertainties are included in the likelihood function as nuisance parameters with Gaussian probability densities. Following the standards used for LHC analyses, p values are computed according to the $\mathrm{CL_s}$ prescription [90] using HistFitter [82].

Model-independent upper limits on the event yields are calculated for each SR except the multibin SR, assuming no signal contribution in the CRs. No such interpretation can be made for the multibin SR, as the relative signal contribution in each bin of the $m_{\mathrm{T}}^{\tau_1} + m_{\mathrm{T}}^{\tau_2}$ distribution is model dependent. The results are derived using profile-likelihood-ratio distributions obtained from pseudoexperiments. Upper limits on signal yields are converted into limits on the visible cross section (σ_{vis}) of BSM processes by dividing by the integrated luminosity of the data. The visible cross section is defined as the product of production cross section, acceptance, and selection efficiency. Results are summarized at the bottom of Tables X and XI. The observed upper limits on the visible cross section range from 0.18 fb for the compressed SR of the 2τ channel to 1.37 fb for the compressed SR of the 1τ channel.

TABLE XI. Number of observed events and predicted background yields in the three signal regions of the 2τ channel. The background prediction is scaled using normalization factors derived in the control regions. The numbers in brackets give the background prediction before application of the fitted normalization factors. All systematic and statistical uncertainties are included in the quoted uncertainties. The bottom part of the table shows the observed and expected model-independent upper limits at 95% C.L. on the number of signal events S^{95}_{obs} and S^{95}_{exp}, respectively, the corresponding observed upper limit on the visible cross section $\langle\sigma_{\mathrm{vis}}\rangle^{95}_{\mathrm{obs}}$, the confidence level observed for the background-only hypothesis $\mathrm{CL_b}$, the p_0 value, and corresponding significance (Z). If the number of observed events is smaller than the expected background yield, the p_0 value is set to 0.5, corresponding to a significance of 0.0 standard deviations.

2τ channel	Compressed SR		High-mass SR		GMSB SR	
Data		5		6		4
Total background	[4.7]	5.4 ± 1.9	[2.3]	2.3 ± 0.7	[1.5]	1.4 ± 0.5
Top quarks	[2.3]	2.9 ± 1.7	[0.9]	1.0 ± 0.5	[0.34]	0.39 ± 0.23
$W(\tau\nu) + \text{jets}$	[0.5]	$0.4^{+0.5}_{-0.4}$	[0.4]	0.4 ± 0.4	[0.4]	0.4 ± 0.4
$Z(\tau\tau) + \text{jets}$	[0.035]	0.030 ± 0.011	[0.37]	0.32 ± 0.11	[0.33]	0.28 ± 0.10
$Z(\nu\nu) + \text{jets}$	[0.47]	0.67 ± 0.35	[0.065]	0.093 ± 0.028	[0.008]	0.011 ± 0.007
Other $V + \text{jets}$	[0.32]	0.30 ± 0.08	[0.019]	0.015 ± 0.012	[< 0.01]	< 0.01
Diboson	[1.06]	1.05 ± 0.25	[0.56]	0.56 ± 0.15	[0.29]	0.29 ± 0.08
Multijet	[0.0261]	0.0241 ± 0.0031	[0.0131]	0.0121 ± 0.0015	[0.065]	0.060 ± 0.008
S^{95}_{obs} (S^{95}_{exp})		6.7 ($6.7^{+2.8}_{-1.5}$)		9.0 ($5.0^{+1.9}_{-1.3}$)		7.3 ($4.4^{+1.5}_{-0.9}$)
$\langle\sigma_{\mathrm{vis}}\rangle^{95}_{\mathrm{obs}}$[fb]		0.18		0.25		0.20
$\mathrm{CL_b}$		0.50		0.96		0.95
p_0(Z)		0.5 (0.0)		0.03 (1.83)		0.05 (1.68)

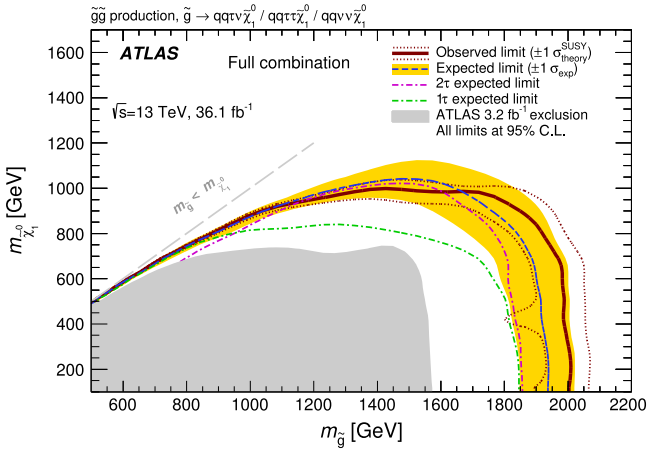

FIG. 9. Exclusion contours at the 95% confidence level as a function of the LSP mass $m_{\tilde{\chi}_1^0}$ and gluino mass $m_{\tilde{g}}$ for the simplified model of gluino pair production. The solid line and the dashed line correspond to the observed and median expected limits, respectively, for the combination of the 1τ and 2τ channels. The band shows the one-standard-deviation spread of expected limits around the median. The effect of the signal cross-section uncertainty on the observed limits is shown as dotted lines. The inward fluctuation of the -1σ line originates from the method employed to perform the combination. The previous ATLAS result [19] obtained with 3.2 fb^{-1} of 13 TeV data is shown as the filled area in the bottom left.

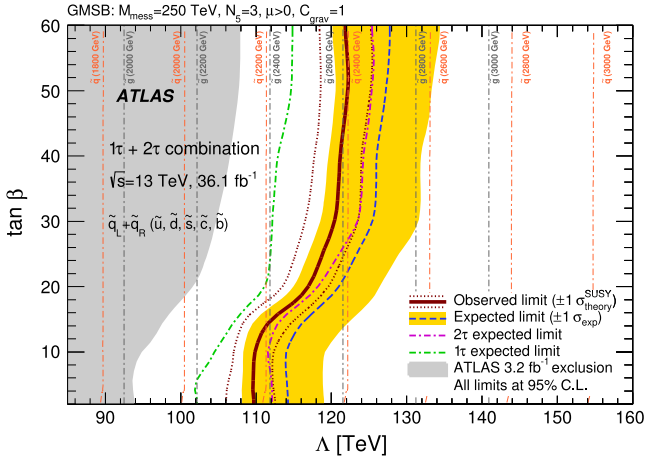

FIG. 10. Exclusion contours at the 95% confidence level as a function of $\tan\beta$ and the SUSY-breaking mass scale Λ for the gauge-mediated supersymmetry-breaking model. The solid line and the dashed line correspond to the observed and median expected limits, respectively, for the combination of the 1τ and 2τ channels. The band shows the one-standard-deviation spread of expected limits around the median. The effect of the signal cross-section uncertainty on the observed limits is shown as dotted lines. The gray and orange dash-dotted lines indicate the masses of gluinos and mass-degenerate squarks, respectively. The previous ATLAS result [19] obtained with 3.2 fb^{-1} of 13 TeV data is shown as the filled area on the left.

Limits are also set for the two SUSY models discussed in Sec. I. Exclusion contours at the 95% C.L. are derived in the $(m_{\tilde{g}}, m_{\tilde{\chi}_1^0})$ parameter space for the simplified model and in the $(\Lambda, \tan\beta)$ parameter space for the GMSB model. In the case of model-dependent interpretations, the signal contribution in the control regions is included in the calculation of upper limits, and asymptotic properties of test-statistic distributions are used [91]. Results are shown in Figs. 9 and 10. The solid line and the dashed line correspond to the observed and median expected limits, respectively. The band shows the one-standard-deviation spread of the expected limits around the median, which originates from statistical and systematic uncertainties in the background and signal. The theoretical uncertainty in the signal cross section is not included in the band. Its effect on the observed limits is shown separately as dotted lines. For both SUSY models, the exclusion limits obtained with 36.1 fb^{-1} of collision data at $\sqrt{s} = 13$ TeV significantly improve upon the previous ATLAS results [19] established with 3.2 fb^{-1} of 13 TeV data. Besides the increase in the integrated luminosity, the results benefit from an improved analysis and statistical treatment. The 1τ and 2τ channels are now statistically combined in a global fit, while in the previous analysis, only the SR with the lowest expected CL_s value was considered for the simplified model, and only the 2τ GMSB SR was used for the GMSB interpretation. In addition, the multibin SR of the 2τ channel provides increased sensitivity to gluino pair production over a large region of the parameter space.

Expected limits in the model parameter space are shown for each channel, to illustrate their complementarity and the gain in sensitivity achieved with their combination. The green dash-dotted line corresponds to a fit that includes all CRs and the two SRs of the 1τ channel. For the 2τ channel, in the case of the simplified model, the magenta dash-dotted line corresponds to the best expected exclusion from fits that include either the 2τ multibin SR or the combination of the 2τ compressed and high-mass SRs. In the GMSB model, the 2τ combination is based on the 2τ GMSB and compressed SRs. In the simplified model, the 1τ and 2τ channels have similar sensitivity at high gluino and low LSP masses. For high LSP masses, the combination is dominated by the 2τ channel, while in the region with a low mass difference between the gluino and the LSP, the 1τ channel drives the exclusion. In the GMSB interpretation, the more stringent limits at high values of $\tan\beta$ are explained by the nature of the NLSP, which is the lightest τ-slepton in this region. For lower values of $\tan\beta$, the $\tilde{\tau}_1$ is nearly mass-degenerate with $\tilde{e}_R$ and $\tilde{\mu}_R$, leading to fewer τ-leptons in squark and gluino decays, and reduced sensitivity of the 2τ GMSB SR. The weaker exclusion at low $\tan\beta$ is mitigated by the SRs from the 1τ channel and the compressed SR of the 2τ channel. For high Λ, the sensitivity is limited by the strong-production cross section.

While the analysis is mainly sensitive to squark and gluino production, the total GMSB production cross section for high Λ is dominated by electroweak production modes.

IX. CONCLUSION

A search for squarks and gluinos in events with jets, hadronically decaying τ-leptons, and missing transverse momentum is performed using pp collision data at $\sqrt{s} = 13$ TeV recorded by the ATLAS detector at the LHC in 2015 and 2016, corresponding to an integrated luminosity of 36.1 fb^{-1}. Two channels with exactly one or at least two τ-leptons are considered, and their results are statistically combined. The observed data are consistent with background expectations from the Standard Model. Upper limits are set at 95% confidence level on the number of events that could be produced by processes beyond the Standard Model. Results are also interpreted in the framework of a simplified model of gluino pairs decaying into τ-leptons via τ-sleptons, and a minimal model of gauge-mediated supersymmetry breaking with the lighter τ-slepton as the NLSP at large $\tan\beta$. At 95% C.L. in the simplified model, gluino masses up to 2000 GeV are excluded for low LSP masses, and LSP masses up to 1000 GeV are excluded for gluino masses around 1400 GeV. In the GMSB model, values of the SUSY-breaking scale Λ below 110 TeV are excluded at 95% C.L. for all values of $\tan\beta$ in the range $2 \leq \tan\beta \leq 60$, while a stronger limit of 120 TeV is achieved for $\tan\beta > 30$.

ACKNOWLEDGMENTS

We thank CERN for the very successful operation of the LHC, as well as the support staff from our institutions without whom ATLAS could not be operated efficiently. We acknowledge the support of ANPCyT, Argentina; YerPhI, Armenia; ARC, Australia; BMWFW and FWF, Austria; ANAS, Azerbaijan; SSTC, Belarus; CNPq and FAPESP, Brazil; NSERC, NRC and CFI, Canada; CERN; CONICYT, Chile; CAS, MOST and NSFC, China; COLCIENCIAS, Colombia; MSMT CR, MPO CR and VSC CR, Czech Republic; DNRF and DNSRC, Denmark; IN2P3-CNRS, CEA-DRF/IRFU, France; SRNSFG, Georgia; BMBF, HGF, and MPG, Germany; GSRT, Greece; RGC, Hong Kong SAR, China; ISF, I-CORE and Benoziyo Center, Israel; INFN, Italy; MEXT and JSPS, Japan; CNRST, Morocco; NWO, Netherlands; RCN, Norway; MNiSW and NCN, Poland; FCT, Portugal; MNE/IFA, Romania; MES of Russia and NRC KI, Russian Federation; JINR; MESTD, Serbia; MSSR, Slovakia; ARRS and MIZŠ, Slovenia; DST/NRF, South Africa; MINECO, Spain; SRC and Wallenberg Foundation, Sweden; SERI, SNSF and Cantons of Bern and Geneva, Switzerland; MOST, Taiwan; TAEK, Turkey; STFC, United Kingdom; DOE and NSF, United States of America. In addition, individual groups and members have received support from BCKDF, the Canada Council, CANARIE, CRC, Compute Canada, FQRNT, and the Ontario Innovation Trust, Canada; EPLANET, ERC, ERDF, FP7, Horizon 2020 and Marie Skłodowska-Curie Actions, European Union; Investissements d'Avenir Labex and Idex, ANR, Région Auvergne and Fondation Partager le Savoir, France; DFG and AvH Foundation, Germany; Herakleitos, Thales and Aristeia programmes co-financed by EU-ESF and the Greek NSRF; BSF, GIF and Minerva, Israel; BRF, Norway; CERCA Programme Generalitat de Catalunya, Generalitat Valenciana, Spain; the Royal Society and Leverhulme Trust, United Kingdom. The crucial computing support from all WLCG partners is acknowledged gratefully, in particular from CERN, the ATLAS Tier-1 facilities at TRIUMF (Canada), NDGF (Denmark, Norway, Sweden), CC-IN2P3 (France), KIT/GridKA (Germany), INFN-CNAF (Italy), NL-T1 (Netherlands), PIC (Spain), ASGC (Taiwan), RAL (UK) and BNL (USA), the Tier-2 facilities worldwide and large non-WLCG resource providers. Major contributors of computing resources are listed in Ref. [92].

[1] Yu. A. Golfand and E. P. Likhtman, Extension of the algebra of Poincare group generators and violation of p invariance, Pis'ma Zh. Eksp. Teor. Fiz. **13**, 452 (1971) [JETP Lett. **13**, 323 (1971)], http://www.jetpletters.ac.ru/ps/1584/article_24309.pdf.

[2] D. V. Volkov and V. P. Akulov, Is the neutrino a goldstone particle?, Phys. Lett. **46B**, 109 (1973).

[3] J. Wess and B. Zumino, Supergauge transformations in four dimensions, Nucl. Phys. **B70**, 39 (1974).

[4] J. Wess and B. Zumino, Supergauge invariant extension of quantum electrodynamics, Nucl. Phys. **B78**, 1 (1974).

[5] S. Ferrara and B. Zumino, Supergauge invariant Yang-Mills theories, Nucl. Phys. **B79**, 413 (1974).

[6] A. Salam and J. A. Strathdee, Supersymmetry and non-Abelian gauges, Phys. Lett. **51B**, 353 (1974).

[7] G. R. Farrar and P. Fayet, Phenomenology of the production, decay, and detection of new hadronic states associated with supersymmetry, Phys. Lett. **76B**, 575 (1978).

[8] D. Albornoz Vásquez, G. Bélanger, and C. Boehm, Revisiting light neutralino scenarios in the MSSM, Phys. Rev. D **84**, 095015 (2011).

[9] E. Bagnaschi *et al.*, Likelihood analysis of the pMSSM11 in light of LHC 13 TeV data, Eur. Phys. J. C **78**, 256 (2018).

[10] P. Bechtle *et al.*, Killing the cMSSM softly, Eur. Phys. J. C **76**, 96 (2016).

[11] J. Alwall, M.-P. Le, M. Lisanti, and J. G. Wacker, Searching for directly decaying gluinos at the Tevatron, Phys. Lett. B **666**, 34 (2008).
[12] J. Alwall, P. C. Schuster, and N. Toro, Simplified models for a first characterization of new physics at the LHC, Phys. Rev. D **79**, 075020 (2009).
[13] D. Alves *et al.*, Simplified models for LHC new physics searches, J. Phys. G **39**, 105005 (2012).
[14] M. Dine and W. Fischler, A phenomenological model of particle physics based on supersymmetry, Phys. Lett. **110B**, 227 (1982).
[15] L. Alvarez-Gaumé, M. Claudson, and M. B. Wise, Low-energy supersymmetry, Nucl. Phys. **B207**, 96 (1982).
[16] C. R. Nappi and B. A. Ovrut, Supersymmetric extension of the $SU(3) \times SU(2) \times U(1)$ model, Phys. Lett. **113B**, 175 (1982).
[17] ATLAS Collaboration, Search for supersymmetry in events with large missing transverse momentum, jets, and at least one tau lepton in 7 TeV proton-proton collision data with the ATLAS detector, Eur. Phys. J. C **72**, 2215 (2012).
[18] ATLAS Collaboration, Search for supersymmetry in events with large missing transverse momentum, jets, and at least one tau lepton in 20 fb^{-1} of $\sqrt{s} = 8$ TeV proton-proton collision data with the ATLAS detector, J. High Energy Phys. 09 (2014) 103.
[19] ATLAS Collaboration, Search for squarks and gluinos in events with hadronically decaying tau leptons, jets and missing transverse momentum in proton-proton collisions at $\sqrt{s} = 13$ TeV recorded with the ATLAS detector, Eur. Phys. J. C **76**, 683 (2016).
[20] CMS Collaboration, Search for physics beyond the standard model in events with τ leptons, jets, and large transverse momentum imbalance in pp collisions at $\sqrt{s} = 7$ TeV, Eur. Phys. J. C **73**, 2493 (2013).
[21] M. Buican, P. Meade, N. Seiberg, and D. Shih, Exploring general gauge mediation, J. High Energy Phys. 03 (2009) 016.
[22] J. Barnard, B. Farmer, T. Gherghetta, and M. White, Natural Gauge Mediation with a Bino Next-to-Lightest Supersymmetric Particle at the LHC, Phys. Rev. Lett. **109**, 241801 (2012).
[23] A. Djouadi *et al.*, The minimal supersymmetric standard model: Group summary report, arXiv:hep-ph/9901246.
[24] C. F. Berger, J. S. Gainer, J. L. Hewett, and T. G. Rizzo, Supersymmetry without prejudice, J. High Energy Phys. 02 (2009) 023.
[25] ATLAS Collaboration, The ATLAS experiment at the CERN Large Hadron Collider, J. Instrum. **3**, S08003 (2008).
[26] ATLAS Collaboration, ATLAS insertable B-layer technical design report, ATLAS-TDR-19, ATLAS insertable B-layer technical design report addendum, Report No. ATLAS-TDR-19-ADD-1, 2012, https://cds.cern.ch/record/1451888; 2010, https://cds.cern.ch/record/1291633.
[27] ATLAS Collaboration, Performance of the ATLAS trigger system in 2015, Eur. Phys. J. C **77**, 317 (2017).
[28] T. Sjöstrand, S. Ask, J. R. Christiansen, R. Corke, N. Desai, P. Ilten, S. Mrenna, S. Prestel, C. O. Rasmussen, and P. Z. Skands, An introduction to PYTHIA 8.2, Comput. Phys. Commun. **191**, 159 (2015).
[29] ATLAS Collaboration, Summary of ATLAS PYTHIA 8 tunes, Report No. ATL-PHYS-PUB-2012-003, 2012, https://cds.cern.ch/record/1474107.
[30] A. D. Martin, W. J. Stirling, R. S. Thorne, and G. Watt, Parton distributions for the LHC, Eur. Phys. J. C **63**, 189 (2009).
[31] ATLAS Collaboration, The ATLAS simulation infrastructure, Eur. Phys. J. C **70**, 823 (2010).
[32] S. Agostinelli *et al.*, GEANT4: A simulation toolkit, Nucl. Instrum. Methods Phys. Res., Sect. A **506**, 250 (2003).
[33] ATLAS Collaboration, Performance of the fast ATLAS tracking simulation (FATRAS) and the ATLAS fast calorimeter simulation (FastCaloSim) with single particles, Report No. ATL-SOFT-PUB-2014-01, 2014, https://cds.cern.ch/record/1669341.
[34] T. Gleisberg, S. Höche, F. Krauss, M. Schönherr, S. Schumann, F. Siegert, and J. Winter, Event generation with SHERPA 1.1, J. High Energy Phys. 02 (2009) 007.
[35] F. Cascioli, P. Maierhöfer, and S. Pozzorini, Scattering Amplitudes with Open Loops, Phys. Rev. Lett. **108**, 111601 (2012).
[36] T. Gleisberg and S. Höche, COMIX, a new matrix element generator, J. High Energy Phys. 12 (2008) 039.
[37] S. Schumann and F. Krauss, A Parton shower algorithm based on Catani-Seymour dipole factorisation, J. High Energy Phys. 03 (2008) 038.
[38] S. Höche, F. Krauss, M. Schönherr, and F. Siegert, QCD matrix elements + parton showers: The NLO case, J. High Energy Phys. 04 (2013) 027.
[39] R. D. Ball *et al.*, Parton distributions for the LHC Run II, J. High Energy Phys. 04 (2015) 040.
[40] S. Catani, L. Cieri, G. Ferrera, D. de Florian, and M. Grazzini, Vector Boson Production at Hadron Colliders: A Fully Exclusive QCD Calculation at Next-to-Next-to-Leading Order, Phys. Rev. Lett. **103**, 082001 (2009).
[41] C. Anastasiou, L. J. Dixon, K. Melnikov, and F. Petriello, High-precision QCD at hadron colliders: Electroweak gauge boson rapidity distributions at next-to-next-to leading order, Phys. Rev. D **69**, 094008 (2004).
[42] J. Alwall, R. Frederix, S. Frixione, V. Hirschi, F. Maltoni, O. Mattelaer, H.-S. Shao, T. Stelzer, P. Torrielli, and M. Zaro, The automated computation of tree-level and next-to-leading order differential cross sections, and their matching to parton shower simulations, J. High Energy Phys. 07 (2014) 079.
[43] ATLAS Collaboration, ATLAS PYTHIA 8 tunes to 7 TeV data, Report No. ATL-PHYS-PUB-2014-021, 2014, https://cds.cern.ch/record/1966419.
[44] R. D. Ball, V. Bertone, S. Carrazza, L. Del Debbio, S. Forte, A. Guffanti, N. P. Hartland, and J. Rojo, Parton distributions with QED corrections, Nucl. Phys. **B877**, 290 (2013).
[45] S. Alioli, P. Nason, C. Oleari, and E. Re, A general framework for implementing NLO calculations in shower Monte Carlo programs: The POWHEG BOX, J. High Energy Phys. 06 (2010) 043.
[46] H.-L. Lai, M. Guzzi, J. Huston, Z. Li, P. M. Nadolsky, J. Pumplin, and C.-P. Yuan, New parton distributions for collider physics, Phys. Rev. D **82**, 074024 (2010).

[47] T. Sjöstrand, S. Mrenna, and P. Z. Skands, PYTHIA 6.4 physics and manual, J. High Energy Phys. 05 (2006) 026.
[48] J. Pumplin, D. R. Stump, J. Huston, H.-L. Lai, P. Nadolsky, and W.-K. Tung, New generation of Parton distributions with uncertainties from global QCD analysis, J. High Energy Phys. 07 (2002) 012.
[49] P. Z. Skands, Tuning Monte Carlo generators: The Perugia tunes, Phys. Rev. D **82**, 074018 (2010).
[50] M. Czakon and A. Mitov, TOP++: A program for the calculation of the top-pair cross-section at hadron colliders, Comput. Phys. Commun. **185**, 2930 (2014).
[51] M. Bähr *et al.*, HERWIG++ physics and manual, Eur. Phys. J. C **58**, 639 (2008).
[52] S. Gieseke, C. Röhr, and A. Siódmok, Colour reconnections in HERWIG++, Eur. Phys. J. C **72**, 2225 (2012).
[53] W. Porod and F. Staub, SPHENO 3.1: Extensions including flavour, *CP*-phases and models beyond the MSSM, Comput. Phys. Commun. **183**, 2458 (2012).
[54] G. Marchesini and B. R. Webber, Simulation of QCD jets including soft gluon interference, Nucl. Phys. **B238**, 1 (1984).
[55] G. Marchesini and B. R. Webber, Monte Carlo simulation of general hard processes with coherent QCD radiation, Nucl. Phys. **B310**, 461 (1988).
[56] S. Gieseke, P. Stephens, and B. Webber, New formalism for QCD parton showers, J. High Energy Phys. 12 (2003) 045.
[57] W. Beenakker, R. Höpker, M. Spira, and P. M. Zerwas, Squark and gluino production at hadron colliders, Nucl. Phys. **B492**, 51 (1997).
[58] A. Kulesza and L. Motyka, Threshold Resummation for Squark-Antisquark and Gluino-Pair Production at the LHC, Phys. Rev. Lett. **102**, 111802 (2009).
[59] A. Kulesza and L. Motyka, Soft gluon resummation for the production of gluino-gluino and squark-antisquark pairs at the LHC, Phys. Rev. D **80**, 095004 (2009).
[60] W. Beenakker, S. Brensing, M. Krämer, A. Kulesza, E. Laenen, and I. Niessen, Soft-gluon resummation for squark and gluino hadroproduction, J. High Energy Phys. 12 (2009) 041.
[61] W. Beenakker, S. Brensing, M. Krämer, A. Kulesza, E. Laenen, L. Motyka, and I. Niessen, Squark and gluino hadroproduction, Int. J. Mod. Phys. A **26**, 2637 (2011).
[62] C. Borschensky, M. Krämer, A. Kulesza, M. Mangano, S. Padhi, T. Plehn, and X. Portell, Squark and gluino production cross sections in pp collisions at $\sqrt{s} = 13$, 14, 33 and 100 TeV, Eur. Phys. J. C **74**, 3174 (2014).
[63] ATLAS Collaboration, Vertex reconstruction performance of the ATLAS detector at $\sqrt{s} = 13$ TeV, Report No. ATL-PHYS-PUB-2015-026, 2015, https://cds.cern.ch/record/2037717.
[64] M. Cacciari, G. P. Salam, and G. Soyez, The anti-k_t jet clustering algorithm, J. High Energy Phys. 04 (2008) 063.
[65] M. Cacciari, G. P. Salam, and G. Soyez, FastJet user manual, Eur. Phys. J. C **72**, 1896 (2012).
[66] ATLAS Collaboration, Topological cell clustering in the ATLAS calorimeters and its performance in LHC Run 1, Eur. Phys. J. C **77**, 490 (2017).
[67] ATLAS Collaboration, Jet global sequential corrections with the ATLAS detector in proton-proton collisions at $\sqrt{s} = 8$ TeV, Report No. ATLAS-CONF-2015-002, 2015, https://cds.cern.ch/record/2001682.
[68] ATLAS Collaboration, Jet calibration and systematic uncertainties for jets reconstructed in the ATLAS detector at $\sqrt{s} = 13$ TeV, Report No. ATL-PHYS-PUB-2015-015, 2015, https://cds.cern.ch/record/2037613.
[69] ATLAS Collaboration, Performance of pile-up mitigation techniques for jets in pp collisions at $\sqrt{s} = 8$ TeV using the ATLAS detector, Eur. Phys. J. C **76**, 581 (2016).
[70] ATLAS Collaboration, Selection of jets produced in 13 TeV proton-proton collisions with the ATLAS detector, Report No. ATLAS-CONF-2015-029, 2015, https://cds.cern.ch/record/2037702.
[71] ATLAS Collaboration, Expected performance of the ATLAS *b*-tagging algorithms in Run-2, Report No. ATL-PHYS-PUB-2015-022, 2015, https://cds.cern.ch/record/2037697.
[72] ATLAS Collaboration, Commissioning of the ATLAS b-tagging algorithms using $t\bar{t}$ events in early Run 2 data, Report No. ATL-PHYS-PUB-2015-039, 2015, https://cds.cern.ch/record/2047871.
[73] ATLAS Collaboration, Muon reconstruction performance of the ATLAS detector in proton-proton collision data at $\sqrt{s} = 13$ TeV, Eur. Phys. J. C **76**, 292 (2016).
[74] ATLAS Collaboration, Electron and photon energy calibration with the ATLAS detector using LHC Run 1 data, Eur. Phys. J. C **74**, 3071 (2014).
[75] ATLAS Collaboration, Electron identification measurements in ATLAS using $\sqrt{s} = 13$ TeV data with 50 ns bunch spacing, Report No. ATL-PHYS-PUB-2015-041, 2015, https://cds.cern.ch/record/2048202.
[76] ATLAS Collaboration, Reconstruction, energy calibration, and identification of hadronically decaying tau leptons in the ATLAS experiment for Run-2 of the LHC, Report No. ATL-PHYS-PUB-2015-045, 2015, http://cdsweb.cern.ch/record/2064383.
[77] ATLAS Collaboration, Jet energy measurement with the ATLAS detector in proton-proton collisions at $\sqrt{s} = 7$ TeV, Eur. Phys. J. C **73**, 2304 (2013).
[78] ATLAS Collaboration, Reconstruction of hadronic decay products of tau leptons with the ATLAS experiment, Eur. Phys. J. C **76**, 295 (2016).
[79] ATLAS Collaboration, Performance of missing transverse momentum reconstruction with the ATLAS detector in the first proton-proton collisions at $\sqrt{s} = 13$ TeV, Report No. ATL-PHYS-PUB-2015-027, 2015, https://cds.cern.ch/record/2037904.
[80] C. G. Lester and D. J. Summers, Measuring masses of semi-invisibly decaying particles pair produced at hadron colliders, Phys. Lett. B **463**, 99 (1999).
[81] C. G. Lester and B. Nachman, Bisection-based asymmetric M_T2 computation: A higher precision calculator than existing symmetric methods, J. High Energy Phys. 03 (2015) 100.
[82] M. Baak, G. J. Besjes, D. Côté, A. Koutsman, J. Lorenz, and D. Short, HISTFITTER software framework for statistical data analysis, Eur. Phys. J. C **75**, 153 (2015).
[83] ATLAS Collaboration, Search for squarks and gluinos with the ATLAS detector in final states with jets and missing transverse momentum using 4.7 fb^{-1} of

$\sqrt{s} = 7$ TeV proton-proton collision data, Phys. Rev. D **87**, 012008 (2013).

[84] ATLAS Collaboration, Jet energy scale measurements and their systematic uncertainties in proton-proton collisions at $\sqrt{s} = 13$ TeV with the ATLAS detector, Phys. Rev. D **96**, 072002 (2017).

[85] ATLAS Collaboration, Jet energy resolution in proton-proton collisions at $\sqrt{s} = 7$ TeV recorded in 2010 with the ATLAS detector, Eur. Phys. J. C **73**, 2306 (2013).

[86] ATLAS Collaboration, Optimisation of the ATLAS b-tagging performance for the 2016 LHC Run, Report No. ATL-PHYS-PUB-2016-012, 2016, https://cds.cern.ch/record/2160731.

[87] ATLAS Collaboration, Measurement of the tau lepton reconstruction and identification performance in the ATLAS experiment using pp collisions at $\sqrt{s} = 13$ TeV, Report No. ATLAS-CONF-2017-029, 2017, https://cds.cern.ch/record/2261772.

[88] ATLAS Collaboration, Expected performance of missing transverse momentum reconstruction for the ATLAS detector at $\sqrt{s} = 13$ TeV, Report No. ATL-PHYS-PUB-2015-023, 2015, https://cds.cern.ch/record/2037700.

[89] ATLAS Collaboration, Luminosity determination in pp collisions at $\sqrt{s} = 8$ TeV using the ATLAS detector at the LHC, Eur. Phys. J. C **76**, 653 (2016).

[90] A. L. Read, Presentation of search results: The CLs technique, J. Phys. G **28**, 2693 (2002).

[91] G. Cowan, K. Cranmer, E. Gross, and O. Vitells, Asymptotic formulae for likelihood-based tests of new physics, Eur. Phys. J. C **71**, 1554 (2011); Erratum **73**, 2501 (2013).

[92] ATLAS Collaboration, ATLAS computing acknowledgements, Report No. ATL-GEN-PUB-2016-002, https://cds.cern.ch/record/2202407.

M. Aaboud,[34d] G. Aad,[99] B. Abbott,[124] O. Abdinov,[13,a] B. Abeloos,[128] D. K. Abhayasinghe,[91] S. H. Abidi,[164] O. S. AbouZeid,[143] N. L. Abraham,[153] H. Abramowicz,[158] H. Abreu,[157] Y. Abulaiti,[6] B. S. Acharya,[64a,64b,b] S. Adachi,[160] L. Adamczyk,[81a] J. Adelman,[119] M. Adersberger,[112] A. Adiguzel,[12c,c] T. Adye,[141] A. A. Affolder,[143] Y. Afik,[157] C. Agheorghiesei,[27c] J. A. Aguilar-Saavedra,[136f,136a] F. Ahmadov,[77,d] G. Aielli,[71a,71b] S. Akatsuka,[83] T. P. A. Åkesson,[94] E. Akilli,[52] A. V. Akimov,[108] G. L. Alberghi,[23b,23a] J. Albert,[173] P. Albicocco,[49] M. J. Alconada Verzini,[86] S. Alderweireldt,[117] M. Aleksa,[35] I. N. Aleksandrov,[77] C. Alexa,[27b] T. Alexopoulos,[10] M. Alhroob,[124] B. Ali,[138] G. Alimonti,[66a] J. Alison,[36] S. P. Alkire,[145] C. Allaire,[128] B. M. M. Allbrooke,[153] B. W. Allen,[127] P. P. Allport,[21] A. Aloisio,[67a,67b] A. Alonso,[39] F. Alonso,[86] C. Alpigiani,[145] A. A. Alshehri,[55] M. I. Alstaty,[99] B. Alvarez Gonzalez,[35] D. Álvarez Piqueras,[171] M. G. Alviggi,[67a,67b] B. T. Amadio,[18] Y. Amaral Coutinho,[78b] L. Ambroz,[131] C. Amelung,[26] D. Amidei,[103] S. P. Amor Dos Santos,[136a,136c] S. Amoroso,[35] C. S. Amrouche,[52] C. Anastopoulos,[146] L. S. Ancu,[52] N. Andari,[21] T. Andeen,[11] C. F. Anders,[59b] J. K. Anders,[20] K. J. Anderson,[36] A. Andreazza,[66a,66b] V. Andrei,[59a] C. R. Anelli,[173] S. Angelidakis,[37] I. Angelozzi,[118] A. Angerami,[38] A. V. Anisenkov,[120b,120a] A. Annovi,[69a] C. Antel,[59a] M. T. Anthony,[146] M. Antonelli,[49] D. J. A. Antrim,[168] F. Anulli,[70a] M. Aoki,[79] L. Aperio Bella,[35] G. Arabidze,[104] Y. Arai,[79] J. P. Araque,[136a] V. Araujo Ferraz,[78b] R. Araujo Pereira,[78b] A. T. H. Arce,[47] R. E. Ardell,[91] F. A. Arduh,[86] J-F. Arguin,[107] S. Argyropoulos,[75] A. J. Armbruster,[35] L. J. Armitage,[90] A Armstrong,[168] O. Arnaez,[164] H. Arnold,[118] M. Arratia,[31] O. Arslan,[24] A. Artamonov,[109,a] G. Artoni,[131] S. Artz,[97] S. Asai,[160] N. Asbah,[44] A. Ashkenazi,[158] E. M. Asimakopoulou,[169] L. Asquith,[153] K. Assamagan,[29] R. Astalos,[28a] R. J. Atkin,[32a] M. Atkinson,[170] N. B. Atlay,[148] K. Augsten,[138] G. Avolio,[35] R. Avramidou,[58a] B. Axen,[18] M. K. Ayoub,[15a] G. Azuelos,[107,e] A. E. Baas,[59a] M. J. Baca,[21] H. Bachacou,[142] K. Bachas,[65a,65b] M. Backes,[131] P. Bagnaia,[70a,70b] M. Bahmani,[82] H. Bahrasemani,[149] A. J. Bailey,[171] J. T. Baines,[141] M. Bajic,[39] C. Bakalis,[10] O. K. Baker,[180] P. J. Bakker,[118] D. Bakshi Gupta,[93] E. M. Baldin,[120b,120a] P. Balek,[177] F. Balli,[142] W. K. Balunas,[133] J. Balz,[97] E. Banas,[82] A. Bandyopadhyay,[24] S. Banerjee,[178,f] A. A. E. Bannoura,[179] L. Barak,[158] W. M. Barbe,[37] E. L. Barberio,[102] D. Barberis,[53b,53a] M. Barbero,[99] T. Barillari,[113] M-S. Barisits,[35] J. Barkeloo,[127] T. Barklow,[150] N. Barlow,[31] R. Barnea,[157] S. L. Barnes,[58c] B. M. Barnett,[141] R. M. Barnett,[18] Z. Barnovska-Blenessy,[58a] A. Baroncelli,[72a] G. Barone,[26] A. J. Barr,[131] L. Barranco Navarro,[171] F. Barreiro,[96] J. Barreiro Guimarães da Costa,[15a] R. Bartoldus,[150] A. E. Barton,[87] P. Bartos,[28a] A. Basalaev,[134] A. Bassalat,[128] R. L. Bates,[55] S. J. Batista,[164] S. Batlamous,[34e] J. R. Batley,[31] M. Battaglia,[143] M. Bauce,[70a,70b] F. Bauer,[142] K. T. Bauer,[168] H. S. Bawa,[150,g] J. B. Beacham,[122] M. D. Beattie,[87] T. Beau,[132] P. H. Beauchemin,[167] P. Bechtle,[24] H. C. Beck,[51] H. P. Beck,[20,h] K. Becker,[50] M. Becker,[97] C. Becot,[44] A. Beddall,[12d] A. J. Beddall,[12a] V. A. Bednyakov,[77] M. Bedognetti,[118] C. P. Bee,[152] T. A. Beermann,[35] M. Begalli,[78b] M. Begel,[29] A. Behera,[152] J. K. Behr,[44] A. S. Bell,[92] G. Bella,[158] L. Bellagamba,[23b] A. Bellerive,[33] M. Bellomo,[157] P. Bellos,[9] K. Belotskiy,[110] N. L. Belyaev,[110] O. Benary,[158,a] D. Benchekroun,[34a] M. Bender,[112] N. Benekos,[10] Y. Benhammou,[158] E. Benhar Noccioli,[180] J. Benitez,[75] D. P. Benjamin,[47] M. Benoit,[52] J. R. Bensinger,[26] S. Bentvelsen,[118] L. Beresford,[131] M. Beretta,[49] D. Berge,[44] E. Bergeaas Kuutmann,[169] N. Berger,[5] L. J. Bergsten,[26] J. Beringer,[18] S. Berlendis,[7] N. R. Bernard,[100] G. Bernardi,[132] C. Bernius,[150]

F. U. Bernlochner,[24] T. Berry,[91] P. Berta,[97] C. Bertella,[15a] G. Bertoli,[43a,43b] I. A. Bertram,[87] G. J. Besjes,[39] O. Bessidskaia Bylund,[43a,43b] M. Bessner,[44] N. Besson,[142] A. Bethani,[98] S. Bethke,[113] A. Betti,[24] A. J. Bevan,[90] J. Beyer,[113] R. M. Bianchi,[135] O. Biebel,[112] D. Biedermann,[19] R. Bielski,[98] K. Bierwagen,[97] N. V. Biesuz,[69a,69b] M. Biglietti,[72a] T. R. V. Billoud,[107] M. Bindi,[51] A. Bingul,[12d] C. Bini,[70a,70b] S. Biondi,[23b,23a] T. Bisanz,[51] J. P. Biswal,[158] C. Bittrich,[46] D. M. Bjergaard,[47] J. E. Black,[150] K. M. Black,[25] R. E. Blair,[6] T. Blazek,[28a] I. Bloch,[44] C. Blocker,[26] A. Blue,[55] U. Blumenschein,[90] Dr. Blunier,[144a] G. J. Bobbink,[118] V. S. Bobrovnikov,[120b,120a] S. S. Bocchetta,[94] A. Bocci,[47] D. Boerner,[179] D. Bogavac,[112] A. G. Bogdanchikov,[120b,120a] C. Bohm,[43a] V. Boisvert,[91] P. Bokan,[169] T. Bold,[81a] A. S. Boldyrev,[111] A. E. Bolz,[59b] M. Bomben,[132] M. Bona,[90] J. S. Bonilla,[127] M. Boonekamp,[142] A. Borisov,[140] G. Borissov,[87] J. Bortfeldt,[35] D. Bortoletto,[131] V. Bortolotto,[71a,61b,61c,71b] D. Boscherini,[23b] M. Bosman,[14] J. D. Bossio Sola,[30] K. Bouaouda,[34a] J. Boudreau,[135] E. V. Bouhova-Thacker,[87] D. Boumediene,[37] C. Bourdarios,[128] S. K. Boutle,[55] A. Boveia,[122] J. Boyd,[35] I. R. Boyko,[77] A. J. Bozson,[91] J. Bracinik,[21] N. Brahimi,[99] A. Brandt,[8] G. Brandt,[179] O. Brandt,[59a] F. Braren,[44] U. Bratzler,[161] B. Brau,[100] J. E. Brau,[127] W. D. Breaden Madden,[55] K. Brendlinger,[44] A. J. Brennan,[102] L. Brenner,[44] R. Brenner,[169] S. Bressler,[177] B. Brickwedde,[97] D. L. Briglin,[21] D. Britton,[55] D. Britzger,[59b] I. Brock,[24] R. Brock,[104] G. Brooijmans,[38] T. Brooks,[91] W. K. Brooks,[144b] E. Brost,[119] J.H Broughton,[21] P. A. Bruckman de Renstrom,[82] D. Bruncko,[28b] A. Bruni,[23b] G. Bruni,[23b] L. S. Bruni,[118] S. Bruno,[71a,71b] B. H. Brunt,[31] M. Bruschi,[23b] N. Bruscino,[135] P. Bryant,[36] L. Bryngemark,[44] T. Buanes,[17] Q. Buat,[35] P. Buchholz,[148] A. G. Buckley,[55] I. A. Budagov,[77] F. Buehrer,[50] M. K. Bugge,[130] O. Bulekov,[110] D. Bullock,[8] T. J. Burch,[119] S. Burdin,[88] C. D. Burgard,[118] A. M. Burger,[5] B. Burghgrave,[119] K. Burka,[82] S. Burke,[141] I. Burmeister,[45] J. T. P. Burr,[131] D. Büscher,[50] V. Büscher,[97] E. Buschmann,[51] P. Bussey,[55] J. M. Butler,[25] C. M. Buttar,[55] J. M. Butterworth,[92] P. Butti,[35] W. Buttinger,[35] A. Buzatu,[155] A. R. Buzykaev,[120b,120a] G. Cabras,[23b,23a] S. Cabrera Urbán,[171] D. Caforio,[138] H. Cai,[170] V. M. M. Cairo,[2] O. Cakir,[4a] N. Calace,[52] P. Calafiura,[18] A. Calandri,[99] G. Calderini,[132] P. Calfayan,[63] G. Callea,[40b,40a] L. P. Caloba,[78b] S. Calvente Lopez,[96] D. Calvet,[37] S. Calvet,[37] T. P. Calvet,[152] M. Calvetti,[69a,69b] R. Camacho Toro,[132] S. Camarda,[35] P. Camarri,[71a,71b] D. Cameron,[130] R. Caminal Armadans,[100] C. Camincher,[35] S. Campana,[35] M. Campanelli,[92] A. Camplani,[39] A. Campoverde,[148] V. Canale,[67a,67b] M. Cano Bret,[58c] J. Cantero,[125] T. Cao,[158] Y. Cao,[170] M. D. M. Capeans Garrido,[35] I. Caprini,[27b] M. Caprini,[27b] M. Capua,[40b,40a] R. M. Carbone,[38] R. Cardarelli,[71a] F. C. Cardillo,[50] I. Carli,[139] T. Carli,[35] G. Carlino,[67a] B. T. Carlson,[135] L. Carminati,[66a,66b] R. M. D. Carney,[43a,43b] S. Caron,[117] E. Carquin,[144b] S. Carrá,[66a,66b] G. D. Carrillo-Montoya,[35] D. Casadei,[32b] M. P. Casado,[14,i] A. F. Casha,[164] M. Casolino,[14] D. W. Casper,[168] R. Castelijn,[118] F. L. Castillo,[171] V. Castillo Gimenez,[171] N. F. Castro,[136a,136e] A. Catinaccio,[35] J. R. Catmore,[130] A. Cattai,[35] J. Caudron,[24] V. Cavaliere,[29] E. Cavallaro,[14] D. Cavalli,[66a] M. Cavalli-Sforza,[14] V. Cavasinni,[69a,69b] E. Celebi,[12b] F. Ceradini,[72a,72b] L. Cerda Alberich,[171] A. S. Cerqueira,[78a] A. Cerri,[153] L. Cerrito,[71a,71b] F. Cerutti,[18] A. Cervelli,[23b,23a] S. A. Cetin,[12b] A. Chafaq,[34a] D Chakraborty,[119] S. K. Chan,[57] W. S. Chan,[118] Y. L. Chan,[61a] J. D. Chapman,[31] D. G. Charlton,[21] C. C. Chau,[33] C. A. Chavez Barajas,[153] S. Che,[122] A. Chegwidden,[104] S. Chekanov,[6] S. V. Chekulaev,[165a] G. A. Chelkov,[77,j] M. A. Chelstowska,[35] C. Chen,[58a] C. H. Chen,[76] H. Chen,[29] J. Chen,[58a] J. Chen,[38] S. Chen,[133] S. J. Chen,[15c] X. Chen,[15b,k] Y. Chen,[80] Y-H. Chen,[44] H. C. Cheng,[103] H. J. Cheng,[15d] A. Cheplakov,[77] E. Cheremushkina,[140] R. Cherkaoui El Moursli,[34e] E. Cheu,[7] K. Cheung,[62] L. Chevalier,[142] V. Chiarella,[49] G. Chiarelli,[69a] G. Chiodini,[65a] A. S. Chisholm,[35] A. Chitan,[27b] I. Chiu,[160] Y. H. Chiu,[173] M. V. Chizhov,[77] K. Choi,[63] A. R. Chomont,[128] S. Chouridou,[159] Y. S. Chow,[118] V. Christodoulou,[92] M. C. Chu,[61a] J. Chudoba,[137] A. J. Chuinard,[101] J. J. Chwastowski,[82] L. Chytka,[126] D. Cinca,[45] V. Cindro,[89] I. A. Cioară,[24] A. Ciocio,[18] F. Cirotto,[67a,67b] Z. H. Citron,[177] M. Citterio,[66a] A. Clark,[52] M. R. Clark,[38] P. J. Clark,[48] C. Clement,[43a,43b] Y. Coadou,[99] M. Cobal,[64a,64c] A. Coccaro,[53b,53a] J. Cochran,[76] A. E. C. Coimbra,[177] L. Colasurdo,[117] B. Cole,[38] A. P. Colijn,[118] J. Collot,[56] P. Conde Muiño,[136a,136b] E. Coniavitis,[50] S. H. Connell,[32b] I. A. Connelly,[98] S. Constantinescu,[27b] F. Conventi,[67a,l] A. M. Cooper-Sarkar,[131] F. Cormier,[172] K. J. R. Cormier,[164] M. Corradi,[70a,70b] E. E. Corrigan,[94] F. Corriveau,[101,m] A. Cortes-Gonzalez,[35] M. J. Costa,[171] D. Costanzo,[146] G. Cottin,[31] G. Cowan,[91] B. E. Cox,[98] J. Crane,[98] K. Cranmer,[121] S. J. Crawley,[55] R. A. Creager,[133] G. Cree,[33] S. Crépé-Renaudin,[56] F. Crescioli,[132] M. Cristinziani,[24] V. Croft,[121] G. Crosetti,[40b,40a] A. Cueto,[96] T. Cuhadar Donszelmann,[146] A. R. Cukierman,[150] M. Curatolo,[49] J. Cúth,[97] S. Czekierda,[82] P. Czodrowski,[35] M. J. Da Cunha Sargedas De Sousa,[58b,136b] C. Da Via,[98] W. Dabrowski,[81a] T. Dado,[28a,n] S. Dahbi,[34e] T. Dai,[103] F. Dallaire,[107] C. Dallapiccola,[100] M. Dam,[39] G. D'amen,[23b,23a] J. Damp,[97] J. R. Dandoy,[133] M. F. Daneri,[30] N. P. Dang,[178,f] N.D Dann,[98] M. Danninger,[172] V. Dao,[35] G. Darbo,[53b] S. Darmora,[8] O. Dartsi,[5] A. Dattagupta,[127] T. Daubney,[44] S. D'Auria,[55] W. Davey,[24] C. David,[44] T. Davidek,[139] D. R. Davis,[47] E. Dawe,[102] I. Dawson,[146] K. De,[8] R. De Asmundis,[67a] A. De Benedetti,[124] S. De Castro,[23b,23a]

S. De Cecco,[70a,70b] N. De Groot,[117] P. de Jong,[118] H. De la Torre,[104] F. De Lorenzi,[76] A. De Maria,[51,o] D. De Pedis,[70a] A. De Salvo,[70a] U. De Sanctis,[71a,71b] A. De Santo,[153] K. De Vasconcelos Corga,[99] J. B. De Vivie De Regie,[128] C. Debenedetti,[143] D. V. Dedovich,[77] N. Dehghanian,[3] M. Del Gaudio,[40b,40a] J. Del Peso,[96] D. Delgove,[128] F. Deliot,[142] C. M. Delitzsch,[7] M. Della Pietra,[67a,67b] D. Della Volpe,[52] A. Dell'Acqua,[35] L. Dell'Asta,[25] M. Delmastro,[5] C. Delporte,[128] P. A. Delsart,[56] D. A. DeMarco,[164] S. Demers,[180] M. Demichev,[77] S. P. Denisov,[140] D. Denysiuk,[118] L. D'Eramo,[132] D. Derendarz,[82] J. E. Derkaoui,[34d] F. Derue,[132] P. Dervan,[88] K. Desch,[24] C. Deterre,[44] K. Dette,[164] M. R. Devesa,[30] P. O. Deviveiros,[35] A. Dewhurst,[141] S. Dhaliwal,[26] F. A. Di Bello,[52] A. Di Ciaccio,[71a,71b] L. Di Ciaccio,[5] W. K. Di Clemente,[133] C. Di Donato,[67a,67b] A. Di Girolamo,[35] B. Di Micco,[72a,72b] R. Di Nardo,[35] K. F. Di Petrillo,[57] A. Di Simone,[50] R. Di Sipio,[164] D. Di Valentino,[33] C. Diaconu,[99] M. Diamond,[164] F. A. Dias,[39] T. Dias Do Vale,[136a] M. A. Diaz,[144a] J. Dickinson,[18] E. B. Diehl,[103] J. Dietrich,[19] S. Díez Cornell,[44] A. Dimitrievska,[18] J. Dingfelder,[24] F. Dittus,[35] F. Djama,[99] T. Djobava,[156b] J. I. Djuvsland,[59a] M. A. B. Do Vale,[78c] M. Dobre,[27b] D. Dodsworth,[26] C. Doglioni,[94] J. Dolejsi,[139] Z. Dolezal,[139] M. Donadelli,[78d] J. Donini,[37] A. D'onofrio,[90] M. D'Onofrio,[88] J. Dopke,[141] A. Doria,[67a] M. T. Dova,[86] A. T. Doyle,[55] E. Drechsler,[51] E. Dreyer,[149] T. Dreyer,[51] M. Dris,[10] Y. Du,[58b] J. Duarte-Campderros,[158] F. Dubinin,[108] M. Dubovsky,[28a] A. Dubreuil,[52] E. Duchovni,[177] G. Duckeck,[112] A. Ducourthial,[132] O. A. Ducu,[107,p] D. Duda,[113] A. Dudarev,[35] A. C. Dudder,[97] E. M. Duffield,[18] L. Duflot,[128] M. Dührssen,[35] C. Dülsen,[179] M. Dumancic,[177] A. E. Dumitriu,[27b,q] A. K. Duncan,[55] M. Dunford,[59a] A. Duperrin,[99] H. Duran Yildiz,[4a] M. Düren,[54] A. Durglishvili,[156b] D. Duschinger,[46] B. Dutta,[44] D. Duvnjak,[1] M. Dyndal,[44] S. Dysch,[98] B. S. Dziedzic,[82] C. Eckardt,[44] K. M. Ecker,[113] R. C. Edgar,[103] T. Eifert,[35] G. Eigen,[17] K. Einsweiler,[18] T. Ekelof,[169] M. El Kacimi,[34c] R. El Kosseifi,[99] V. Ellajosyula,[99] M. Ellert,[169] F. Ellinghaus,[179] A. A. Elliot,[90] N. Ellis,[35] J. Elmsheuser,[29] M. Elsing,[35] D. Emeliyanov,[141] Y. Enari,[160] J. S. Ennis,[175] M. B. Epland,[47] J. Erdmann,[45] A. Ereditato,[20] S. Errede,[170] M. Escalier,[128] C. Escobar,[171] B. Esposito,[49] O. Estrada Pastor,[171] A. I. Etienvre,[142] E. Etzion,[158] H. Evans,[63] A. Ezhilov,[134] M. Ezzi,[34e] F. Fabbri,[55] L. Fabbri,[23b,23a] V. Fabiani,[117] G. Facini,[92] R. M. Faisca Rodrigues Pereira,[136a] R. M. Fakhrutdinov,[140] S. Falciano,[70a] P. J. Falke,[5] S. Falke,[5] J. Faltova,[139] Y. Fang,[15a] M. Fanti,[66a,66b] A. Farbin,[8] A. Farilla,[72a] E. M. Farina,[68a,68b] T. Farooque,[104] S. Farrell,[18] S. M. Farrington,[175] P. Farthouat,[35] F. Fassi,[34e] P. Fassnacht,[35] D. Fassouliotis,[9] M. Faucci Giannelli,[48] A. Favareto,[53b,53a] W. J. Fawcett,[52] L. Fayard,[128] O. L. Fedin,[134,r] W. Fedorko,[172] M. Feickert,[41] S. Feigl,[130] L. Feligioni,[99] C. Feng,[58b] E. J. Feng,[35] M. Feng,[47] M. J. Fenton,[55] A. B. Fenyuk,[140] L. Feremenga,[8] J. Ferrando,[44] A. Ferrari,[169] P. Ferrari,[118] R. Ferrari,[68a] D. E. Ferreira de Lima,[59b] A. Ferrer,[171] D. Ferrere,[52] C. Ferretti,[103] F. Fiedler,[97] A. Filipčič,[89] F. Filthaut,[117] K. D. Finelli,[25] M. C. N. Fiolhais,[136a,136c,s] L. Fiorini,[171] C. Fischer,[14] W. C. Fisher,[104] N. Flaschel,[44] I. Fleck,[148] P. Fleischmann,[103] R. R. M. Fletcher,[133] T. Flick,[179] B. M. Flierl,[112] L. M. Flores,[133] L. R. Flores Castillo,[61a] N. Fomin,[17] G. T. Forcolin,[98] A. Formica,[142] F. A. Förster,[14] A. C. Forti,[98] A. G. Foster,[21] D. Fournier,[128] H. Fox,[87] S. Fracchia,[146] P. Francavilla,[69a,69b] M. Franchini,[23b,23a] S. Franchino,[59a] D. Francis,[35] L. Franconi,[130] M. Franklin,[57] M. Frate,[168] M. Fraternali,[68a,68b] D. Freeborn,[92] S. M. Fressard-Batraneanu,[35] B. Freund,[107] W. S. Freund,[78b] D. Froidevaux,[35] J. A. Frost,[131] C. Fukunaga,[161] T. Fusayasu,[114] J. Fuster,[171] O. Gabizon,[157] A. Gabrielli,[23b,23a] A. Gabrielli,[18] G. P. Gach,[81a] S. Gadatsch,[52] P. Gadow,[113] G. Gagliardi,[53b,53a] L. G. Gagnon,[107] C. Galea,[27b] B. Galhardo,[136a,136c] E. J. Gallas,[131] B. J. Gallop,[141] P. Gallus,[138] G. Galster,[39] R. Gamboa Goni,[90] K. K. Gan,[122] S. Ganguly,[177] Y. Gao,[88] Y. S. Gao,[150,g] C. García,[171] J. E. García Navarro,[171] J. A. García Pascual,[15a] M. Garcia-Sciveres,[18] R. W. Gardner,[36] N. Garelli,[150] V. Garonne,[130] K. Gasnikova,[44] A. Gaudiello,[53b,53a] G. Gaudio,[68a] I. L. Gavrilenko,[108] A. Gavrilyuk,[109] C. Gay,[172] G. Gaycken,[24] E. N. Gazis,[10] C. N. P. Gee,[141] J. Geisen,[51] M. Geisen,[97] M. P. Geisler,[59a] K. Gellerstedt,[43a,43b] C. Gemme,[53b] M. H. Genest,[56] C. Geng,[103] S. Gentile,[70a,70b] C. Gentsos,[159] S. George,[91] D. Gerbaudo,[14] G. Gessner,[45] S. Ghasemi,[148] M. Ghasemi Bostanabad,[173] M. Ghneimat,[24] B. Giacobbe,[23b] S. Giagu,[70a,70b] N. Giangiacomi,[23b,23a] P. Giannetti,[69a] S. M. Gibson,[91] M. Gignac,[143] D. Gillberg,[33] G. Gilles,[179] D. M. Gingrich,[3,e] M. P. Giordani,[64a,64c] F. M. Giorgi,[23b] P. F. Giraud,[142] P. Giromini,[57] G. Giugliarelli,[64a,64c] D. Giugni,[66a] F. Giuli,[131] M. Giulini,[59b] S. Gkaitatzis,[159] I. Gkialas,[9,t] E. L. Gkougkousis,[14] P. Gkountoumis,[10] L. K. Gladilin,[111] C. Glasman,[96] J. Glatzer,[14] P. C. F. Glaysher,[44] A. Glazov,[44] M. Goblirsch-Kolb,[26] J. Godlewski,[82] S. Goldfarb,[102] T. Golling,[52] D. Golubkov,[140] A. Gomes,[136a,136b,136d] R. Goncalves Gama,[78a] R. Gonçalo,[136a] G. Gonella,[50] L. Gonella,[21] A. Gongadze,[77] F. Gonnella,[21] J. L. Gonski,[57] S. González de la Hoz,[171] S. Gonzalez-Sevilla,[52] L. Goossens,[35] P. A. Gorbounov,[109] H. A. Gordon,[29] B. Gorini,[35] E. Gorini,[65a,65b] A. Gorišek,[89] A. T. Goshaw,[47] C. Gössling,[45] M. I. Gostkin,[77] C. A. Gottardo,[24] C. R. Goudet,[128] D. Goujdami,[34c] A. G. Goussiou,[145] N. Govender,[32b,u] C. Goy,[5] E. Gozani,[157] I. Grabowska-Bold,[81a] P. O. J. Gradin,[169] E. C. Graham,[88] J. Gramling,[168] E. Gramstad,[130] S. Grancagnolo,[19] V. Gratchev,[134] P. M. Gravila,[27f] C. Gray,[55] H. M. Gray,[18]

Z. D. Greenwood,[93,v] C. Grefe,[24] K. Gregersen,[92] I. M. Gregor,[44] P. Grenier,[150] K. Grevtsov,[44] J. Griffiths,[8] A. A. Grillo,[143] K. Grimm,[150,w] S. Grinstein,[14,x] Ph. Gris,[37] J.-F. Grivaz,[128] S. Groh,[97] E. Gross,[177] J. Grosse-Knetter,[51] G. C. Grossi,[93] Z. J. Grout,[92] C. Grud,[103] A. Grummer,[116] L. Guan,[103] W. Guan,[178] J. Guenther,[35] A. Guerguichon,[128] F. Guescini,[165a] D. Guest,[168] R. Gugel,[50] B. Gui,[122] T. Guillemin,[5] S. Guindon,[35] U. Gul,[55] C. Gumpert,[35] J. Guo,[58c] W. Guo,[103] Y. Guo,[58a,y] Z. Guo,[99] R. Gupta,[41] S. Gurbuz,[12c] G. Gustavino,[124] B. J. Gutelman,[157] P. Gutierrez,[124] C. Gutschow,[92] C. Guyot,[142] M. P. Guzik,[81a] C. Gwenlan,[131] C. B. Gwilliam,[88] A. Haas,[121] C. Haber,[18] H. K. Hadavand,[8] N. Haddad,[34e] A. Hadef,[58a] S. Hageböck,[24] M. Hagihara,[166] H. Hakobyan,[181,a] M. Haleem,[174] J. Haley,[125] G. Halladjian,[104] G. D. Hallewell,[99] K. Hamacher,[179] P. Hamal,[126] K. Hamano,[173] A. Hamilton,[32a] G. N. Hamity,[146] K. Han,[58a,z] L. Han,[58a] S. Han,[15d] K. Hanagaki,[79,aa] M. Hance,[143] D. M. Handl,[112] B. Haney,[133] R. Hankache,[132] P. Hanke,[59a] E. Hansen,[94] J. B. Hansen,[39] J. D. Hansen,[39] M. C. Hansen,[24] P. H. Hansen,[39] K. Hara,[166] A. S. Hard,[178] T. Harenberg,[179] S. Harkusha,[105] P. F. Harrison,[175] N. M. Hartmann,[112] Y. Hasegawa,[147] A. Hasib,[48] S. Hassani,[142] S. Haug,[20] R. Hauser,[104] L. Hauswald,[46] L. B. Havener,[38] M. Havranek,[138] C. M. Hawkes,[21] R. J. Hawkings,[35] D. Hayden,[104] C. Hayes,[152] C. P. Hays,[131] J. M. Hays,[90] H. S. Hayward,[88] S. J. Haywood,[141] M. P. Heath,[48] V. Hedberg,[94] L. Heelan,[8] S. Heer,[24] K. K. Heidegger,[50] J. Heilman,[33] S. Heim,[44] T. Heim,[18] B. Heinemann,[44,bb] J. J. Heinrich,[112] L. Heinrich,[121] C. Heinz,[54] J. Hejbal,[137] L. Helary,[35] A. Held,[172] S. Hellesund,[130] S. Hellman,[43a,43b] C. Helsens,[35] R. C. W. Henderson,[87] Y. Heng,[178] S. Henkelmann,[172] A. M. Henriques Correia,[35] G. H. Herbert,[19] H. Herde,[26] V. Herget,[174] Y. Hernández Jiménez,[32c] H. Herr,[97] G. Herten,[50] R. Hertenberger,[112] L. Hervas,[35] T. C. Herwig,[133] G. G. Hesketh,[92] N. P. Hessey,[165a] J. W. Hetherly,[41] S. Higashino,[79] E. Higón-Rodriguez,[171] K. Hildebrand,[36] E. Hill,[173] J. C. Hill,[31] K. K. Hill,[29] K. H. Hiller,[44] S. J. Hillier,[21] M. Hils,[46] I. Hinchliffe,[18] M. Hirose,[129] D. Hirschbuehl,[179] B. Hiti,[89] O. Hladik,[137] D. R. Hlaluku,[32c] X. Hoad,[48] J. Hobbs,[152] N. Hod,[165a] M. C. Hodgkinson,[146] A. Hoecker,[35] M. R. Hoeferkamp,[116] F. Hoenig,[112] D. Hohn,[24] D. Hohov,[128] T. R. Holmes,[36] M. Holzbock,[112] M. Homann,[45] S. Honda,[166] T. Honda,[79] T. M. Hong,[135] A. Hönle,[113] B. H. Hooberman,[170] W. H. Hopkins,[127] Y. Horii,[115] P. Horn,[46] A. J. Horton,[149] L. A. Horyn,[36] J-Y. Hostachy,[56] A. Hostiuc,[145] S. Hou,[155] A. Hoummada,[34a] J. Howarth,[98] J. Hoya,[86] M. Hrabovsky,[126] J. Hrdinka,[35] I. Hristova,[19] J. Hrivnac,[128] A. Hrynevich,[106] T. Hryn'ova,[5] P. J. Hsu,[62] S.-C. Hsu,[145] Q. Hu,[29] S. Hu,[58c] Y. Huang,[15a] Z. Hubacek,[138] F. Hubaut,[99] M. Huebner,[24] F. Huegging,[24] T. B. Huffman,[131] E. W. Hughes,[38] M. Huhtinen,[35] R. F. H. Hunter,[33] P. Huo,[152] A. M. Hupe,[33] N. Huseynov,[77,d] J. Huston,[104] J. Huth,[57] R. Hyneman,[103] G. Iacobucci,[52] G. Iakovidis,[29] I. Ibragimov,[148] L. Iconomidou-Fayard,[128] Z. Idrissi,[34e] P. Iengo,[35] R. Ignazzi,[39] O. Igonkina,[118,cc] R. Iguchi,[160] T. Iizawa,[52] Y. Ikegami,[79] M. Ikeno,[79] D. Iliadis,[159] N. Ilic,[150] F. Iltzsche,[46] G. Introzzi,[68a,68b] M. Iodice,[72a] K. Iordanidou,[38] V. Ippolito,[70a,70b] M. F. Isacson,[169] N. Ishijima,[129] M. Ishino,[160] M. Ishitsuka,[162] W. Islam,[125] C. Issever,[131] S. Istin,[12c,dd] F. Ito,[166] J. M. Iturbe Ponce,[61a] R. Iuppa,[73a,73b] A. Ivina,[177] H. Iwasaki,[79] J. M. Izen,[42] V. Izzo,[67a] S. Jabbar,[3] P. Jacka,[137] P. Jackson,[1] R. M. Jacobs,[24] V. Jain,[2] G. Jäkel,[179] K. B. Jakobi,[97] K. Jakobs,[50] S. Jakobsen,[74] T. Jakoubek,[137] D. O. Jamin,[125] D. K. Jana,[93] R. Jansky,[52] J. Janssen,[24] M. Janus,[51] P. A. Janus,[81a] G. Jarlskog,[94] N. Javadov,[77,d] T. Javůrek,[50] M. Javurkova,[50] F. Jeanneau,[142] L. Jeanty,[18] J. Jejelava,[156a,ee] A. Jelinskas,[175] P. Jenni,[50,ff] J. Jeong,[44] C. Jeske,[175] S. Jézéquel,[5] H. Ji,[178] J. Jia,[152] H. Jiang,[76] Y. Jiang,[58a] Z. Jiang,[150,gg] S. Jiggins,[50] F. A. Jimenez Morales,[37] J. Jimenez Pena,[171] S. Jin,[15c] A. Jinaru,[27b] O. Jinnouchi,[162] H. Jivan,[32c] P. Johansson,[146] K. A. Johns,[7] C. A. Johnson,[63] W. J. Johnson,[145] K. Jon-And,[43a,43b] R. W. L. Jones,[87] S. D. Jones,[153] S. Jones,[7] T. J. Jones,[88] J. Jongmanns,[59a] P. M. Jorge,[136a,136b] J. Jovicevic,[165a] X. Ju,[178] J. J. Junggeburth,[113] A. Juste Rozas,[14,x] A. Kaczmarska,[82] M. Kado,[128] H. Kagan,[122] M. Kagan,[150] T. Kaji,[176] E. Kajomovitz,[157] C. W. Kalderon,[94] A. Kaluza,[97] S. Kama,[41] A. Kamenshchikov,[140] L. Kanjir,[89] Y. Kano,[160] V. A. Kantserov,[110] J. Kanzaki,[79] B. Kaplan,[121] L. S. Kaplan,[178] D. Kar,[32c] M. J. Kareem,[165b] E. Karentzos,[10] S. N. Karpov,[77] Z. M. Karpova,[77] V. Kartvelishvili,[87] A. N. Karyukhin,[140] K. Kasahara,[166] L. Kashif,[178] R. D. Kass,[122] A. Kastanas,[151] Y. Kataoka,[160] C. Kato,[160] J. Katzy,[44] K. Kawade,[80] K. Kawagoe,[85] T. Kawamoto,[160] G. Kawamura,[51] E. F. Kay,[88] V. F. Kazanin,[120b,120a] R. Keeler,[173] R. Kehoe,[41] J. S. Keller,[33] E. Kellermann,[94] J. J. Kempster,[21] J. Kendrick,[21] O. Kepka,[137] S. Kersten,[179] B. P. Kerševan,[89] R. A. Keyes,[101] M. Khader,[170] F. Khalil-Zada,[13] A. Khanov,[125] A. G. Kharlamov,[120b,120a] T. Kharlamova,[120b,120a] A. Khodinov,[163] T. J. Khoo,[52] E. Khramov,[77] J. Khubua,[156b] S. Kido,[80] M. Kiehn,[52] C. R. Kilby,[91] S. H. Kim,[166] Y. K. Kim,[36] N. Kimura,[64a,64c] O. M. Kind,[19] B. T. King,[88] D. Kirchmeier,[46] J. Kirk,[141] A. E. Kiryunin,[113] T. Kishimoto,[160] D. Kisielewska,[81a] V. Kitali,[44] O. Kivernyk,[5] E. Kladiva,[28b,a] T. Klapdor-Kleingrothaus,[50] M. H. Klein,[103] M. Klein,[88] U. Klein,[88] K. Kleinknecht,[97] P. Klimek,[119] A. Klimentov,[29] R. Klingenberg,[45,a] T. Klingl,[24] T. Klioutchnikova,[35] F. F. Klitzner,[112] P. Kluit,[118] S. Kluth,[113] E. Kneringer,[74] E. B. F. G. Knoops,[99] A. Knue,[50] A. Kobayashi,[160] D. Kobayashi,[85] T. Kobayashi,[160] M. Kobel,[46] M. Kocian,[150] P. Kodys,[139]

T. Koffas,[33] E. Koffeman,[118] N. M. Köhler,[113] T. Koi,[150] M. Kolb,[59b] I. Koletsou,[5] T. Kondo,[79] N. Kondrashova,[58c] K. Köneke,[50] A. C. König,[117] T. Kono,[79] R. Konoplich,[121,hh] V. Konstantinides,[92] N. Konstantinidis,[92] B. Konya,[94] R. Kopeliansky,[63] S. Koperny,[81a] K. Korcyl,[82] K. Kordas,[159] A. Korn,[92] I. Korolkov,[14] E. V. Korolkova,[146] O. Kortner,[113] S. Kortner,[113] T. Kosek,[139] V. V. Kostyukhin,[24] A. Kotwal,[47] A. Koulouris,[10] A. Kourkoumeli-Charalampidi,[68a,68b] C. Kourkoumelis,[9] E. Kourlitis,[146] V. Kouskoura,[29] A. B. Kowalewska,[82] R. Kowalewski,[173] T. Z. Kowalski,[81a] C. Kozakai,[160] W. Kozanecki,[142] A. S. Kozhin,[140] V. A. Kramarenko,[111] G. Kramberger,[89] D. Krasnopevtsev,[110] M. W. Krasny,[132] A. Krasznahorkay,[35] D. Krauss,[113] J. A. Kremer,[81a] J. Kretzschmar,[88] P. Krieger,[164] K. Krizka,[18] K. Kroeninger,[45] H. Kroha,[113] J. Kroll,[137] J. Kroll,[133] J. Krstic,[16] U. Kruchonak,[77] H. Krüger,[24] N. Krumnack,[76] M. C. Kruse,[47] T. Kubota,[102] S. Kuday,[4b] J. T. Kuechler,[179] S. Kuehn,[35] A. Kugel,[59a] F. Kuger,[174] T. Kuhl,[44] V. Kukhtin,[77] R. Kukla,[99] Y. Kulchitsky,[105] S. Kuleshov,[144b] Y. P. Kulinich,[170] M. Kuna,[56] T. Kunigo,[83] A. Kupco,[137] T. Kupfer,[45] O. Kuprash,[158] H. Kurashige,[80] L. L. Kurchaninov,[165a] Y. A. Kurochkin,[105] M. G. Kurth,[15d] E. S. Kuwertz,[173] M. Kuze,[162] J. Kvita,[126] T. Kwan,[101] A. La Rosa,[113] J. L. La Rosa Navarro,[78d] L. La Rotonda,[40b,40a] F. La Ruffa,[40b,40a] C. Lacasta,[171] F. Lacava,[70a,70b] J. Lacey,[44] D. P. J. Lack,[98] H. Lacker,[19] D. Lacour,[132] E. Ladygin,[77] R. Lafaye,[5] B. Laforge,[132] T. Lagouri,[32c] S. Lai,[51] S. Lammers,[63] W. Lampl,[7] E. Lançon,[29] U. Landgraf,[50] M. P. J. Landon,[90] M. C. Lanfermann,[52] V. S. Lang,[44] J. C. Lange,[14] R. J. Langenberg,[35] A. J. Lankford,[168] F. Lanni,[29] K. Lantzsch,[24] A. Lanza,[68a] A. Lapertosa,[53b,53a] S. Laplace,[132] J. F. Laporte,[142] T. Lari,[66a] F. Lasagni Manghi,[23b,23a] M. Lassnig,[35] T. S. Lau,[61a] A. Laudrain,[128] A. T. Law,[143] P. Laycock,[88] M. Lazzaroni,[66a,66b] B. Le,[102] O. Le Dortz,[132] E. Le Guirriec,[99] E. P. Le Quilleuc,[142] M. LeBlanc,[7] T. LeCompte,[6] F. Ledroit-Guillon,[56] C. A. Lee,[29] G. R. Lee,[144a] L. Lee,[57] S. C. Lee,[155] B. Lefebvre,[101] M. Lefebvre,[173] F. Legger,[112] C. Leggett,[18] N. Lehmann,[179] G. Lehmann Miotto,[35] W. A. Leight,[44] A. Leisos,[159,ii] M. A. L. Leite,[78d] R. Leitner,[139] D. Lellouch,[177] B. Lemmer,[51] K. J. C. Leney,[92] T. Lenz,[24] B. Lenzi,[35] R. Leone,[7] S. Leone,[69a] C. Leonidopoulos,[48] G. Lerner,[153] C. Leroy,[107] R. Les,[164] A. A. J. Lesage,[142] C. G. Lester,[31] M. Levchenko,[134] J. Levêque,[5] D. Levin,[103] L. J. Levinson,[177] D. Lewis,[90] B. Li,[103] C-Q. Li,[58a,jj] H. Li,[58b] L. Li,[58c] Q. Li,[15d] Q. Y. Li,[58a] S. Li,[58d,58c] X. Li,[58c] Y. Li,[148] Z. Liang,[15a] B. Liberti,[71a] A. Liblong,[164] K. Lie,[61c] S. Liem,[118] A. Limosani,[154] C. Y. Lin,[31] K. Lin,[104] T. H. Lin,[97] R. A. Linck,[63] B. E. Lindquist,[152] A. L. Lionti,[52] E. Lipeles,[133] A. Lipniacka,[17] M. Lisovyi,[59b] T. M. Liss,[170,kk] A. Lister,[172] A. M. Litke,[143] J. D. Little,[8] B. Liu,[76] B.L Liu,[6] H. B. Liu,[29] H. Liu,[103] J. B. Liu,[58a] J. K. K. Liu,[131] K. Liu,[132] M. Liu,[58a] P. Liu,[18] Y. Liu,[15a] Y. L. Liu,[58a] Y. W. Liu,[58a] M. Livan,[68a,68b] A. Lleres,[56] J. Llorente Merino,[15a] S. L. Lloyd,[90] C. Y. Lo,[61b] F. Lo Sterzo,[41] E. M. Lobodzinska,[44] P. Loch,[7] F. K. Loebinger,[98] K. M. Loew,[26] T. Lohse,[19] K. Lohwasser,[146] M. Lokajicek,[137] B. A. Long,[25] J. D. Long,[170] R. E. Long,[87] L. Longo,[65a,65b] K. A. Looper,[122] J. A. Lopez,[144b] I. Lopez Paz,[14] A. Lopez Solis,[146] J. Lorenz,[112] N. Lorenzo Martinez,[5] M. Losada,[22] P. J. Lösel,[112] A. Lösle,[50] X. Lou,[44] X. Lou,[15a] A. Lounis,[128] J. Love,[6] P. A. Love,[87] J. J. Lozano Bahilo,[171] H. Lu,[61a] M. Lu,[58a] N. Lu,[103] Y. J. Lu,[62] H. J. Lubatti,[145] C. Luci,[70a,70b] A. Lucotte,[56] C. Luedtke,[50] F. Luehring,[63] I. Luise,[132] W. Lukas,[74] L. Luminari,[70a] B. Lund-Jensen,[151] M. S. Lutz,[100] P. M. Luzi,[132] D. Lynn,[29] R. Lysak,[137] E. Lytken,[94] F. Lyu,[15a] V. Lyubushkin,[77] H. Ma,[29] L. L. Ma,[58b] Y. Ma,[58b] G. Maccarrone,[49] A. Macchiolo,[113] C. M. Macdonald,[146] J. Machado Miguens,[133,136b] D. Madaffari,[171] R. Madar,[37] W. F. Mader,[46] A. Madsen,[44] N. Madysa,[46] J. Maeda,[80] K. Maekawa,[160] S. Maeland,[17] T. Maeno,[29] A. S. Maevskiy,[111] V. Magerl,[50] C. Maidantchik,[78b] T. Maier,[112] A. Maio,[136a,136b,136d] O. Majersky,[28a] S. Majewski,[127] Y. Makida,[79] N. Makovec,[128] B. Malaescu,[132] Pa. Malecki,[82] V. P. Maleev,[134] F. Malek,[56] U. Mallik,[75] D. Malon,[6] C. Malone,[31] S. Maltezos,[10] S. Malyukov,[35] J. Mamuzic,[171] G. Mancini,[49] I. Mandić,[89] J. Maneira,[136a] L. Manhaes de Andrade Filho,[78a] J. Manjarres Ramos,[46] K. H. Mankinen,[94] A. Mann,[112] A. Manousos,[74] B. Mansoulie,[142] J. D. Mansour,[15a] M. Mantoani,[51] S. Manzoni,[66a,66b] G. Marceca,[30] L. March,[52] L. Marchese,[131] G. Marchiori,[132] M. Marcisovsky,[137] C. A. Marin Tobon,[35] M. Marjanovic,[37] D. E. Marley,[103] F. Marroquim,[78b] Z. Marshall,[18] M. U. F Martensson,[169] S. Marti-Garcia,[171] C. B. Martin,[122] T. A. Martin,[175] V. J. Martin,[48] B. Martin dit Latour,[17] M. Martinez,[14,x] V. I. Martinez Outschoorn,[100] S. Martin-Haugh,[141] V. S. Martoiu,[27b] A. C. Martyniuk,[92] A. Marzin,[35] L. Masetti,[97] T. Mashimo,[160] R. Mashinistov,[108] J. Masik,[98] A. L. Maslennikov,[120b,120a] L. H. Mason,[102] L. Massa,[71a,71b] P. Mastrandrea,[5] A. Mastroberardino,[40b,40a] T. Masubuchi,[160] P. Mättig,[179] J. Maurer,[27b] B. Maček,[89] S. J. Maxfield,[88] D. A. Maximov,[120b,120a] R. Mazini,[155] I. Maznas,[159] S. M. Mazza,[143] N. C. Mc Fadden,[116] G. Mc Goldrick,[164] S. P. Mc Kee,[103] A. McCarn,[103] T. G. McCarthy,[113] L. I. McClymont,[92] E. F. McDonald,[102] J. A. Mcfayden,[35] G. Mchedlidze,[51] M. A. McKay,[41] K. D. McLean,[173] S. J. McMahon,[141] P. C. McNamara,[102] C. J. McNicol,[175] R. A. McPherson,[173,m] J. E. Mdhluli,[32c] Z. A. Meadows,[100] S. Meehan,[145] T. M. Megy,[50] S. Mehlhase,[112] A. Mehta,[88] T. Meideck,[56] B. Meirose,[42] D. Melini,[171,ll] B. R. Mellado Garcia,[32c] J. D. Mellenthin,[51] M. Melo,[28a] F. Meloni,[20] A. Melzer,[24] S. B. Menary,[98]

E. D. Mendes Gouveia,[136a] L. Meng,[88] X. T. Meng,[103] A. Mengarelli,[23b,23a] S. Menke,[113] E. Meoni,[40b,40a] S. Mergelmeyer,[19] C. Merlassino,[20] P. Mermod,[52] L. Merola,[67a,67b] C. Meroni,[66a] F. S. Merritt,[36] A. Messina,[70a,70b] J. Metcalfe,[6] A. S. Mete,[168] C. Meyer,[133] J. Meyer,[157] J-P. Meyer,[142] H. Meyer Zu Theenhausen,[59a] F. Miano,[153] R. P. Middleton,[141] L. Mijović,[48] G. Mikenberg,[177] M. Mikestikova,[137] M. Mikuž,[89] M. Milesi,[102] A. Milic,[164] D. A. Millar,[90] D. W. Miller,[36] A. Milov,[177] D. A. Milstead,[43a,43b] A. A. Minaenko,[140] M. Miñano Moya,[171] I. A. Minashvili,[156b] A. I. Mincer,[121] B. Mindur,[81a] M. Mineev,[77] Y. Minegishi,[160] Y. Ming,[178] L. M. Mir,[14] A. Mirto,[65a,65b] K. P. Mistry,[133] T. Mitani,[176] J. Mitrevski,[112] V. A. Mitsou,[171] A. Miucci,[20] P. S. Miyagawa,[146] A. Mizukami,[79] J. U. Mjörnmark,[94] T. Mkrtchyan,[181] M. Mlynarikova,[139] T. Moa,[43a,43b] K. Mochizuki,[107] P. Mogg,[50] S. Mohapatra,[38] S. Molander,[43a,43b] R. Moles-Valls,[24] M. C. Mondragon,[104] K. Mönig,[44] J. Monk,[39] E. Monnier,[99] A. Montalbano,[149] J. Montejo Berlingen,[35] F. Monticelli,[86] S. Monzani,[66a] R. W. Moore,[3] N. Morange,[128] D. Moreno,[22] M. Moreno Llácer,[35] P. Morettini,[53b] M. Morgenstern,[118] S. Morgenstern,[35] D. Mori,[149] T. Mori,[160] M. Morii,[57] M. Morinaga,[176] V. Morisbak,[130] A. K. Morley,[35] G. Mornacchi,[35] A. P. Morris,[92] J. D. Morris,[90] L. Morvaj,[152] P. Moschovakos,[10] M. Mosidze,[156b] H. J. Moss,[146] J. Moss,[150,mm] K. Motohashi,[162] R. Mount,[150] E. Mountricha,[35] E. J. W. Moyse,[100] S. Muanza,[99] F. Mueller,[113] J. Mueller,[135] R. S. P. Mueller,[112] D. Muenstermann,[87] P. Mullen,[55] G. A. Mullier,[20] F. J. Munoz Sanchez,[98] P. Murin,[28b] W. J. Murray,[175,141] A. Murrone,[66a,66b] M. Muškinja,[89] C. Mwewa,[32a] A. G. Myagkov,[140,nn] J. Myers,[127] M. Myska,[138] B. P. Nachman,[18] O. Nackenhorst,[45] K. Nagai,[131] K. Nagano,[79] Y. Nagasaka,[60] K. Nagata,[166] M. Nagel,[50] E. Nagy,[99] A. M. Nairz,[35] Y. Nakahama,[115] K. Nakamura,[79] T. Nakamura,[160] I. Nakano,[123] H. Nanjo,[129] F. Napolitano,[59a] R. F. Naranjo Garcia,[44] R. Narayan,[11] D. I. Narrias Villar,[59a] I. Naryshkin,[134] T. Naumann,[44] G. Navarro,[22] R. Nayyar,[7] H. A. Neal,[103,a] P. Y. Nechaeva,[108] T. J. Neep,[142] A. Negri,[68a,68b] M. Negrini,[23b] S. Nektarijevic,[117] C. Nellist,[51] M. E. Nelson,[131] S. Nemecek,[137] P. Nemethy,[121] M. Nessi,[35,oo] M. S. Neubauer,[170] M. Neumann,[179] P. R. Newman,[21] T. Y. Ng,[61c] Y. S. Ng,[19] H. D. N. Nguyen,[99] T. Nguyen Manh,[107] E. Nibigira,[37] R. B. Nickerson,[131] R. Nicolaidou,[142] J. Nielsen,[143] N. Nikiforou,[11] V. Nikolaenko,[140,nn] I. Nikolic-Audit,[132] K. Nikolopoulos,[21] P. Nilsson,[29] Y. Ninomiya,[79] A. Nisati,[70a] N. Nishu,[58c] R. Nisius,[113] I. Nitsche,[45] T. Nitta,[176] T. Nobe,[160] Y. Noguchi,[83] M. Nomachi,[129] I. Nomidis,[132] M. A. Nomura,[29] T. Nooney,[90] M. Nordberg,[35] N. Norjoharuddeen,[131] T. Novak,[89] O. Novgorodova,[46] R. Novotny,[138] M. Nozaki,[79] L. Nozka,[126] K. Ntekas,[168] E. Nurse,[92] F. Nuti,[102] F. G. Oakham,[33,e] H. Oberlack,[113] T. Obermann,[24] J. Ocariz,[132] A. Ochi,[80] I. Ochoa,[38] J. P. Ochoa-Ricoux,[144a] K. O'Connor,[26] S. Oda,[85] S. Odaka,[79] A. Oh,[98] S. H. Oh,[47] C. C. Ohm,[151] H. Oide,[53b,53a] H. Okawa,[166] Y. Okazaki,[83] Y. Okumura,[160] T. Okuyama,[79] A. Olariu,[27b] L. F. Oleiro Seabra,[136a] S. A. Olivares Pino,[144a] D. Oliveira Damazio,[29] J. L. Oliver,[1] M. J. R. Olsson,[36] A. Olszewski,[82] J. Olszowska,[82] D. C. O'Neil,[149] A. Onofre,[136a,136e] K. Onogi,[115] P. U. E. Onyisi,[11] H. Oppen,[130] M. J. Oreglia,[36] Y. Oren,[158] D. Orestano,[72a,72b] E. C. Orgill,[98] N. Orlando,[61b] A. A. O'Rourke,[44] R. S. Orr,[164] B. Osculati,[53b,53a,a] V. O'Shea,[55] R. Ospanov,[58a] G. Otero y Garzon,[30] H. Otono,[85] M. Ouchrif,[34d] F. Ould-Saada,[130] A. Ouraou,[142] Q. Ouyang,[15a] M. Owen,[55] R. E. Owen,[21] V. E. Ozcan,[12c] N. Ozturk,[8] J. Pacalt,[126] H. A. Pacey,[31] K. Pachal,[149] A. Pacheco Pages,[14] L. Pacheco Rodriguez,[142] C. Padilla Aranda,[14] S. Pagan Griso,[18] M. Paganini,[180] G. Palacino,[63] S. Palazzo,[40b,40a] S. Palestini,[35] M. Palka,[81b] D. Pallin,[37] I. Panagoulias,[10] C. E. Pandini,[35] J. G. Panduro Vazquez,[91] P. Pani,[35] G. Panizzo,[64a,64c] L. Paolozzi,[52] T. D. Papadopoulou,[10] K. Papageorgiou,[9,t] A. Paramonov,[6] D. Paredes Hernandez,[61b] S. R. Paredes Saenz,[131] B. Parida,[58c] A. J. Parker,[87] K. A. Parker,[44] M. A. Parker,[31] F. Parodi,[53b,53a] J. A. Parsons,[38] U. Parzefall,[50] V. R. Pascuzzi,[164] J. M. P. Pasner,[143] E. Pasqualucci,[70a] S. Passaggio,[53b] F. Pastore,[91] P. Pasuwan,[43a,43b] S. Pataraia,[97] J. R. Pater,[98] A. Pathak,[178,f] T. Pauly,[35] B. Pearson,[113] M. Pedersen,[130] L. Pedraza Diaz,[117] S. Pedraza Lopez,[171] R. Pedro,[136a,136b] S. V. Peleganchuk,[120b,120a] O. Penc,[137] C. Peng,[15d] H. Peng,[58a] B. S. Peralva,[78a] M. M. Perego,[142] A. P. Pereira Peixoto,[136a] D. V. Perepelitsa,[29] F. Peri,[19] L. Perini,[66a,66b] H. Pernegger,[35] S. Perrella,[67a,67b] V. D. Peshekhonov,[77,a] K. Peters,[44] R. F. Y. Peters,[98] B. A. Petersen,[35] T. C. Petersen,[39] E. Petit,[56] A. Petridis,[1] C. Petridou,[159] P. Petroff,[128] E. Petrolo,[70a] M. Petrov,[131] F. Petrucci,[72a,72b] M. Pettee,[180] N. E. Pettersson,[100] A. Peyaud,[142] R. Pezoa,[144b] T. Pham,[102] F. H. Phillips,[104] P. W. Phillips,[141] G. Piacquadio,[152] E. Pianori,[18] A. Picazio,[100] M. A. Pickering,[131] R. Piegaia,[30] J. E. Pilcher,[36] A. D. Pilkington,[98] M. Pinamonti,[71a,71b] J. L. Pinfold,[3] M. Pitt,[177] M-A. Pleier,[29] V. Pleskot,[139] E. Plotnikova,[77] D. Pluth,[76] P. Podberezko,[120b,120a] R. Poettgen,[94] R. Poggi,[52] L. Poggioli,[128] I. Pogrebnyak,[104] D. Pohl,[24] I. Pokharel,[51] G. Polesello,[68a] A. Poley,[44] A. Policicchio,[40b,40a] R. Polifka,[35] A. Polini,[23b] C. S. Pollard,[44] V. Polychronakos,[29] D. Ponomarenko,[110] L. Pontecorvo,[70a] G. A. Popeneciu,[27d] D. M. Portillo Quintero,[132] S. Pospisil,[138] K. Potamianos,[44] I. N. Potrap,[77] C. J. Potter,[31] H. Potti,[11] T. Poulsen,[94] J. Poveda,[35] T. D. Powell,[146] M. E. Pozo Astigarraga,[35] P. Pralavorio,[99] S. Prell,[76] D. Price,[98] M. Primavera,[65a] S. Prince,[101] N. Proklova,[110] K. Prokofiev,[61c] F. Prokoshin,[144b] S. Protopopescu,[29] J. Proudfoot,[6] M. Przybycien,[81a]

A. Puri,[170] P. Puzo,[128] J. Qian,[103] Y. Qin,[98] A. Quadt,[51] M. Queitsch-Maitland,[44] A. Qureshi,[1] P. Rados,[102] F. Ragusa,[66a,66b] G. Rahal,[95] J. A. Raine,[98] S. Rajagopalan,[29] A. Ramirez Morales,[90] T. Rashid,[128] S. Raspopov,[5] M. G. Ratti,[66a,66b] D. M. Rauch,[44] F. Rauscher,[112] S. Rave,[97] B. Ravina,[146] I. Ravinovich,[177] J. H. Rawling,[98] M. Raymond,[35] A. L. Read,[130] N. P. Readioff,[56] M. Reale,[65a,65b] D. M. Rebuzzi,[68a,68b] A. Redelbach,[174] G. Redlinger,[29] R. Reece,[143] R. G. Reed,[32c] K. Reeves,[42] L. Rehnisch,[19] J. Reichert,[133] A. Reiss,[97] C. Rembser,[35] H. Ren,[15d] M. Rescigno,[70a] S. Resconi,[66a] E. D. Resseguie,[133] S. Rettie,[172] E. Reynolds,[21] O. L. Rezanova,[120b,120a] P. Reznicek,[139] R. Richter,[113] S. Richter,[92] E. Richter-Was,[81b] O. Ricken,[24] M. Ridel,[132] P. Rieck,[113] C. J. Riegel,[179] O. Rifki,[44] M. Rijssenbeek,[152] A. Rimoldi,[68a,68b] M. Rimoldi,[20] L. Rinaldi,[23b] G. Ripellino,[151] B. Ristić,[87] E. Ritsch,[35] I. Riu,[14] J. C. Rivera Vergara,[144a] F. Rizatdinova,[125] E. Rizvi,[90] C. Rizzi,[14] R. T. Roberts,[98] S. H. Robertson,[101,m] A. Robichaud-Veronneau,[101] D. Robinson,[31] J. E. M. Robinson,[44] A. Robson,[55] E. Rocco,[97] C. Roda,[69a,69b] Y. Rodina,[99] S. Rodriguez Bosca,[171] A. Rodriguez Perez,[14] D. Rodriguez Rodriguez,[171] A. M. Rodríguez Vera,[165b] S. Roe,[35] C. S. Rogan,[57] O. Røhne,[130] R. Röhrig,[113] C. P. A. Roland,[63] J. Roloff,[57] A. Romaniouk,[110] M. Romano,[23b,23a] N. Rompotis,[88] M. Ronzani,[121] L. Roos,[132] S. Rosati,[70a] K. Rosbach,[50] P. Rose,[143] N-A. Rosien,[51] E. Rossi,[67a,67b] L. P. Rossi,[53b] L. Rossini,[66a,66b] J. H. N. Rosten,[31] R. Rosten,[14] M. Rotaru,[27b] J. Rothberg,[145] D. Rousseau,[128] D. Roy,[32c] A. Rozanov,[99] Y. Rozen,[157] X. Ruan,[32c] F. Rubbo,[150] F. Rühr,[50] A. Ruiz-Martinez,[33] Z. Rurikova,[50] N. A. Rusakovich,[77] H. L. Russell,[101] J. P. Rutherfoord,[7] N. Ruthmann,[35] E. M. Rüttinger,[44,pp] Y. F. Ryabov,[134] M. Rybar,[170] G. Rybkin,[128] S. Ryu,[6] A. Ryzhov,[140] G. F. Rzehorz,[51] P. Sabatini,[51] G. Sabato,[118] S. Sacerdoti,[128] H. F-W. Sadrozinski,[143] R. Sadykov,[77] F. Safai Tehrani,[70a] P. Saha,[119] M. Sahinsoy,[59a] A. Sahu,[179] M. Saimpert,[44] M. Saito,[160] T. Saito,[160] H. Sakamoto,[160] A. Sakharov,[121,hh] D. Salamani,[52] G. Salamanna,[72a,72b] J. E. Salazar Loyola,[144b] D. Salek,[118] P. H. Sales De Bruin,[169] D. Salihagic,[113] A. Salnikov,[150] J. Salt,[171] D. Salvatore,[40b,40a] F. Salvatore,[153] A. Salvucci,[61a,61b,61c] A. Salzburger,[35] J. Samarati,[35] D. Sammel,[50] D. Sampsonidis,[159] D. Sampsonidou,[159] J. Sánchez,[171] A. Sanchez Pineda,[64a,64c] H. Sandaker,[130] C. O. Sander,[44] M. Sandhoff,[179] C. Sandoval,[22] D. P. C. Sankey,[141] M. Sannino,[53b,53a] Y. Sano,[115] A. Sansoni,[49] C. Santoni,[37] H. Santos,[136a] I. Santoyo Castillo,[153] A. Sapronov,[77] J. G. Saraiva,[136a,136d] O. Sasaki,[79] K. Sato,[166] E. Sauvan,[5] P. Savard,[164,e] N. Savic,[113] R. Sawada,[160] C. Sawyer,[141] L. Sawyer,[93,v] C. Sbarra,[23b] A. Sbrizzi,[23b,23a] T. Scanlon,[92] J. Schaarschmidt,[145] P. Schacht,[113] B. M. Schachtner,[112] D. Schaefer,[36] L. Schaefer,[133] J. Schaeffer,[97] S. Schaepe,[35] U. Schäfer,[97] A. C. Schaffer,[128] D. Schaile,[112] R. D. Schamberger,[152] N. Scharmberg,[98] V. A. Schegelsky,[134] D. Scheirich,[139] F. Schenck,[19] M. Schernau,[168] C. Schiavi,[53b,53a] S. Schier,[143] L. K. Schildgen,[24] Z. M. Schillaci,[26] E. J. Schioppa,[35] M. Schioppa,[40b,40a] K. E. Schleicher,[50] S. Schlenker,[35] K. R. Schmidt-Sommerfeld,[113] K. Schmieden,[35] C. Schmitt,[97] S. Schmitt,[44] S. Schmitz,[97] U. Schnoor,[50] L. Schoeffel,[142] A. Schoening,[59b] E. Schopf,[24] M. Schott,[97] J. F. P. Schouwenberg,[117] J. Schovancova,[35] S. Schramm,[52] A. Schulte,[97] H-C. Schultz-Coulon,[59a] M. Schumacher,[50] B. A. Schumm,[143] Ph. Schune,[142] A. Schwartzman,[150] T. A. Schwarz,[103] H. Schweiger,[98] Ph. Schwemling,[142] R. Schwienhorst,[104] A. Sciandra,[24] G. Sciolla,[26] M. Scornajenghi,[40b,40a] F. Scuri,[69a] F. Scutti,[102] L. M. Scyboz,[113] J. Searcy,[103] C. D. Sebastiani,[70a,70b] P. Seema,[24] S. C. Seidel,[116] A. Seiden,[143] T. Seiss,[36] J. M. Seixas,[78b] G. Sekhniaidze,[67a] K. Sekhon,[103] S. J. Sekula,[41] N. Semprini-Cesari,[23b,23a] S. Sen,[47] S. Senkin,[37] C. Serfon,[130] L. Serin,[128] L. Serkin,[64a,64b] M. Sessa,[72a,72b] H. Severini,[124] F. Sforza,[167] A. Sfyrla,[52] E. Shabalina,[51] J. D. Shahinian,[143] N. W. Shaikh,[43a,43b] L. Y. Shan,[15a] R. Shang,[170] J. T. Shank,[25] M. Shapiro,[18] A. S. Sharma,[1] A. Sharma,[131] P. B. Shatalov,[109] K. Shaw,[153] S. M. Shaw,[98] A. Shcherbakova,[134] Y. Shen,[124] N. Sherafati,[33] A. D. Sherman,[25] P. Sherwood,[92] L. Shi,[155,qq] S. Shimizu,[80] C. O. Shimmin,[180] M. Shimojima,[114] I. P. J. Shipsey,[131] S. Shirabe,[85] M. Shiyakova,[77] J. Shlomi,[177] A. Shmeleva,[108] D. Shoaleh Saadi,[107] M. J. Shochet,[36] S. Shojaii,[102] D. R. Shope,[124] S. Shrestha,[122] E. Shulga,[110] P. Sicho,[137] A. M. Sickles,[170] P. E. Sidebo,[151] E. Sideras Haddad,[32c] O. Sidiropoulou,[174] A. Sidoti,[23b,23a] F. Siegert,[46] Dj. Sijacki,[16] J. Silva,[136a] M. Silva Jr.,[178] M. V. Silva Oliveira,[78a] S. B. Silverstein,[43a] L. Simic,[77] S. Simion,[128] E. Simioni,[97] M. Simon,[97] P. Sinervo,[164] N. B. Sinev,[127] M. Sioli,[23b,23a] G. Siragusa,[174] I. Siral,[103] S. Yu. Sivoklokov,[111] J. Sjölin,[43a,43b] M. B. Skinner,[87] P. Skubic,[124] M. Slater,[21] T. Slavicek,[138] M. Slawinska,[82] K. Sliwa,[167] R. Slovak,[139] V. Smakhtin,[177] B. H. Smart,[5] J. Smiesko,[28a] N. Smirnov,[110] S. Yu. Smirnov,[110] Y. Smirnov,[110] L. N. Smirnova,[111] O. Smirnova,[94] J. W. Smith,[51] M. N. K. Smith,[38] R. W. Smith,[38] M. Smizanska,[87] K. Smolek,[138] A. A. Snesarev,[108] I. M. Snyder,[127] S. Snyder,[29] R. Sobie,[173,m] A. M. Soffa,[168] A. Soffer,[158] A. Søgaard,[48] D. A. Soh,[155] G. Sokhrannyi,[89] C. A. Solans Sanchez,[35] M. Solar,[138] E. Yu. Soldatov,[110] U. Soldevila,[171] A. A. Solodkov,[140] A. Soloshenko,[77] O. V. Solovyanov,[140] V. Solovyev,[134] P. Sommer,[146] H. Son,[167] W. Song,[141] A. Sopczak,[138] F. Sopkova,[28b] D. Sosa,[59b] C. L. Sotiropoulou,[69a,69b] S. Sottocornola,[68a,68b] R. Soualah,[64a,64c,rr] A. M. Soukharev,[120b,120a] D. South,[44] B. C. Sowden,[91] S. Spagnolo,[65a,65b] M. Spalla,[113] M. Spangenberg,[175] F. Spanò,[91]

D. Sperlich,[19] F. Spettel,[113] T. M. Spieker,[59a] R. Spighi,[23b] G. Spigo,[35] L. A. Spiller,[102] D. P. Spiteri,[55] M. Spousta,[139] A. Stabile,[66a,66b] R. Stamen,[59a] S. Stamm,[19] E. Stanecka,[82] R. W. Stanek,[6] C. Stanescu,[72a] B. Stanislaus,[131] M. M. Stanitzki,[44] B. Stapf,[118] S. Stapnes,[130] E. A. Starchenko,[140] G. H. Stark,[36] J. Stark,[56] S.H Stark,[39] P. Staroba,[137] P. Starovoitov,[59a] S. Stärz,[35] R. Staszewski,[82] M. Stegler,[44] P. Steinberg,[29] B. Stelzer,[149] H. J. Stelzer,[35] O. Stelzer-Chilton,[165a] H. Stenzel,[54] T. J. Stevenson,[90] G. A. Stewart,[55] M. C. Stockton,[127] G. Stoicea,[27b] P. Stolte,[51] S. Stonjek,[113] A. Straessner,[46] J. Strandberg,[151] S. Strandberg,[43a,43b] M. Strauss,[124] P. Strizenec,[28b] R. Ströhmer,[174] D. M. Strom,[127] R. Stroynowski,[41] A. Strubig,[48] S. A. Stucci,[29] B. Stugu,[17] J. Stupak,[124] N. A. Styles,[44] D. Su,[150] J. Su,[135] S. Suchek,[59a] Y. Sugaya,[129] M. Suk,[138] V. V. Sulin,[108] D. M. S. Sultan,[52] S. Sultansoy,[4c] T. Sumida,[83] S. Sun,[103] X. Sun,[3] K. Suruliz,[153] C. J. E. Suster,[154] M. R. Sutton,[153] S. Suzuki,[79] M. Svatos,[137] M. Swiatlowski,[36] S. P. Swift,[2] A. Sydorenko,[97] I. Sykora,[28a] T. Sykora,[139] D. Ta,[97] K. Tackmann,[44,ss] J. Taenzer,[158] A. Taffard,[168] R. Tafirout,[165a] E. Tahirovic,[90] N. Taiblum,[158] H. Takai,[29] R. Takashima,[84] E. H. Takasugi,[113] K. Takeda,[80] T. Takeshita,[147] Y. Takubo,[79] M. Talby,[99] A. A. Talyshev,[120b,120a] J. Tanaka,[160] M. Tanaka,[162] R. Tanaka,[128] R. Tanioka,[80] B. B. Tannenwald,[122] S. Tapia Araya,[144b] S. Tapprogge,[97] A. Tarek Abouelfadl Mohamed,[132] S. Tarem,[157] G. Tarna,[27b,q] G. F. Tartarelli,[66a] P. Tas,[139] M. Tasevsky,[137] T. Tashiro,[83] E. Tassi,[40b,40a] A. Tavares Delgado,[136a,136b] Y. Tayalati,[34e] A. C. Taylor,[116] A. J. Taylor,[48] G. N. Taylor,[102] P. T. E. Taylor,[102] W. Taylor,[165b] A. S. Tee,[87] P. Teixeira-Dias,[91] H. Ten Kate,[35] P. K. Teng,[155] J. J. Teoh,[129] F. Tepel,[179] S. Terada,[79] K. Terashi,[160] J. Terron,[96] S. Terzo,[14] M. Testa,[49] R. J. Teuscher,[164,m] S. J. Thais,[180] T. Theveneaux-Pelzer,[44] F. Thiele,[39] J. P. Thomas,[21] A. S. Thompson,[55] P. D. Thompson,[21] L. A. Thomsen,[180] E. Thomson,[133] Y. Tian,[38] R. E. Ticse Torres,[51] V. O. Tikhomirov,[108,tt] Yu. A. Tikhonov,[120b,120a] S. Timoshenko,[110] P. Tipton,[180] S. Tisserant,[99] K. Todome,[162] S. Todorova-Nova,[5] S. Todt,[46] J. Tojo,[85] S. Tokár,[28a] K. Tokushuku,[79] E. Tolley,[122] K. G. Tomiwa,[32c] M. Tomoto,[115] L. Tompkins,[150,gg] K. Toms,[116] B. Tong,[57] P. Tornambe,[50] E. Torrence,[127] H. Torres,[46] E. Torró Pastor,[145] C. Tosciri,[131] J. Toth,[99,uu] F. Touchard,[99] D. R. Tovey,[146] C. J. Treado,[121] T. Trefzger,[174] F. Tresoldi,[153] A. Tricoli,[29] I. M. Trigger,[165a] S. Trincaz-Duvoid,[132] M. F. Tripiana,[14] W. Trischuk,[164] B. Trocmé,[56] A. Trofymov,[128] C. Troncon,[66a] M. Trovatelli,[173] F. Trovato,[153] L. Truong,[32b] M. Trzebinski,[82] A. Trzupek,[82] F. Tsai,[44] J.C-L. Tseng,[131] P. V. Tsiareshka,[105] N. Tsirintanis,[9] V. Tsiskaridze,[152] E. G. Tskhadadze,[156a] I. I. Tsukerman,[109] V. Tsulaia,[18] S. Tsuno,[79] D. Tsybychev,[152] Y. Tu,[61b] A. Tudorache,[27b] V. Tudorache,[27b] T. T. Tulbure,[27a] A. N. Tuna,[57] S. Turchikhin,[77] D. Turgeman,[177] I. Turk Cakir,[4b,vv] R. Turra,[66a] P. M. Tuts,[38] E. Tzovara,[97] G. Ucchielli,[23b,23a] I. Ueda,[79] M. Ughetto,[43a,43b] F. Ukegawa,[166] G. Unal,[35] A. Undrus,[29] G. Unel,[168] F. C. Ungaro,[102] Y. Unno,[79] K. Uno,[160] J. Urban,[28b] P. Urquijo,[102] P. Urrejola,[97] G. Usai,[8] J. Usui,[79] L. Vacavant,[99] V. Vacek,[138] B. Vachon,[101] K. O. H. Vadla,[130] A. Vaidya,[92] C. Valderanis,[112] E. Valdes Santurio,[43a,43b] M. Valente,[52] S. Valentinetti,[23b,23a] A. Valero,[171] L. Valéry,[44] R. A. Vallance,[21] A. Vallier,[5] J. A. Valls Ferrer,[171] T. R. Van Daalen,[14] W. Van Den Wollenberg,[118] H. Van der Graaf,[118] P. Van Gemmeren,[6] J. Van Nieuwkoop,[149] I. Van Vulpen,[118] M. C. van Woerden,[118] M. Vanadia,[71a,71b] W. Vandelli,[35] A. Vaniachine,[163] P. Vankov,[118] R. Vari,[70a] E. W. Varnes,[7] C. Varni,[53b,53a] T. Varol,[41] D. Varouchas,[128] K. E. Varvell,[154] G. A. Vasquez,[144b] J. G. Vasquez,[180] F. Vazeille,[37] D. Vazquez Furelos,[14] T. Vazquez Schroeder,[101] J. Veatch,[51] V. Vecchio,[72a,72b] L. M. Veloce,[164] F. Veloso,[136a,136c] S. Veneziano,[70a] A. Ventura,[65a,65b] M. Venturi,[173] N. Venturi,[35] V. Vercesi,[68a] M. Verducci,[72a,72b] C. M. Vergel Infante,[76] W. Verkerke,[118] A. T. Vermeulen,[118] J. C. Vermeulen,[118] M. C. Vetterli,[149,e] N. Viaux Maira,[144b] O. Viazlo,[94] I. Vichou,[170,a] T. Vickey,[146] O. E. Vickey Boeriu,[146] G. H. A. Viehhauser,[131] S. Viel,[18] L. Vigani,[131] M. Villa,[23b,23a] M. Villaplana Perez,[66a,66b] E. Vilucchi,[49] M. G. Vincter,[33] V. B. Vinogradov,[77] A. Vishwakarma,[44] C. Vittori,[23b,23a] I. Vivarelli,[153] S. Vlachos,[10] M. Vogel,[179] P. Vokac,[138] G. Volpi,[14] S. E. von Buddenbrock,[32c] E. Von Toerne,[24] V. Vorobel,[139] K. Vorobev,[110] M. Vos,[171] J. H. Vossebeld,[88] N. Vranjes,[16] M. Vranjes Milosavljevic,[16] V. Vrba,[138] M. Vreeswijk,[118] T. Šfiligoj,[89] R. Vuillermet,[35] I. Vukotic,[36] T. Ženiš,[28a] L. Živković,[16] P. Wagner,[24] W. Wagner,[179] J. Wagner-Kuhr,[112] H. Wahlberg,[86] S. Wahrmund,[46] K. Wakamiya,[80] V. M. Walbrecht,[113] J. Walder,[87] R. Walker,[112] W. Walkowiak,[148] V. Wallangen,[43a,43b] A. M. Wang,[57] C. Wang,[58b,q] F. Wang,[178] H. Wang,[18] H. Wang,[3] J. Wang,[154] J. Wang,[59b] P. Wang,[41] Q. Wang,[124] R.-J. Wang,[132] R. Wang,[58a] R. Wang,[6] S. M. Wang,[155] W. T. Wang,[58a] W. Wang,[155,ww] W. X. Wang,[58a,xx] Y. Wang,[58a,jj] Z. Wang,[58c] C. Wanotayaroj,[44] A. Warburton,[101] C. P. Ward,[31] D. R. Wardrope,[92] A. Washbrook,[48] P. M. Watkins,[21] A. T. Watson,[21] M. F. Watson,[21] G. Watts,[145] S. Watts,[98] B. M. Waugh,[92] A. F. Webb,[11] S. Webb,[97] C. Weber,[180] M. S. Weber,[20] S. A. Weber,[33] S. M. Weber,[59a] J. S. Webster,[6] A. R. Weidberg,[131] B. Weinert,[63] J. Weingarten,[51] M. Weirich,[97] C. Weiser,[50] P. S. Wells,[35] T. Wenaus,[29] T. Wengler,[35] S. Wenig,[35] N. Wermes,[24] M. D. Werner,[76] P. Werner,[35] M. Wessels,[59a] T. D. Weston,[20] K. Whalen,[127] N. L. Whallon,[145] A. M. Wharton,[87] A. S. White,[103] A. White,[8] M. J. White,[1] R. White,[144b] D. Whiteson,[168] B. W. Whitmore,[87]

F. J. Wickens,[141] W. Wiedenmann,[178] M. Wielers,[141] C. Wiglesworth,[39] L. A. M. Wiik-Fuchs,[50] A. Wildauer,[113] F. Wilk,[98] H. G. Wilkens,[35] L. J. Wilkins,[91] H. H. Williams,[133] S. Williams,[31] C. Willis,[104] S. Willocq,[100] J. A. Wilson,[21] I. Wingerter-Seez,[5] E. Winkels,[153] F. Winklmeier,[127] O. J. Winston,[153] B. T. Winter,[24] M. Wittgen,[150] M. Wobisch,[93] A. Wolf,[97] T. M. H. Wolf,[118] R. Wolff,[99] M. W. Wolter,[82] H. Wolters,[136a,136c] V. W. S. Wong,[172] N. L. Woods,[143] S. D. Worm,[21] B. K. Wosiek,[82] K. W. Woźniak,[82] K. Wraight,[55] M. Wu,[36] S. L. Wu,[178] X. Wu,[52] Y. Wu,[58a] T. R. Wyatt,[98] B. M. Wynne,[48] S. Xella,[39] Z. Xi,[103] L. Xia,[175] D. Xu,[15a] H. Xu,[58a,q] L. Xu,[29] T. Xu,[142] W. Xu,[103] B. Yabsley,[154] S. Yacoob,[32a] K. Yajima,[129] D. P. Yallup,[92] D. Yamaguchi,[162] Y. Yamaguchi,[162] A. Yamamoto,[79] T. Yamanaka,[160] F. Yamane,[80] M. Yamatani,[160] T. Yamazaki,[160] Y. Yamazaki,[80] Z. Yan,[25] H. J. Yang,[58c,58d] H. T. Yang,[18] S. Yang,[75] Y. Yang,[160] Z. Yang,[17] W-M. Yao,[18] Y. C. Yap,[44] Y. Yasu,[79] E. Yatsenko,[58c,58d] J. Ye,[41] S. Ye,[29] I. Yeletskikh,[77] E. Yigitbasi,[25] E. Yildirim,[97] K. Yorita,[176] K. Yoshihara,[133] C. J. S. Young,[35] C. Young,[150] J. Yu,[8] J. Yu,[76] X. Yue,[59a] S. P. Y. Yuen,[24] I. Yusuff,[31,yy] B. Zabinski,[82] G. Zacharis,[10] E. Zaffaroni,[52] R. Zaidan,[14] A. M. Zaitsev,[140,nn] N. Zakharchuk,[44] J. Zalieckas,[17] S. Zambito,[57] D. Zanzi,[35] D. R. Zaripovas,[55] S. V. Zeißner,[45] C. Zeitnitz,[179] G. Zemaityte,[131] J. C. Zeng,[170] Q. Zeng,[150] O. Zenin,[140] D. Zerwas,[128] M. Zgubič,[131] D. F. Zhang,[58b] D. Zhang,[103] F. Zhang,[178] G. Zhang,[58a,xx] H. Zhang,[15c] J. Zhang,[6] L. Zhang,[50] L. Zhang,[58a] M. Zhang,[170] P. Zhang,[15c] R. Zhang,[58a,q] R. Zhang,[24] X. Zhang,[58b] Y. Zhang,[15d] Z. Zhang,[128] P. Zhao,[47] X. Zhao,[41] Y. Zhao,[58b,128,z] Z. Zhao,[58a] A. Zhemchugov,[77] B. Zhou,[103] C. Zhou,[178] L. Zhou,[41] M. S. Zhou,[15d] M. Zhou,[152] N. Zhou,[58c] Y. Zhou,[7] C. G. Zhu,[58b] H. L. Zhu,[58a] H. Zhu,[15a] J. Zhu,[103] Y. Zhu,[58a] X. Zhuang,[15a] K. Zhukov,[108] V. Zhulanov,[120b,120a] A. Zibell,[174] D. Zieminska,[63] N. I. Zimine,[77] S. Zimmermann,[50] Z. Zinonos,[113] M. Zinser,[97] M. Ziolkowski,[148] G. Zobernig,[178] A. Zoccoli,[23b,23a] K. Zoch,[51] T. G. Zorbas,[146] R. Zou,[36] M. Zur Nedden,[19] and L. Zwalinski[35]

(ATLAS Collaboration)

[1]*Department of Physics, University of Adelaide, Adelaide, Australia*
[2]*Physics Department, SUNY Albany, Albany, New York, USA*
[3]*Department of Physics, University of Alberta, Edmonton, Alberta, Canada*
[4a]*Department of Physics, Ankara University, Ankara, Turkey*
[4b]*Istanbul Aydin University, Istanbul, Turkey*
[4c]*Division of Physics, TOBB University of Economics and Technology, Ankara, Turkey*
[5]*LAPP, Université Grenoble Alpes, Université Savoie Mont Blanc, CNRS/IN2P3, Annecy, France*
[6]*High Energy Physics Division, Argonne National Laboratory, Argonne, Illinois, USA*
[7]*Department of Physics, University of Arizona, Tucson, Arizona, USA*
[8]*Department of Physics, University of Texas at Arlington, Arlington, Texas, USA*
[9]*Physics Department, National and Kapodistrian University of Athens, Athens, Greece*
[10]*Physics Department, National Technical University of Athens, Zografou, Greece*
[11]*Department of Physics, University of Texas at Austin, Austin, Texas, USA*
[12a]*Bahcesehir University, Faculty of Engineering and Natural Sciences, Istanbul, Turkey*
[12b]*Istanbul Bilgi University, Faculty of Engineering and Natural Sciences, Istanbul, Turkey*
[12c]*Department of Physics, Bogazici University, Istanbul, Turkey*
[12d]*Department of Physics Engineering, Gaziantep University, Gaziantep, Turkey*
[13]*Institute of Physics, Azerbaijan Academy of Sciences, Baku, Azerbaijan*
[14]*Institut de Física d'Altes Energies (IFAE), Barcelona Institute of Science and Technology, Barcelona, Spain*
[15a]*Institute of High Energy Physics, Chinese Academy of Sciences, Beijing, China*
[15b]*Physics Department, Tsinghua University, Beijing, China*
[15c]*Department of Physics, Nanjing University, Nanjing, China*
[15d]*University of Chinese Academy of Science (UCAS), Beijing, China*
[16]*Institute of Physics, University of Belgrade, Belgrade, Serbia*
[17]*Department for Physics and Technology, University of Bergen, Bergen, Norway*
[18]*Physics Division, Lawrence Berkeley National Laboratory and University of California, Berkeley, California, USA*
[19]*Institut für Physik, Humboldt Universität zu Berlin, Berlin, Germany*
[20]*Albert Einstein Center for Fundamental Physics and Laboratory for High Energy Physics, University of Bern, Bern, Switzerland*
[21]*School of Physics and Astronomy, University of Birmingham, Birmingham, United Kingdom*
[22]*Centro de Investigaciónes, Universidad Antonio Nariño, Bogota, Colombia*

[23a]*Dipartimento di Fisica e Astronomia, Università di Bologna, Bologna, Italy*
[23b]*INFN Sezione di Bologna, Italy*
[24]*Physikalisches Institut, Universität Bonn, Bonn, Germany*
[25]*Department of Physics, Boston University, Boston, Massachusetts, USA*
[26]*Department of Physics, Brandeis University, Waltham, Massachusetts, USA*
[27a]*Transilvania University of Brasov, Brasov, Romania*
[27b]*Horia Hulubei National Institute of Physics and Nuclear Engineering, Bucharest, Romania*
[27c]*Department of Physics, Alexandru Ioan Cuza University of Iasi, Iasi, Romania*
[27d]*National Institute for Research and Development of Isotopic and Molecular Technologies, Physics Department, Cluj-Napoca, Romania*
[27e]*University Politehnica Bucharest, Bucharest, Romania*
[27f]*West University in Timisoara, Timisoara, Romania*
[28a]*Faculty of Mathematics, Physics and Informatics, Comenius University, Bratislava, Slovak Republic*
[28b]*Department of Subnuclear Physics, Institute of Experimental Physics of the Slovak Academy of Sciences, Kosice, Slovak Republic*
[29]*Physics Department, Brookhaven National Laboratory, Upton, New York, USA*
[30]*Departamento de Física, Universidad de Buenos Aires, Buenos Aires, Argentina*
[31]*Cavendish Laboratory, University of Cambridge, Cambridge, United Kingdom*
[32a]*Department of Physics, University of Cape Town, Cape Town, South Africa*
[32b]*Department of Mechanical Engineering Science, University of Johannesburg, Johannesburg, South Africa*
[32c]*School of Physics, University of the Witwatersrand, Johannesburg, South Africa*
[33]*Department of Physics, Carleton University, Ottawa, Ontario, Canada*
[34a]*Faculté des Sciences Ain Chock, Réseau Universitaire de Physique des Hautes Energies—Université Hassan II, Casablanca, Morocco*
[34b]*Centre National de l'Energie des Sciences Techniques Nucleaires (CNESTEN), Rabat, Morocco*
[34c]*Faculté des Sciences Semlalia, Université Cadi Ayyad, LPHEA-Marrakech, Morocco*
[34d]*Faculté des Sciences, Université Mohamed Premier and LPTPM, Oujda, Morocco*
[34e]*Faculté des sciences, Université Mohammed V, Rabat, Morocco*
[35]*CERN, Geneva, Switzerland*
[36]*Enrico Fermi Institute, University of Chicago, Chicago, Illinois, USA*
[37]*LPC, Université Clermont Auvergne, CNRS/IN2P3, Clermont-Ferrand, France*
[38]*Nevis Laboratory, Columbia University, Irvington, New York, USA*
[39]*Niels Bohr Institute, University of Copenhagen, Copenhagen, Denmark*
[40a]*Dipartimento di Fisica, Università della Calabria, Rende, Italy*
[40b]*INFN Gruppo Collegato di Cosenza, Laboratori Nazionali di Frascati, Italy*
[41]*Physics Department, Southern Methodist University, Dallas, Texas, USA*
[42]*Physics Department, University of Texas at Dallas, Richardson, Texas, USA*
[43a]*Department of Physics, Stockholm University, Sweden*
[43b]*Oskar Klein Centre, Stockholm, Sweden*
[44]*Deutsches Elektronen-Synchrotron DESY, Hamburg and Zeuthen, Germany*
[45]*Lehrstuhl für Experimentelle Physik IV, Technische Universität Dortmund, Dortmund, Germany*
[46]*Institut für Kern- und Teilchenphysik, Technische Universität Dresden, Dresden, Germany*
[47]*Department of Physics, Duke University, Durham, North Carolina, USA*
[48]*SUPA—School of Physics and Astronomy, University of Edinburgh, Edinburgh, United Kingdom*
[49]*INFN e Laboratori Nazionali di Frascati, Frascati, Italy*
[50]*Physikalisches Institut, Albert-Ludwigs-Universität Freiburg, Freiburg, Germany*
[51]*II. Physikalisches Institut, Georg-August-Universität Göttingen, Göttingen, Germany*
[52]*Département de Physique Nucléaire et Corpusculaire, Université de Genève, Genève, Switzerland*
[53a]*Dipartimento di Fisica, Università di Genova, Genova, Italy*
[53b]*INFN Sezione di Genova, Italy*
[54]*II. Physikalisches Institut, Justus-Liebig-Universität Giessen, Giessen, Germany*
[55]*SUPA—School of Physics and Astronomy, University of Glasgow, Glasgow, United Kingdom*
[56]*LPSC, Université Grenoble Alpes, CNRS/IN2P3, Grenoble INP, Grenoble, France*
[57]*Laboratory for Particle Physics and Cosmology, Harvard University, Cambridge, Massachusetts, USA*
[58a]*Department of Modern Physics and State Key Laboratory of Particle Detection and Electronics, University of Science and Technology of China, Hefei, China*
[58b]*Institute of Frontier and Interdisciplinary Science and Key Laboratory of Particle Physics and Particle Irradiation (MOE), Shandong University, Qingdao, China*

[58c]School of Physics and Astronomy, Shanghai Jiao Tong University, KLPPAC-MoE, SKLPPC, Shanghai, China
[58d]Tsung-Dao Lee Institute, Shanghai, China
[59a]Kirchhoff-Institut für Physik, Ruprecht-Karls-Universität Heidelberg, Heidelberg, Germany
[59b]Physikalisches Institut, Ruprecht-Karls-Universität Heidelberg, Heidelberg, Germany
[60]Faculty of Applied Information Science, Hiroshima Institute of Technology, Hiroshima, Japan
[61a]Department of Physics, Chinese University of Hong Kong, Shatin, N.T., Hong Kong, China
[61b]Department of Physics, University of Hong Kong, Hong Kong, China
[61c]Department of Physics and Institute for Advanced Study, Hong Kong University of Science and Technology, Clear Water Bay, Kowloon, Hong Kong, China
[62]Department of Physics, National Tsing Hua University, Hsinchu, Taiwan
[63]Department of Physics, Indiana University, Bloomington, Indiana, USA
[64a]INFN Gruppo Collegato di Udine, Sezione di Trieste, Udine, Italy
[64b]ICTP, Trieste, Italy
[64c]Dipartimento di Chimica, Fisica e Ambiente, Università di Udine, Udine, Italy
[65a]INFN Sezione di Lecce, Italy
[65b]Dipartimento di Matematica e Fisica, Università del Salento, Lecce, Italy
[66a]INFN Sezione di Milano, Italy
[66b]Dipartimento di Fisica, Università di Milano, Milano, Italy
[67a]INFN Sezione di Napoli, Italy
[67b]Dipartimento di Fisica, Università di Napoli, Napoli, Italy
[68a]INFN Sezione di Pavia, Italy
[68b]Dipartimento di Fisica, Università di Pavia, Pavia, Italy
[69a]INFN Sezione di Pisa, Italy
[69b]Dipartimento di Fisica E. Fermi, Università di Pisa, Pisa, Italy
[70a]INFN Sezione di Roma, Italy
[70b]Dipartimento di Fisica, Sapienza Università di Roma, Roma, Italy
[71a]INFN Sezione di Roma Tor Vergata, Italy
[71b]Dipartimento di Fisica, Università di Roma Tor Vergata, Roma, Italy
[72a]INFN Sezione di Roma Tre, Italy
[72b]Dipartimento di Matematica e Fisica, Università Roma Tre, Roma, Italy
[73a]INFN-TIFPA, Italy
[73b]Università degli Studi di Trento, Trento, Italy
[74]Institut für Astro- und Teilchenphysik, Leopold-Franzens-Universität, Innsbruck, Austria
[75]University of Iowa, Iowa City, Iowa, USA
[76]Department of Physics and Astronomy, Iowa State University, Ames, Iowa, USA
[77]Joint Institute for Nuclear Research, Dubna, Russia
[78a]Departamento de Engenharia Elétrica, Universidade Federal de Juiz de Fora (UFJF), Juiz de Fora, Brazil
[78b]Universidade Federal do Rio De Janeiro COPPE/EE/IF, Rio de Janeiro, Brazil
[78c]Universidade Federal de São João del Rei (UFSJ), São João del Rei, Brazil
[78d]Instituto de Física, Universidade de São Paulo, São Paulo, Brazil
[79]KEK, High Energy Accelerator Research Organization, Tsukuba, Japan
[80]Graduate School of Science, Kobe University, Kobe, Japan
[81a]AGH University of Science and Technology, Faculty of Physics and Applied Computer Science, Krakow, Poland
[81b]Marian Smoluchowski Institute of Physics, Jagiellonian University, Krakow, Poland
[82]Institute of Nuclear Physics Polish Academy of Sciences, Krakow, Poland
[83]Faculty of Science, Kyoto University, Kyoto, Japan
[84]Kyoto University of Education, Kyoto, Japan
[85]Research Center for Advanced Particle Physics and Department of Physics, Kyushu University, Fukuoka, Japan
[86]Instituto de Física La Plata, Universidad Nacional de La Plata and CONICET, La Plata, Argentina
[87]Physics Department, Lancaster University, Lancaster, United Kingdom
[88]Oliver Lodge Laboratory, University of Liverpool, Liverpool, United Kingdom
[89]Department of Experimental Particle Physics, Jožef Stefan Institute and Department of Physics, University of Ljubljana, Ljubljana, Slovenia
[90]School of Physics and Astronomy, Queen Mary University of London, London, United Kingdom
[91]Department of Physics, Royal Holloway University of London, Egham, United Kingdom
[92]Department of Physics and Astronomy, University College London, London, United Kingdom

[93]*Louisiana Tech University, Ruston, Louisiana, USA*
[94]*Fysiska institutionen, Lunds universitet, Lund, Sweden*
[95]*Centre de Calcul de l'Institut National de Physique Nucléaire et de Physique des Particules (IN2P3), Villeurbanne, France*
[96]*Departamento de Física Teorica C-15 and CIAFF, Universidad Autónoma de Madrid, Madrid, Spain*
[97]*Institut für Physik, Universität Mainz, Mainz, Germany*
[98]*School of Physics and Astronomy, University of Manchester, Manchester, United Kingdom*
[99]*CPPM, Aix-Marseille Université, CNRS/IN2P3, Marseille, France*
[100]*Department of Physics, University of Massachusetts, Amherst, Massachusetts, USA*
[101]*Department of Physics, McGill University, Montreal, Quebec, Canada*
[102]*School of Physics, University of Melbourne, Victoria, Australia*
[103]*Department of Physics, University of Michigan, Ann Arbor, Michigan, USA*
[104]*Department of Physics and Astronomy, Michigan State University, East Lansing, Michigan, USA*
[105]*B.I. Stepanov Institute of Physics, National Academy of Sciences of Belarus, Minsk, Belarus*
[106]*Research Institute for Nuclear Problems of Byelorussian State University, Minsk, Belarus*
[107]*Group of Particle Physics, University of Montreal, Montreal, Quebec, Canada*
[108]*P.N. Lebedev Physical Institute of the Russian Academy of Sciences, Moscow, Russia*
[109]*Institute for Theoretical and Experimental Physics (ITEP), Moscow, Russia*
[110]*National Research Nuclear University MEPhI, Moscow, Russia*
[111]*D.V. Skobeltsyn Institute of Nuclear Physics, M.V. Lomonosov Moscow State University, Moscow, Russia*
[112]*Fakultät für Physik, Ludwig-Maximilians-Universität München, München, Germany*
[113]*Max-Planck-Institut für Physik (Werner-Heisenberg-Institut), München, Germany*
[114]*Nagasaki Institute of Applied Science, Nagasaki, Japan*
[115]*Graduate School of Science and Kobayashi-Maskawa Institute, Nagoya University, Nagoya, Japan*
[116]*Department of Physics and Astronomy, University of New Mexico, Albuquerque, New Mexico, USA*
[117]*Institute for Mathematics, Astrophysics and Particle Physics, Radboud University Nijmegen/Nikhef, Nijmegen, Netherlands*
[118]*Nikhef National Institute for Subatomic Physics and University of Amsterdam, Amsterdam, Netherlands*
[119]*Department of Physics, Northern Illinois University, DeKalb, Illinois, USA*
[120a]*Budker Institute of Nuclear Physics, SB RAS, Novosibirsk, Russia*
[120b]*Novosibirsk State University Novosibirsk, Russia*
[121]*Department of Physics, New York University, New York, New York, USA*
[122]*The Ohio State University, Columbus, Ohio, USA*
[123]*Faculty of Science, Okayama University, Okayama, Japan*
[124]*Homer L. Dodge Department of Physics and Astronomy, University of Oklahoma, Norman, Oklahoma, USA*
[125]*Department of Physics, Oklahoma State University, Stillwater, Oklahoma, USA*
[126]*Palacký University, RCPTM, Joint Laboratory of Optics, Olomouc, Czech Republic*
[127]*Center for High Energy Physics, University of Oregon, Eugene, Oregon, USA*
[128]*LAL, Université Paris-Sud, CNRS/IN2P3, Université Paris-Saclay, Orsay, France*
[129]*Graduate School of Science, Osaka University, Osaka, Japan*
[130]*Department of Physics, University of Oslo, Oslo, Norway*
[131]*Department of Physics, Oxford University, Oxford, United Kingdom*
[132]*LPNHE, Sorbonne Université, Paris Diderot Sorbonne Paris Cité, CNRS/IN2P3, Paris, France*
[133]*Department of Physics, University of Pennsylvania, Philadelphia, Pennsylvania, USA*
[134]*Konstantinov Nuclear Physics Institute of National Research Centre "Kurchatov Institute", PNPI, St. Petersburg, Russia*
[135]*Department of Physics and Astronomy, University of Pittsburgh, Pittsburgh, Pennsylvania, USA*
[136a]*Laboratório de Instrumentação e Física Experimental de Partículas—LIP, Portugal*
[136b]*Departamento de Física, Faculdade de Ciências, Universidade de Lisboa, Lisboa, Portugal*
[136c]*Departamento de Física, Universidade de Coimbra, Coimbra, Portugal*
[136d]*Centro de Física Nuclear da Universidade de Lisboa, Lisboa, Portugal*
[136e]*Departamento de Física, Universidade do Minho, Braga, Portugal*
[136f]*Departamento de Física Teorica y del Cosmos, Universidad de Granada, Granada (Spain), Spain*
[136g]*Dep Física and CEFITEC of Faculdade de Ciências e Tecnologia, Universidade Nova de Lisboa, Caparica, Portugal*
[137]*Institute of Physics, Academy of Sciences of the Czech Republic, Prague, Czech Republic*
[138]*Czech Technical University in Prague, Prague, Czech Republic*
[139]*Charles University, Faculty of Mathematics and Physics, Prague, Czech Republic*

[140]State Research Center Institute for High Energy Physics, NRC KI, Protvino, Russia
[141]Particle Physics Department, Rutherford Appleton Laboratory, Didcot, United Kingdom
[142]IRFU, CEA, Université Paris-Saclay, Gif-sur-Yvette, France
[143]Santa Cruz Institute for Particle Physics, University of California Santa Cruz, Santa Cruz, California, USA
[144a]Departamento de Física, Pontificia Universidad Católica de Chile, Santiago, Chile
[144b]Departamento de Física, Universidad Técnica Federico Santa María, Valparaíso, Chile
[145]Department of Physics, University of Washington, Seattle, Washington, USA
[146]Department of Physics and Astronomy, University of Sheffield, Sheffield, United Kingdom
[147]Department of Physics, Shinshu University, Nagano, Japan
[148]Department Physik, Universität Siegen, Siegen, Germany
[149]Department of Physics, Simon Fraser University, Burnaby, British Columbia, Canada
[150]SLAC National Accelerator Laboratory, Stanford, California, USA
[151]Physics Department, Royal Institute of Technology, Stockholm, Sweden
[152]Departments of Physics and Astronomy, Stony Brook University, Stony Brook, New York, USA
[153]Department of Physics and Astronomy, University of Sussex, Brighton, United Kingdom
[154]School of Physics, University of Sydney, Sydney, Australia
[155]Institute of Physics, Academia Sinica, Taipei, Taiwan
[156a]E. Andronikashvili Institute of Physics, Iv. Javakhishvili Tbilisi State University, Tbilisi, Georgia
[156b]High Energy Physics Institute, Tbilisi State University, Tbilisi, Georgia
[157]Department of Physics, Technion, Israel Institute of Technology, Haifa, Israel
[158]Raymond and Beverly Sackler School of Physics and Astronomy, Tel Aviv University, Tel Aviv, Israel
[159]Department of Physics, Aristotle University of Thessaloniki, Thessaloniki, Greece
[160]International Center for Elementary Particle Physics and Department of Physics, University of Tokyo, Tokyo, Japan
[161]Graduate School of Science and Technology, Tokyo Metropolitan University, Tokyo, Japan
[162]Department of Physics, Tokyo Institute of Technology, Tokyo, Japan
[163]Tomsk State University, Tomsk, Russia
[164]Department of Physics, University of Toronto, Toronto, Ontario, Canada
[165a]TRIUMF, Vancouver, British Columbia, Canada
[165b]Department of Physics and Astronomy, York University, Toronto, Ontario, Canada
[166]Division of Physics and Tomonaga Center for the History of the Universe, Faculty of Pure and Applied Sciences, University of Tsukuba, Tsukuba, Japan
[167]Department of Physics and Astronomy, Tufts University, Medford, Massachusetts, USA
[168]Department of Physics and Astronomy, University of California Irvine, Irvine, California, USA
[169]Department of Physics and Astronomy, University of Uppsala, Uppsala, Sweden
[170]Department of Physics, University of Illinois, Urbana, Illinois, USA
[171]Instituto de Física Corpuscular (IFIC), Centro Mixto Universidad de Valencia—CSIC, Valencia, Spain
[172]Department of Physics, University of British Columbia, Vancouver, British Columbia, Canada
[173]Department of Physics and Astronomy, University of Victoria, Victoria, British Columbia, Canada
[174]Fakultät für Physik und Astronomie, Julius-Maximilians-Universität Würzburg, Würzburg, Germany
[175]Department of Physics, University of Warwick, Coventry, United Kingdom
[176]Waseda University, Tokyo, Japan
[177]Department of Particle Physics, Weizmann Institute of Science, Rehovot, Israel
[178]Department of Physics, University of Wisconsin, Madison, Wisconsin, USA
[179]Fakultät für Mathematik und Naturwissenschaften, Fachgruppe Physik, Bergische Universität Wuppertal, Wuppertal, Germany
[180]Department of Physics, Yale University, New Haven, Connecticut, USA
[181]Yerevan Physics Institute, Yerevan, Armenia

[a]Deceased.
[b]Also at Department of Physics, King's College London, London, United Kingdom.
[c]Also at Istanbul University, Department of Physics, Istanbul, Turkey.
[d]Also at Institute of Physics, Azerbaijan Academy of Sciences, Baku, Azerbaijan.
[e]Also at TRIUMF, Vancouver, British Columbia, Canada.
[f]Also at Department of Physics and Astronomy, University of Louisville, Louisville, Kentucky, USA.
[g]Also at Department of Physics, California State University, Fresno, California, USA.
[h]Also at Department of Physics, University of Fribourg, Fribourg, Switzerland.
[i]Also at Departament de Fisica de la Universitat Autonoma de Barcelona, Barcelona, Spain.
[j]Also at Tomsk State University, Tomsk, and Moscow Institute of Physics and Technology State University, Dolgoprudny, Russia.

[k]Also at The Collaborative Innovation Center of Quantum Matter (CICQM), Beijing, China.
[l]Also at Universita di Napoli Parthenope, Napoli, Italy.
[m]Also at Institute of Particle Physics (IPP), Canada.
[n]Also at II. Physikalisches Institut, Georg-August-Universität Göttingen, Göttingen, Germany.
[o]Also at Dipartimento di Fisica E. Fermi, Università di Pisa, Pisa, Italy.
[p]Also at Horia Hulubei National Institute of Physics and Nuclear Engineering, Bucharest, Romania.
[q]Also at CPPM, Aix-Marseille Université, CNRS/IN2P3, Marseille, France.
[r]Also at Department of Physics, St. Petersburg State Polytechnical University, St. Petersburg, Russia.
[s]Also at Borough of Manhattan Community College, City University of New York, New York, USA.
[t]Also at Department of Financial and Management Engineering, University of the Aegean, Chios, Greece.
[u]Also at Centre for High Performance Computing, CSIR Campus, Rosebank, Cape Town, South Africa.
[v]Also at Louisiana Tech University, Ruston, Louisiana, USA.
[w]Also at California State University, East Bay, USA.
[x]Also at Institucio Catalana de Recerca i Estudis Avancats, ICREA, Barcelona, Spain.
[y]Also at Department of Physics, University of Michigan, Ann Arbor, Michigan, USA.
[z]Also at LAL, Université Paris-Sud, CNRS/IN2P3, Université Paris-Saclay, Orsay, France.
[aa]Also at Graduate School of Science, Osaka University, Osaka, Japan.
[bb]Also at Physikalisches Institut, Albert-Ludwigs-Universität Freiburg, Freiburg, Germany.
[cc]Also at Institute for Mathematics, Astrophysics and Particle Physics, Radboud University Nijmegen/Nikhef, Nijmegen, Netherlands.
[dd]Also at Near East University, Nicosia, North Cyprus, Mersin, Turkey.
[ee]Also at Institute of Theoretical Physics, Ilia State University, Tbilisi, Georgia.
[ff]Also at CERN, Geneva, Switzerland.
[gg]Also at Department of Physics, Stanford University, Stanford, California, USA.
[hh]Also at Manhattan College, New York, New York, USA.
[ii]Also at Hellenic Open University, Patras, Greece.
[jj]Also at LPNHE, Sorbonne Université, Paris Diderot Sorbonne Paris Cité, CNRS/IN2P3, Paris, France.
[kk]Also at The City College of New York, New York, New York, USA.
[ll]Also at Departamento de Física Teorica y del Cosmos, Universidad de Granada, Granada (Spain), Spain.
[mm]Also at Department of Physics, California State University, Sacramento, California, USA.
[nn]Also at Moscow Institute of Physics and Technology State University, Dolgoprudny, Russia.
[oo]Also at Département de Physique Nucléaire et Corpusculaire, Université de Genève, Genève, Switzerland.
[pp]Also at Department of Physics and Astronomy, University of Sheffield, Sheffield, United Kingdom.
[qq]Also at School of Physics, Sun Yat-sen University, Guangzhou, China.
[rr]Also at Department of Applied Physics and Astronomy, University of Sharjah, Sharjah, United Arab Emirates.
[ss]Also at Institut für Experimentalphysik, Universität Hamburg, Hamburg, Germany.
[tt]Also at National Research Nuclear University MEPhI, Moscow, Russia.
[uu]Also at Institute for Particle and Nuclear Physics, Wigner Research Centre for Physics, Budapest, Hungary.
[vv]Also at Giresun University, Faculty of Engineering, Giresun, Turkey.
[ww]Also at Department of Physics, Nanjing University, Nanjing, China.
[xx]Also at Institute of Physics, Academia Sinica, Taipei, Taiwan.
[yy]Also at Department of Physics, University of Malaya, Kuala Lumpur, Malaysia.